

AD-756 243

A FEASIBILITY STUDY OF AN ASW SEARCH  
DIRECTOR CONCEPT

William H. Brune, et al

Cornell Aeronautical Laboratory, Incorporated

Prepared for:

Office of Naval Research

31 October 1972

DISTRIBUTED BY:

**NTIS**

National Technical Information Service  
U. S. DEPARTMENT OF COMMERCE  
5285 Port Royal Road, Springfield Va. 22151

AD 756243

# TECHNICAL REPORT

## A FEASIBILITY STUDY OF AN ASW SEARCH DIRECTOR CONCEPT

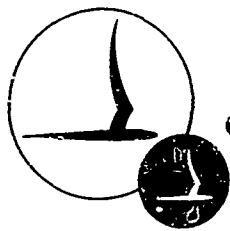
By: W.H. Brune and R.J. Taylor

CAL No. SC-5062-G-1

Prepared For:  
AERONAUTICS PROGRAMS  
OFFICE OF NAVAL RESEARCH

ANNUAL REPORT  
ONR Contract No. N00014-72-C-0103  
Task Number NR220-041-1  
31 October 1972

On November 17, 1972 Cornell Aeronautical Laboratory (CAL) changed its name to Calspan Corporation and converted to for-profit operations. Calspan is dedicated to carrying on CAL's long-standing tradition of advanced research and development from an independent viewpoint. All of CAL's diverse scientific and engineering programs for government and industry are being continued in the aerosciences, electronics and avionics, computer sciences, transportation and vehicle research, and the environmental sciences. Calspan is composed of the same staff, management, and facilities as CAL, which operated since 1946 under federal income tax exemption.



**CORNELL AERONAUTICAL LABORATORY, INC.**

OF CORNELL UNIVERSITY, BUFFALO, N. Y. 14221

For  
to be put  
distributed

176



CORNELL AERONAUTICAL LABORATORY, INC.  
BUFFALO, NEW YORK 14221

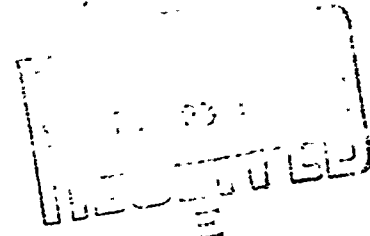
TECHNICAL REPORT

A FEASIBILITY STUDY OF AN ASW  
SEARCH DIRECTOR CONCEPT

CAL REPORT NO. SC-5052-G-1  
ANNUAL REPORT  
CONTRACT NO. N00014-72-C-0103

31 OCTOBER 1972

Prepared For:  
AERONAUTICS PROGRAMS  
OFFICE OF NAVAL RESEARCH



Prepared By: William A. Brune

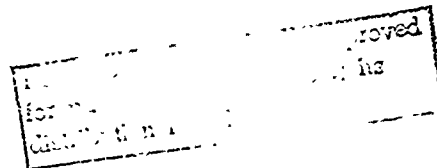
W H Brune  
Operations Research Department

Approved By: Robert M. Stevens

Robert M. Stevens, Head  
Operations Research Department

Richard J. Taylor

R.J. Taylor  
Operations Research Department



UNCLASSIFIED

Security Classification

## DOCUMENT CONTROL DATA - R &amp; D

*Security classification of title, body of abstract, and indexing annotation must be entered when the overall report is classified*

1. ORIGINATING ACTIVITY (Corporate author) Cornell Aeronautical Laboratory, Inc. P. O. Box 235, Buffalo, New York 14221		2a. REPORT SECURITY CLASSIFICATION Unclassified	
		2b. GROUP - - - -	
3. REPORT TITLE A Feasibility Study of an ASW Search Director Concept			
4. DESCRIPTIVE NOTES (Type of report and Inclusive Dates) Annual Report, 1 November 1971 to 31 October 1972			
5. AUTHOR(S) (First name, middle initial, last name) William H. Brune Richard J. Taylor			
6. REPORT DATE 31 October 1972	7a. TOTAL NO. OF PAGES	7b. NO. OF REFS Three	
7a. CONTRACT OR GRANT NO. N00014-72-C-0103	9a. ORIGINATOR'S REPORT NUMBER(S) SC-5062-G-1		
b. PROJECT NO. SC-5062-G			
c. TASK NO: VR220-04i-1	9b. OTHER REPORT NO(S) (Any other numbers that may be assigned this report) - - - -		
10. DISTRIBUTION STATEMENT See Distribution List in rear of report			
11. SUPPLEMENTARY NOTES - - - -		12. SPONSORING MILITARY ACTIVITY Aeronautics Programs (Code 461) Office of Naval Research Arlington, Virginia 22217	
13. ABSTRACT An exploratory investigation is performed of the feasibility and applicability of a Search Director concept for use by U.S. Navy ASW personnel in determining optimal search tactics and sonobuoy drop patterns to detect and localize submarines. Problems arise in conducting these operations which are due to the use of imprecise information from acoustic sensor surveillance systems. The purpose of the Search Director is to (1) assemble this information in terms of target heading, motion, initial size and orientation of the uncertainty area, time late, uncertainty area growth, search time, etc. into coherent and easily computer-processed forms, (2) update the processed information as operations progress and (3) produce displays of the current and future status of these operations. The Search Director principle makes use of negative information that the target has not been detected up to the present time by deployed sonobuoys. As areas covered by each of the sonobuoys are searched and the target is undetected, the probability that the target is in the searched area decreases whereas the probability that it is elsewhere in unsearched areas increases. A dynamic display of this probability density map over the expanding uncertainty area shows where the target might be at any time and, indicates where the next sonobuoys should be dropped. Trial sonobuoy patterns and monitoring schedules can be examined on a real or accelerated time basis and the most efficient sonobuoy patterns selected prior to actual deployment of the sonobuoys. This report (1) summarizes the computer programs that have been formulated to date for this purpose (2) presents sample results to show the feasibility and applicability of this concept and (3) discusses display techniques for presenting the maps.			

DD FORM 1473  
1 NOV 55

14 KEY WORDS	LINK A		LINK B		LINK C	
	ROLE	WT	ROLE	WT	ROLE	WT
ASW Search Director Concept						
VP Aircraft ASW Search Operations						
Submarine Target Uncertainty Areas						
Sonobuoy Search Patterns						
Submarine Target Probability Density Maps						
Search Director Computer Programs						
Probability Density Map Display Techniques						

ACCESSION BY	
YES	Write Section <input checked="" type="checkbox"/>
NO	Edit Section <input type="checkbox"/>
POSITION	<input type="checkbox"/>
BY	
DATE	AVAILABILITY CODES
	REASON FOR SPECIAL

## PREFACE

This report has been prepared by the Cornell Aeronautical Laboratory, Inc. (CAL) for the Office of Aeronautics Programs, Office of Naval Research, Department of the Navy. The results presented herein represent an annual report of the tasks associated with Task Number NR 220-041-1 of Contract No. N00014-72-C-0103.

The Search Director concept originated at CAL. It was initiated as an internal research project as a result of various ASW studies conducted at CAL which were concerned with ASW surveillance systems and VP aircraft operations including detection and localization of target submarines. This study for ONR is the first phase of a continuing effort to:

1. Formulate the mathematical relationships and computer software programs that form the basis of the Search Director concept.
2. Demonstrate the feasibility and applicability of the concept for use by ASW aircraft crews in detecting and localizing submarines.

An abstract of this study is contained in DD Form 1473 which is included in the ii and iii pages of this report.

This study has been co-sponsored by Aeronautics Programs, Code 461 and Naval Analysis, Code 462 of the Office of Naval Research. Appreciation is expressed to Cmdrs. E. R. Doering and W. L. Smith, Code 461 and to J. G. Smith, Code 462 for their help and guidance during the course of the study and during program progress reviews conducted at ONR and CAL. This study has been performed under the technical direction of Cmdrs. E. R. Doering and W. L. Smith.

The following Cornell Aeronautical Laboratory, Inc. personnel have contributed directly to the accomplishment of this study:

William H. Brune  
Richard J. Taylor  
Daryl A. Travnicek

Hamilton M. Maynard  
James L. Douglas  
Vanig V. Abrahamian

TABLE OF CONTENTS

<u>SECTION</u>	<u>TITLE</u>	<u>PAGE NO.</u>
	PREFACE. . . . .	iv
	LIST OF FIGURES. . . . .	ix
	LIST OF TABLES . . . . .	xiv
I.	SUMMARY, CONCLUSIONS AND RECOMMENDATIONS . . . . .	I-1
	A. STUDY SUMMARY . . . . .	I-1
	1. Purpose. . . . .	I-1
	2. Approach . . . . .	I-2
	a. Analysis. . . . .	I-2
	b. Tactical Cases Analyzed . . . . .	I-3
	3. Principal Results. . . . .	I-5
	B. CONCLUSIONS . . . . .	I-10
	C. RECOMMENDATIONS . . . . .	I-10
II.	INTRODUCTION . . . . .	II-1
	A. BACKGROUND. . . . .	II-1
	B. STUDY OBJECTIVES AND SCOPE. . . . .	II-6
III.	STUDY ANALYSES AND RESULTS . . . . .	III-1
	A. BASIC MATHEMATICAL RELATIONSHIPS UNDERLYING TARGET UNCERTAINTY AREA PROBABILITY DENSITY MAPS. . . . .	III-1
	1. Initial Target Uncertainty Area Probability Density Map. . . . .	III-1
	2. Effect of Target Motion on Probability Density Map Versus Time. . . . .	III-2
	3. Acoustic Sensor Employment Effects on Probability Density Map. . . . .	III-4
	a. Sensor Nondetection at Successive Time Increments . . . . .	III-6
	4. Target Motion Changes at $t^*$ . . . . .	III-7
	5. Target Location Probability Density Versus Time . . . . .	III-7



TABLE OF CONTENTS (Continued)

<u>SECTION</u>	<u>TITLE</u>	<u>PAGE NO.</u>
B.	DESCRIPTION OF "EXACT" SOLUTION COMPUTER PROGRAM . . . . .	III-8
1.	Method of Determining Probability Density Map of Target Position With Time . . . . .	III-8
2.	Method of Inserting Sonobuoy Field . . . . .	III-9
C.	DESCRIPTION OF MONTE CARLO COMPUTER PROGRAM . . . . .	III-10
1.	Method of Determining Probability Density of Target Position With Time . . . . .	III-10
2.	Comparison of Monte Carlo Computer Program Results With Exact Solution For Initial Probability Density Distribution . . . . .	III-11
3.	Methods of Inserting Sonobuoy Field Into Monte Carlo Program. . . . .	III-13
a.	Method I. . . . .	III-14
b.	Method II . . . . .	III-15
c.	Sample Results Utilizing Method II. . . . .	III-17
d.	Method III. . . . .	III-20
e.	Sample Computer Run Results for Methods I, II and III . . . . .	III-21
4.	Start and End Grids Development. . . . .	III-28
5.	Probability-of-Miss (PM) Grid Development. . . . .	III-29
6.	Methods of Assigning Velocity Components to MC Submarines . . . . .	III-30
a.	Uniform Heading Case. . . . .	III-30
b.	Biased Heading Case . . . . .	III-30
c.	Random Velocity Component Case. . . . .	III-35
7.	Sub-Optimal Sonobuoy Drop Point Determination. . . . .	III-40
8.	Analog/Hybrid Computer Program . . . . .	III-41
9.	Possible Search Director Display Techniques. . . . .	III-44

TABLE OF CONTENTS (Continued)

<u>SECTION</u>	<u>TITLE</u>	<u>PAGE NO.</u>
IV.	GENERAL STUDY RESULTS. . . . .	IV-1
	1. Comparison of Sample Results for Exact Solution and Monte Carlo Program . . . . .	IV-1
	2. Effect of Varying Start Grid Size. . . . .	IV-1
	3. Effect of Varying the Variance in Target Heading. . . . .	IV-6
	4. Effect of Varying the Variance in Target Velocity. . . . .	IV-8
	5. Effect of Varying the Number of MC Submarines/Start Grid. . . . .	IV-10
	6. Effect of Varying Search Aircraft Time Late in Arriving at Datum . . . . .	IV-12
	7. Effect of Varying ASW Aircraft Search Time .	IV-14
	8. Effect of Linear Smoothing Between Grid Points . . . . .	IV-16
	9. Effect of a Large Variation in Number of MC Submarines/Grid For a Uniform Target Heading and Rayleigh Distribution in Velocity . . . . .	IV-19
	10. Effect of Changes in Target Velocity on Probability of Detection . . . . .	IV-19
	11. Effect of Variance of Variations in Target's Velocity . . . . .	IV-22
	12. Effect of Biasing Target Heading . . . . .	IV-24
	13. Accumulated Probability Density of Target Position with Search Time. . . . .	IV-26
V.	APPENDIX A: CAL FLYING SPOT SCANNER . . . . .	A-1

LIST OF FIGURES

<u>FIGURE NO.</u>	<u>TITLE</u>	<u>PAGE NO.</u>
2-1	Operational Employment of Search Director. . . . .	II-5
3-1	Effect of Target Motion on Probability Density Map Geometry . . . . .	III-3
3-2	Effect of Deploying an Acoustic Sensor on Probability Density Map Geometry . . . . .	III-5
3-3	Distribution of a Moving Target: X and Y Velocities are $N(0,1)$ . . . . .	III-12
3-4	Distribution of a Moving Target With Known Constant Velocity and Uniform Heading: Random Walk . . . . .	III-18
3-5	Distribution of a Moving Target When X and Y Velocity Components are $N(0,1)$ : Random Walk. . . . .	III-19
3-6	Probability Density of Submarine's Position With Known Constant Velocity and Uniform Heading: Method I . . . . .	III-22
3-7	Probability Density of Submarine's Position With Known Constant Velocity and Uniform Heading: Method II. . . . .	III-23
3-8	Probability Density of Submarine's Position With Known Constant Velocity and Uniform Heading: Method III . . . . .	III-24
3-9	Probability Density of Submarine's Position With Rayleigh Distribution of Velocity and Uniform Heading: Method I . . . . .	III-25
3-10	Probability Density of Submarine's Position With Rayleigh Distribution of Velocity and Uniform Heading: Method II. . . . .	III-26
3-11	Probability Density of Submarine's Position With Rayleigh Distribution of Velocity and Uniform Heading: Method III . . . . .	III-27

LIST OF FIGURES (Continued)

<u>FIGURE NO.</u>	<u>TITLE</u>	<u>PAGE NO.</u>
3-12	Distribution of a Moving Target With Constant Velocity and Uniform Heading: For Two Methods of Assigning Velocity Components of MC Submarines. . .	III-32
3-13	Probability Density of Submarine's Position With Constant Velocity and Random Heading: For Two Methods of Assigning Velocity Components of MC Submarines . . . . .	III-34
3-14	Probability Density of Submarine's Position With Rayleigh Distribution in Velocity and Uniform Heading: For Two Methods of Assigning Velocity Components to MC Submarines. . . . .	III-38
3-15	Probability Density of Submarine's Position With Rayleigh Distribution in Velocity and Uniform Heading: For Two Variations in Number of MC Submarines/Grid. . . . .	III-39
3-16	Accumulated Probability Density of Submarines Position With Known Constant Velocity and Uniform Heading: Effect of Correction Factor. . . . .	III-42
3-17	CRT Display of Probability Density of Submarines Position With Known Constant Velocity and Uniform Heading: Utilizing Analog Computer. . . . .	III-43
3-18	CRT Display Techniques of the Probability Density Map. . . . .	III-45
3-19	Gray Scale for Black and White Photographs . . . . .	III-46
3-20	Flying Spot Scanner Display of Probability Density Map: Example 1. . . . .	III-48
3-21	Flying Spot Scanner Display of Probability Density Map: Example 2. . . . .	III-49
3-22	Flying Spot Scanner Display of Probability Density Map: Example 3. . . . .	III-50
3-23	Flying Spot Scanner Display of Probability Density Map: Example 4. . . . .	III-51

LIST OF FIGURES (Continued)

<u>FIGURE NO.</u>	<u>TITLE</u>	<u>PAGE NO.</u>
3-24	Flying Spot Scanner Display of Probability Density Map: Example 5. . . . .	III-52
3-25	Flying Spot Scanner Display of Probability Density Map: Example 6. . . . .	III-54
3-26	Flying Spot Scanner Display of Probability Density Map: Example 7. . . . .	III-55
3-27	Probability Density Contour Map of Submarine's Position With Known Constant Velocity and Uniform Heading: Elapsed Time = 0 Units . . . . .	III-56
3-28	Probability Density Contour Map of Submarine's Position With Known Constant Velocity and Uniform Heading: Elapsed Time = 1 Unit. . . . .	III-57
3-29	Probability Density Contour Map of Submarine's Position With Known Constant Velocity and Uniform Heading: Elapsed Time = 2 Units . . . . .	III-58
4-1	Probability Density of Submarine's Position With Rayleigh Distribution in Velocity and Uniform Heading: Exact Computational Method . . . . .	IV-2
4-2	Probability Density of Submarine's Position With Rayleigh Distribution in Velocity and Uniform Heading: Monte Carlo Method . . . . .	IV-3
4-3	Probability Density of Submarine's Position With Known Constant Velocity and Uniform Heading: For Variations in Start Grid Size. . . . .	IV-4
4-4	Probability Density of Submarine's Position With Rayleigh Distribution in Velocity and Uniform Heading: For Variations in Start Grid Size. . . . .	IV-5
4-5	Probability Density of Submarine's Position With Random Velocity and Heading: For Variance Variations in Heading Distribution . . . . .	IV-7
4-6	Probability Density of Submarine's Position With Random Velocity and Uniform Heading: For Variance Variations in Velocity Distribution. . . . .	IV-9

LIST OF FIGURES (Continued)

<u>FIGURE NO.</u>	<u>TITLE</u>	<u>PAGE NO.</u>
4-7	Probability Density of Submarine's Position With Known Constant Velocity and Uniform Heading: For Variation in Number of MC Submarines/Grid. . . . .	IV-11
4-8	Probability Density of Submarine's Position With X and Y Velocity Components Normally Distributed: Effect of Time Late. . . . .	IV-15
4-9	Probability Density of Submarine's Position With X and Y Velocity Components Normally Distributed: For Selected Search Times. . . . .	IV-15
4-10	Probability Density of Submarine's Position With Known Medium Velocity and Uniform Heading: Effect of Linear Smoothing Between Calculated Grid Points . . .	IV-17
4-11	Probability Density of Submarine's Position With Known High Velocity and Uniform Heading: Effect of Linear Smoothing Between Calculated Grid Points. . . .	IV-18
4-12	Probability Density of Submarine's Position With Rayleigh Distribution in Velocity and Uniform Heading: For Variation in Number of MC Submarines/Grid. . . . .	IV-20
4-13	Probability of Submarine's Position With Rayleigh Distribution in Velocity and Uniform Heading: Effect of PM Grid as a Function of Target's Velocity .	IV-21
4-14	Probability Density of Submarine's Position With X and Y Velocity Components Normally Distributed: For Variance Variations in Velocity. . . . .	IV-23
4-15	Probability Density of Submarine's Position With X and Y Velocity Components Normally Distributed: Effect of Biased Heading . . . . .	IV-25
4-16	Accumulated Probability Density of Submarine's Position With Known Constant Velocity and Random Heading: No Sonobuoys Deployed. . . . .	IV-27
4-17	Accumulated Probability Density of Submarine's Position With Known Constant Velocity and Random Heading: One Sonobuoy Deployed. . . . .	IV-28

LIST OF FIGURES (Continued)

<u>FIGURE NO.</u>	<u>TITLE</u>	<u>PAGE NO.</u>
4-18	Accumulated Probability Density of Submarine's Position With Known Constant Velocity and Uniform Heading Between 0 and $\pi/2$ : No Sonobuoys Deployed. . . . .	IV-29

LIST OF TABLES

<u>TABLE NO.</u>	<u>TITLE</u>	<u>PAGE NO.</u>
3-1	Probability Density Levels for Zero and One Unit of Elapsed Time . . . . .	III-59
3-2	Probability Density Levels for Two Units of Elapsed Time . . . . .	III-59



# I. SUMMARY, CONCLUSIONS AND RECOMMENDATIONS

## A. STUDY SUMMARY

### 1. Purpose

This report summarizes the significant results achieved in an exploratory study to determine the feasibility and applicability of a Search Director concept for use by ASW aircraft crews in determining optimal search tactics and deployment of sonobuoys to detect and localize target submarines. Imprecise target information from acoustic sensor surveillance systems create problems in successfully conducting these operations. The purpose, therefore, of the Search Director is to:

- a. Assemble this information in terms of estimated target heading, motion, initial size and orientation of the target uncertainty area, time late, growth of the uncertainty area, ASW aircraft search time, etc. into coherent and readily computer-processed forms,
- b. Analyze, process and update this information, and
- c. Provide the Tactical Airborne Control and Coordination Officer (TACCO) with a dynamic probability density map display of the target's location.

Probability density functions are employed as a measure of the uncertainty of the exact location of the target and its speed and heading. These probability density distributions also provide measures for estimating the growth of the uncertainty area with time.

The Search Director principle makes use of negative information that the target has not been detected up to the present time by deployed

sonobuoys. As areas covered within the overall target uncertainty area by each of the sonobuoys are searched and the target remains undetected, the probability that the target is in the searched area decreases whereas the probability that it is elsewhere in unsearched areas increases. A dynamic display of this probability density pattern over the expanding uncertainty area shows where the target might be at any particular time (highest probability density) and indicates where the next sonobuoys should be dropped. The TACCO can utilize the Search Director to examine various trial sonobuoy patterns and monitoring schedules on a real or accelerated time basis and select the most efficient sonobuoy patterns prior to actual deployment of the sonobuoys.

In order to accomplish previously stated objectives, it has been necessary in this study to:

- a. Determine the mathematical formulations required for developing computer software programs to achieve this capability,
- b. Program these mathematical formulations for use on computers, and
- c. Demonstrate the feasibility and applicability of employing the concept on a real and accelerated time basis by dynamic presentation of results on displays and hard copy.

2. Approach

a. Analysis

Basic mathematical relationships which underly the target uncertainty area probability density maps are developed. These include analytical procedures for determining initial target uncertainty area

probability density maps. Also included are subsequent growth factors and changes in these maps with elapsed time for differing inputs on target motion and effects caused by the inclusion of various patterns and numbers of sonobuoys. A computer program incorporating these relationships and procedures is developed for use in determining and displaying exact solutions for various tactical situations. A Monte Carlo computer program is also developed utilizing various algorithms formulated from the basic mathematical relationships. The purpose of this program is to substantially reduce computing time and core storage requirements while maintaining output results that closely approximate those for exact solutions.

The feasibility and applicability of the Search Director concept are demonstrated utilizing additional computer programming, the CAL Flying Spot Scanner and a large CRT to dynamically display the probability density maps. An analog/hybrid computer system, program and CRT are also utilized to obtain and display these maps. Additional subroutines are formulated as adjuncts to the Monte Carlo computer program for use in determining sub-optimal sonobuoy drop-point patterns. Several techniques are investigated and compared for displaying the probability density maps on a CRT in various shades of gray or color. Two computer programs have been formulated to generate the map displays as hard copy on paper.

b. Tactical Cases Analyzed

A comparison is made of distribution results from the Monte Carlo computer program with those from the Exact Solution program for an example problem. Three methods are analyzed and results are compared for inserting a field of sonobuoys into the Monte Carlo program. Mathematical analyses are presented for development of the start and end grids and the Probability-of-miss (PM) grid.

Three methods are analyzed for assigning velocity components to Monte Carlo (MC) submarines. Method I utilizes a random number generator. Method II utilizes equally spaced headings of MC submarines between 0 and  $2\pi$ , whereas in Method III the headings are spaced at equal probability increments between 0 and  $2\pi$ . A comparison is made of distribution results from the Monte Carlo program utilizing Methods I and II.

A biased heading tactical situation is analyzed in which the target submarine's velocity is known and its heading is a random variable which is described by a probability distribution. A comparison for this case is made utilizing Method II (equally spaced headings) and Method III (equal probability heading increments).

A tactical situation is analyzed in which the target submarine's velocity is a random variable. Random number generator and expected value techniques are utilized in assigning velocity components to MC submarines. Computer results are compared for a Rayleigh distribution in velocity and uniform heading utilizing the random number generator and expected value methods with the exact solution. Additional results are compared using the expected value method in the first case where the number of MC submarines assigned to each sampled velocity is small and in the second case where it is large.

A subroutine has been added to the Monte Carlo computer program for use as a possible improved aid in determining sub-optimal sonobuoy drop points. A correction factor has been added to the program to overcome a problem caused by the use of a rectangular coordinate system. Sample computer results are compared without and with the use of this factor.

In a sensitivity analysis, computer results are compared for changes in the probability density maps caused by variation of the input values of the principal parameters. These include the effects of varying the following:

- (1) Start grid size,
- (2) Variance in target submarine heading and velocity,
- (3) Number of MC submarines per start grid,
- (4) Search aircraft time late in arriving at datum,
- (5) ASW aircraft search time,
- (6) Number of MC submarines assigned per grid for a uniform target heading and a Rayleigh distribution in velocity, and
- (7) Target velocity on probability of detection.

Also compared are the effects of linear smoothing between grid points, biasing target submarine heading and accumulated probability density of target position with search time.

### 3. Principal Results

Two computer programs have been developed toward implementation of the Search Director Concept.

- a. Exact Solution computer program, and
- b. Monte Carlo computer program.

#### Comparison of Monte Carlo Program With Exact Solution Results

Probability density distributions obtained utilizing the Monte Carlo method closely approximate those obtained from the exact solution method. The Monte Carlo computer program has considerably less run time for specified tactical situations than the Exact Solution computer program (see Section III, page III-11).

A comparison of sample results from the exact solution and the Monte Carlo computer program indicates that the similarity in probability density maps appears to be excellent. The computing time on the IBM 370/165 computer for the exact solution is 92 seconds compared to less than 2.5 seconds for the Monte Carlo program (see Section IV, page IV-1).

For a tactical situation in which the velocity of a target is known and its heading is uniformly distributed, a one-step random walk (change in target heading during a specified time interval) most closely approximates the exact solution distribution, whereas considerable deviation occurs for a 2-step and 4-step random walk. On the other hand, for a tactical situation in which the target velocity components have a normal distribution with zero mean and variance = 1, results for both a one and 4-step random walk closely approximate those for the exact solution (see Section III, page III-17).

#### Comparison of Methods for Inserting Sensors in Monte Carlo Program

Of three methods analyzed for inserting a field of sonobuoys into the Monte Carlo computer program, Method I provides the best results. In this method, "looks" by each sonobuoy are monitored at equal time increments so that one PM grid can be used for all sonobuoys and looks. A two dimensional grid is then calculated as a function of  $x$  and  $y$  offsets of the target from each sonobuoy (see Section III, page III-14).

The correction factor which has been applied to the subroutine for determining sub-optimal sonobuoy drop point determination appears to provide results which compare favorably with those which are expected. However, a complete analytical justification for this factor has not been made (see Section III, page III-40).

## Comparison of Methods for Assignment of Submarine Velocity Components in Monte Carlo Program

Of three methods analyzed for assigning velocity components to MC submarines, Method II is best. In this method MC submarine headings are equally spaced between 0 and  $2\pi$  and results correspond closely to those obtained from the exact solution. The results indicate that equally spaced headings allow the minimum number of MC submarines to be utilized in each grid. In Method III, the headings of the MC submarines are spaced at equal probability increments between 0 and  $2\pi$ . Results for the biased heading case indicate that Method II provides a better representation in the direction of the biased heading while equally spacing the MC submarines provides a better representation in headings of low probability (see Section III, page III-30).

The expected value method of assigning velocity components is much better than the random number generator method. Results indicate that the expected value method closely approximates those shown for the exact solution, whereas they deviate considerably utilizing the random number generator method (see Section III, page III-37).

## Monte Carlo Program Start Grid Size, Linear Smoothing and Submarine Assignment Considerations

It is important to limit the size of the start grid to the minimum required. Doubling the size of the grid increases the computer run time of the Monte Carlo program by more than a factor of four. The results indicate that a  $2\sigma$  bounding appears satisfactory for use in analyses. This encompasses approximately 90% of the probability density area describing the SPA (see Section IV, page IV-1).

The use of a linear smoothing technique can reduce computing time by a factor of approximately four for a specified size grid. Very little difference in probability density is shown on a display in comparing the case where smoothing is employed versus the case in which no smoothing is utilized (see Section IV, page IV-16).

It is important to limit the number of MC submarines assigned to each grid since computing time on the IBM 370/165 computer increases linearly as the number of MC submarines increases. For a probability density of submarines position with known constant velocity and uniform heading, the computing time for 40 submarines/grid is 4.1 seconds whereas it is 2.7 seconds for 24 submarines/grid. A similar case for a Rayleigh distribution in velocity and uniform heading requires 6.53 and 11.64 seconds respectively. These times are for the case in which the size of the start grid is determined by a  $2\sigma$  boundary. It appears that from 18 to 24 MC submarines/grid is sufficient to provide a good probability density map (see Section IV, page IV-10).

#### Analog/Hybrid Computer System

Results of the analog/hybrid computer system study to obtain probability density maps indicate that a general purpose (GP) computer could be used in conjunction with an Analog Computer (a Hybrid system). This system would use the G.P. Computer primarily for storage while the analog computer would be used to compute the probability density maps. A capability exists for the analog computer to pass the output grid through a non-linear amplifier. This technique provides a method for investigating the effects of intensifying the highest probability density levels on a CRT display (see Section III, page III-41).

#### Sensitivity Analysis Selected Results

Varying search aircraft time late in arriving at datum changes probability densities considerably as time late increases from 3 to 5 hours to



a maximum of 7 hours. The results for varying ASW aircraft search time indicate that the sonobuoys in effect search out an increasing portion of the SPA as search time and the number of "looks" by the sonobuoy field increases from 9 to 13 hours and from 8 to 24 "looks" respectively (see Section IV, page IV-12).

For a probability density of submarine's position with random velocity and heading, increasing the variance variation in heading distribution narrows the high probability density area from a circle to an increasingly narrower ellipse. For a probability density of submarine's position with random velocity and uniform heading, increasing the variance variation in velocity distribution spreads the high probability areas more toward datum than away from it (see Section IV, page IV-6).

A comparison of results of the effects of changes in target velocity on the probability of detection show the increased capability of the sonobuoys to detect the target submarine as its' speed increases beyond 9 knots. This is indicated by changes in the probability density in the second quadrant for the variable PM grid compared to that for the constant PM grid (see Section IV, page IV-19).

The effect of biasing target heading is to shift the high probability density area of probable target positions to a sector located outside the ring of deployed sonobuoys (see Section IV, page IV-24).

## B. CONCLUSIONS

The following principal conclusions are made based on results achieved in attaining the objectives and accomplishing the five major tasks of this study program:

1. An assessment of the principal findings of this study indicates that the Search Director concept is technically feasible and has general applicability for use by ASW personnel in determining optimum search patterns for detecting and localizing submarines.
2. Various simulated searches utilizing sonobuoys deployed in submarine target uncertainty areas have been successfully demonstrated on a real and accelerated time basis by visual display of the Search Director program computer output on a CRT, CAL Flying Spot Scanner and hard copy utilizing an IBM 370-model 165 computer printer in a strike-over process.
3. Based on limited research conducted during this study on various types of display presentations in shades of gray or color it is concluded that only a few levels of either gray or color may be necessary in operations required for determining optimum search patterns.
4. The computer printer strike-over process of printing a probability density map on paper appears to be an attractive and useful technique since the displayed results can be readily interpreted and understood by an operator. Such a display is particularly advantageous in vehicles where a CRT is not available.

5. Successful development and computer programming of both exact mathematical relationships and simplified algorithms (Monte Carlo program for computer application) have been achieved for use in determining (1) initial uncertainty area probability density distributions and redistributions due to growth of the area with time and differing assumptions of target motion, (2) redistributions of probability density of target location within the uncertainty area as a result of no detections (negative information) from emplaced sensors and (3) combinations of (1) and (2).
6. The small differences in probability density distributions obtained from the exact solution computer program versus those from the simplified Monte Carlo program are considered to be negligible and thus completely justify the use of the Monte Carlo program for the Search Director concept. By using the Monte Carlo program computer time can be reduced by up to a factor of 35 over that required for the exact solution computer program.
7. The present simplified computer program of approximately 16,000 words could be reduced to approximately 8000 words by utilizing half-word techniques. Additional reductions could be achieved by time sharing of some of the dimensional statements in the program. Thus, it is concluded that the smaller program could be accommodated and would not overload ASW computer systems such as that in the P3-C aircraft or the system being contemplated for the P3-C 1975 update program.
8. The use of negative information by the Search Director concept (i.e., the fact that deployed sonobuoys have not detected a target up to the present time) has a substantial

effect on redistribution of probability densities to unsearched portions of an uncertainty area and, therefore, on where additional sonobuoys should be emplaced in these areas.

9. Maximum use should be made of linear smoothing techniques between calculated points in the Monte Carlo computer program because (1) computing time can be substantially reduced by up to a factor of four and (2) very little if any differences (with or without smoothing) can be seen on probability density map displays.
10. If computer run time is a critical consideration in actual ASW operations, it is important to limit start grid size in the Monte Carlo program to only that required for the tactical situation at hand since a doubling of grid size, for example, increases run time by more than a factor of four.
11. It is important to limit the number of Monte Carlo submarines assigned to each grid in the program since computer time increases linearly with increases in the number of assigned submarines. Assigned values of from 18 to 24 submarine per grid are sufficient to provide high quality probability density maps.
12. In general, results of sensitivity analyses show that varying parameters such as time late to datum, submarine target speed and associated radiated noise, acoustic sensor detection capability, variances in target heading and velocity distributions, etc. can have a marked effect in changing probability density distributions with time, and, therefore, search tactics.

### C. RECOMMENDATIONS

The following recommendations are made as a result of the principal findings of this study:

1. In addition to the P3-C aircraft and P3-C 1975 update program an investigation should be made of the need for and desirability of utilizing the Search Director computer program and associated display in S3-A aircraft, and as a command and control tool by the shore commander, shore-based Tactical Support Centers and in surface ships that include CV's, LAMPS equipped destroyers and the Sea Control Ship.
2. Upon establishment of specific Navy needs for employing the Search Director computer software program and associated display in ASW operations, an investigation should be made to determine the compatability of the program with Navy ASW computer systems in terms of computer core storage limits, format, computer language etc.
3. Utilizing results of the above investigation as a basis, conduct analyses to make required (1) improvements and extensions to the Search Director computer program, (2) reductions in program size and (3) revisions to program in terms of computer language, format etc.
4. Formulate a test program and conduct an at-sea experimental evaluation of a prototype Search Director software computer program and display during ASW exercises.
5. During the interim, effort should be continued to (1) improve and expand the Search Director computer program and (2) determine a preferred method(s) for displaying results to an operator.

## II. INTRODUCTION

### A. BACKGROUND

In certain U. S. Navy ASW missions, a problem arises in searching for and locating a submarine target utilizing imprecise information concerning its position, speed, heading, etc. which is obtained initially from surveillance sensor systems. In order to increase the probability of success in search, detection and localization operations, some means are required to:

1. Assemble all available information (such as target submarine heading, motion, position fix area of uncertainty and orientation, time late, growth of area of uncertainty, search time, etc.) into coherent and easily computer-processed forms,
2. Update the processed information as search and localization operations progress, and
3. Produce a pictorial representation of current and future status of search and localization operations associated with various tactical options which would be of assistance in conducting ASW missions.

The above situation occurs frequently in ASW search and localization, search and rescue, and other missions.

In attempting to accomplish these objectives a concept called the "Search Director" has evolved as the result of a number of ASW studies conducted at the Cornell Aeronautical Laboratory in which search and localization operations have been analyzed. This report presents results accomplished to date from an ongoing ONR study program that addresses the problems of performing these operations by an ASW aircraft in tactical situations where imprecise and limited information is available on a

submarine target's location and motion within a specified initial uncertainty area. It is expected that improved usage of all available information provided to ASW aircraft would increase the probability of successful search operations in terms of initial detection of a submarine by sonobuoys which are dropped in a prescribed pattern in an uncertainty area. The sonobuoys drop points would be determined on the basis of information displayed by the Search Director.

The operations performed by an ASW aircraft as assisted by a Search Director are depicted graphically in Figure 2-1. The purpose of the Search Director is to assemble all the available information (such as initial area of uncertainty (SPA), target speed and heading, the aircraft's time late and the search time, etc.) into a coherent form, analyze this information, and provide the TACCO with a probability density map display of the submarine's location. Probability density functions are used as a measure of the uncertainty of the true location of the target, and its speed and heading. These distributions provide estimated growth factors of the uncertainty areas with time. At each stage of the search operation, the associated map display is indicated as shown on Figure 2-1. Also shown are the target parameter inputs which determine the characteristics of the map displays associated with particular tactical situations.

The probability maps are displayed on a video display screen. Changes in the search situation due to the passage of time, the introduction of aircraft sensors, and changes in target motion cause probability density levels (light intensities) to change on the displayed maps. The maps may be projected into future time to further assist the TACCO in conducting an effective search.

In estimating the probability density map of the submarine target's location, the Search Director principle makes use of negative information that the target has not been detected up to the present time by any of the deployed sonobuoys. As areas covered by each of the sonobuoys are searched and the target is undetected, the probability that the target is in the

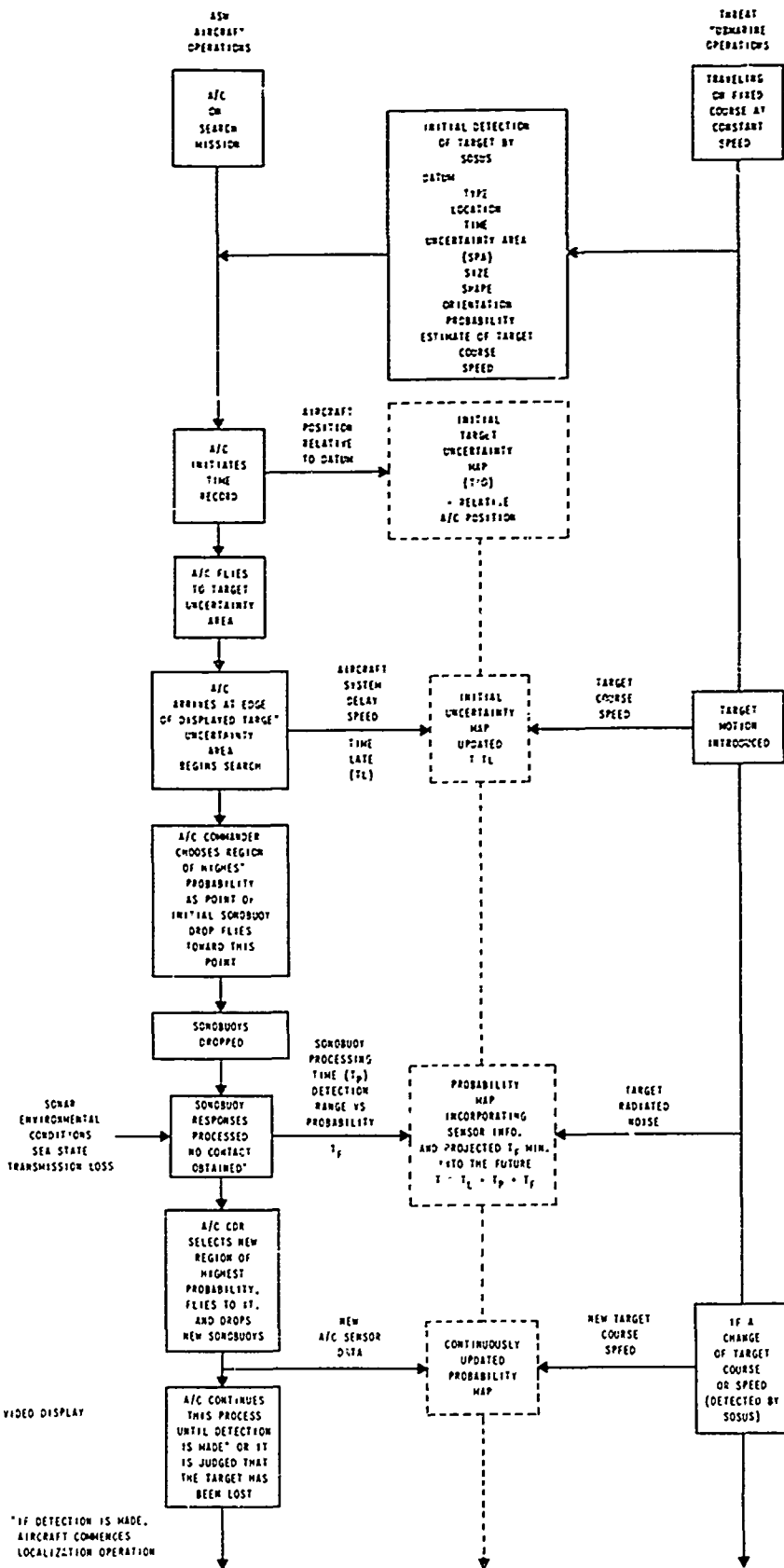


Figure 2-1 OPERATIONAL EMPLOYMENT OF SEARCH DIRECTOR



searched area decreases and the probability that the target is elsewhere in unsearched areas increases. A dynamic display of this changing probability density pattern over the expanding area of uncertainty shows the areas of highest probability where the submarine might be at any particular time and, therefore, indicates where the next sonobuoys should be dropped. The TACCO can, therefore, examine various trial sonobuoy patterns and monitoring schedules on an accelerated time basis and select the most efficient sonobuoy patterns prior to actual deployment of the sonobuoys.

In summary, it is believed that a Search Director could be effectively used to assist the TACCO of an ASW aircraft in determining optimum search patterns to be used in detecting and localizing target submarines. A probabilistic process utilizing Bayesian statistics would be employed to compute and display on a real-time or accelerated time basis those areas which are most likely to contain the target. This information would assist the TACCO in formulating logical tactics and search patterns in attempting to detect and localize a submarine. Continuous updating of the displayed information would permit (1) real-time evaluation of the effect of selected tactics and search patterns on detection and localization operations and (2) changes in tactics and search patterns accordingly as results are displayed.

Thus, a Search Director could provide a continuously updated visual display of those areas having the highest probability of containing the target. The TACCO can observe these changing probability densities as they develop, and modify his search pattern (and/or the operational mode of his sensors) to search out the most fruitful areas. Once having detected a target Search Director operations would cease and localization operations would then be initiated.

Application of the Search Director as presented in this report has centered around its potential use in P3-C ASW aircraft or an updated 1975 version of the P3-C. This selection has been made primarily for illustrative purposes in order to provide a means for detailed discussion of how it could

be employed in ASW search operations. Other potential applications include its use by S3-A ASW aircraft and as a command and control tool by Navy ASW shore commanders, ASW tactical support centers (TSC) or at sea in surface ships such as ASW support carriers (CV's), LAMPS equipped destroyers and the Sea Control ship.

The Search Director could be used in S3-A's in a manner similar to that described in this report for P3-C's. On the other hand, information from a Search Director located in the ASW command and control center on a CV could be transmitted to S3-A's and displayed for use by crews in the aircraft. In a manner similar to the latter case Search Director information could be used by helicopters deployed from destroyers or Sea Control ships to carry out ASW search operations.

The Search Director could also be utilized by ASW shore commanders, TSC's, and ship command and control centers in planning ASW search operations, allocation of available forces, and command, control and coordination of single and multiple vehicle operations. In other applications the Search Director could be employed in TSC's to provide information that would be transmitted to P3-C's. In addition, it could also be used as a tool at TSC's in post-operational analysis of ASW missions and in training crews in ASW search tactics and operations.

## B. STUDY OBJECTIVES AND SCOPE

The principal objective of this study is to conduct an exploratory investigation of the feasibility and applicability of the Search Director concept for use by U.S. Navy ASW personnel in determining optimal search tactics and sonobuoy drop patterns for detection and initial coarse localization of target submarines. In order to accomplish this objective it is necessary to (1) determine the mathematical formulations that are required for computer software programs to achieve this capability, (2) program the mathematical formulations for use on computers and (3) demonstrate the feasibility and applicability of employing the concept on a real and accelerated time basis by dynamic presentation of results on displays and hard copy.

The scope of this study and analytical approach are to determine the basic mathematical relationships which underly the target uncertainty area probability density maps. These include analytical procedures for determining initial target uncertainty area probability density maps, subsequent growth and changes in these maps with elapsed time for differing assumptions of target motion, and effects caused by inclusion of various patterns and numbers of sonobuoys. A computer program incorporating these relationships and procedures developed for use in determining and displaying "exact" solutions for various ASW tactical situations.

In a subsequent effort the above relationships and procedures are modified and/or simplified for use in the development of a Monte Carlo computer program. The purpose in developing this program is to substantially reduce computing time and core storage requirements while maintaining output results that closely approximate those obtained from the Exact Solution computer program. Sample results for identical ASW tactical situations and associated variations in the values of key input parameters are compared utilizing these programs.

The feasibility and applicability of the Search Director concept are demonstrated utilizing additional computer programming, the CAL Flying Spot Scanner and a large CRT to dynamically display the target uncertainty area probability density maps. Limited efforts are also conducted to (1) determine the feasibility of this concept using an analog/hybrid computer system and large CRT to obtain and display these maps and (2) formulate subroutines to the Monte Carlo computer program for use as an aid to the TACCO in determining sub-optimal sonobuoy drop point patterns.

Several techniques are investigated and compared for displaying the probability density maps on a CRT. In one technique the amount of fill-in is varied between calculated points in which the probability levels are indicated by both the intensity of the points and their size. In a second technique the number of shades of gray presented on a display are varied from a few levels up to a maximum of 61 levels on the gray scale where each shade is coded to represent a specified probability level (interval). A third technique examined is similar to the second technique except that the various colors are used to represent the probability levels.

Two computer programs are also formulated to generate probability density map displays as hard copy on paper. One program utilizes a computer printer in an over-striking process of various letters and symbols to print out the maps. A second computer program utilizes a Houston plotter to draw the maps as a series of contour lines representing the various iso-probability density levels.

### III. STUDY ANALYSES AND RESULTS

#### A. BASIC MATHEMATICAL RELATIONSHIPS UNDERLYING TARGET UNCERTAINTY AREA PROBABILITY DENSITY MAPS

##### 1. Initial Target Uncertainty Area Probability Density Map

In airborne search and localization operations the problem arises of locating a submarine target within an area of uncertainty such as provided by the Sound Surveillance System (SOSUS). This area is known as a SOSUS probability area (SPA). One approach in analyzing this problem is to interpret the uncertainties which arise in these tactical situations in probabilistic terms. This approach suggests the development of uncertainty area probability density maps to indicate those portions of the total area which have the highest probability of containing the target. The first step in this development is to determine the basic mathematical relationships in terms of probability functions which underly these maps. In developing these relationships consideration must be given to:

- a. Probability density map of the initial uncertainty area
- b. Probability density maps of the growth of the initial uncertainty area with elapsed time as functions of time late to datum, target motion and the deployment of acoustic sensors within the area by the ASW aircraft.

In developing the probability density map of an initial target uncertainty area  $A$ , it's size, shape, orientation, location and datum must be known. In addition, the kind of probability density function which best describes the probable location within the area, e.g.,  $f(x, y)$  must be specified. It should be noted that the function  $f(x, y) dx dy$  is the conditional probability that the target is located at coordinates  $x, y$  within the area  $A$ , given that the target is located within the area  $A$ .

Having this information the incremental probabilities can be computed for use in developing an initial probability density map.

## 2. Effect of Target Motion on Probability Density Map Versus Time

Subject to the constraints on target motion imposed by a particular tactical situation, probability densities are chosen which are reasonable approximations of the target's probable actual motion. In developing these mathematical relationships it is assumed that submarine target velocity and heading remain constant during the search operation unless otherwise specified. Let  $g_1(v) \Delta v, g_2(\phi) \Delta \phi$  denote the probabilities that the target's velocity has values in  $(v, v + \Delta v)$  and its track heading has values in  $(\phi, \phi + \Delta \phi)$ .

The first step is to compute  $P_t(u, v) \Delta u \Delta v$  the probability that the target is in  $(u, u + \Delta u) \times (v, v + \Delta v)$  at time  $t$ . Referring to Figure 3-1, then  $P_t$  is given by:

$$P_t(u, v) \Delta u \Delta v = \sum_{(x, y) \in A_t(u, v)} P[\text{target moves from } (x, y) \text{ to } (u, v) \text{ in time } t] \\ \cdot P[\text{target initially at } (x, y)]$$

where the summation is made over all points  $(x, y)$  from which transit to  $(u, v)$  in time  $t$  is possible as denoted by  $A_t(u, v)$ .

$$(*) P_t(u, v) \Delta u \Delta v = \sum_{(x, y) \in A_t(u, v)} \frac{1}{t} g_1(\rho/t) \cdot g_2(\phi) \frac{1}{\rho} f(x, y) \Delta x \Delta y \Delta u \Delta v$$

where

$$vt = \rho = [(u-x)^2 + (v-y)^2]^{1/2}, \quad \phi = \tan^{-1} \left( \frac{v-y}{u-x} \right)$$

This representation is valid for any time  $t$ , subject to the same initial distributions on submarine target location, track heading and speed described above.

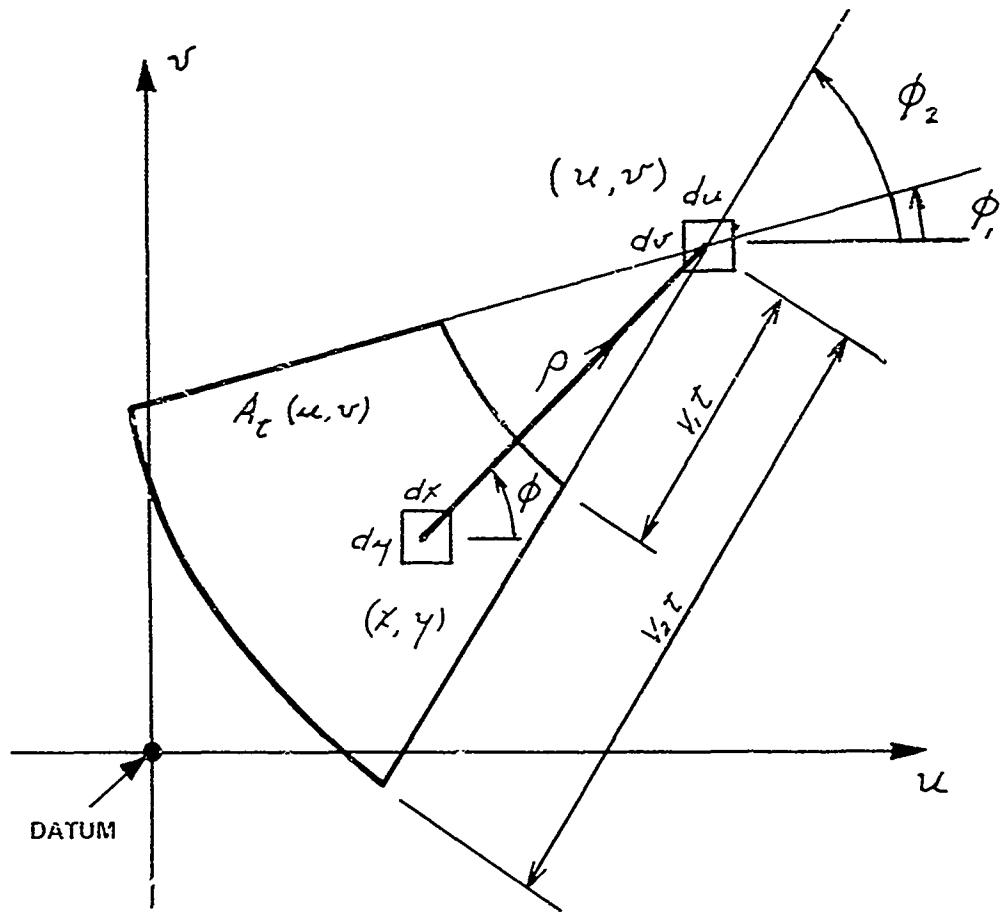


Figure 3-1 EFFECT OF TARGET MOTION ON PROBABILITY DENSITY MAP GEOMETRY

### 3. Acoustic Sensor Employment Effects on Probability Density Map

The next step is to compute the probability density map for time  $t_2$  ( $t_2 > t_1$ ) given that an acoustic sensor has been placed at  $(x, y)_s$  at time  $t_1$ , as shown in Figure 3-2 and has failed to detect the target.

Let  $G(R)$  be the probability of detection by the sensor as a function of range. No deviation in the target's motion is assumed from time  $t=0$  to time  $t=t_2$ . If the target's location at  $t=0$  is  $(x, y)$  and at  $t=t_2$  it is  $(u, v)$  then the target's location at  $t=t_1$  is given by:

$$(u', v') = \left( x + \frac{t_1}{t_2}(u-x), y + \frac{t_1}{t_2}(v-y) \right)$$

This means that the target is just the fraction  $t_1/t_2$  of the way between  $(x, y)$  and  $(u, v)$ . Thus, the probability of the target being at  $(u, v)$  at time  $t_2$  given that no detection has taken place at time  $t_1$  is given by:

$$\begin{aligned} & P_{t_2} [u, v \mid \text{no detection at } t_1] \\ &= P[\text{target is at } (u, v) \text{ at time } t_2 \text{ with no detection at time } t_1] \\ &\div P[\text{no detection at time } t_1] \\ &= \sum_{(x,y) \in A_{t_2}(u,v)} P[\text{target moves from } (x, y) \text{ to } (u, v) \text{ in time } t_2] \\ &\quad *P[\text{target not detected at time } t_1 \text{ while at } (u', v') \text{ and in} \\ &\quad \text{transit from } (x, y) \text{ to } (u, v)] \\ &\quad *P[\text{target at } (x, y) \text{ initially}] \\ &\quad \text{divided by} \\ &\sum_{\text{all}(x,y)} P[\text{target not detected at time } t_1, \text{ given that the target is} \\ &\quad \text{at } (x, y) \text{ at time } t_1] \\ &\quad *P[\text{target is at } (x, y) \text{ at time } t_1] \end{aligned}$$



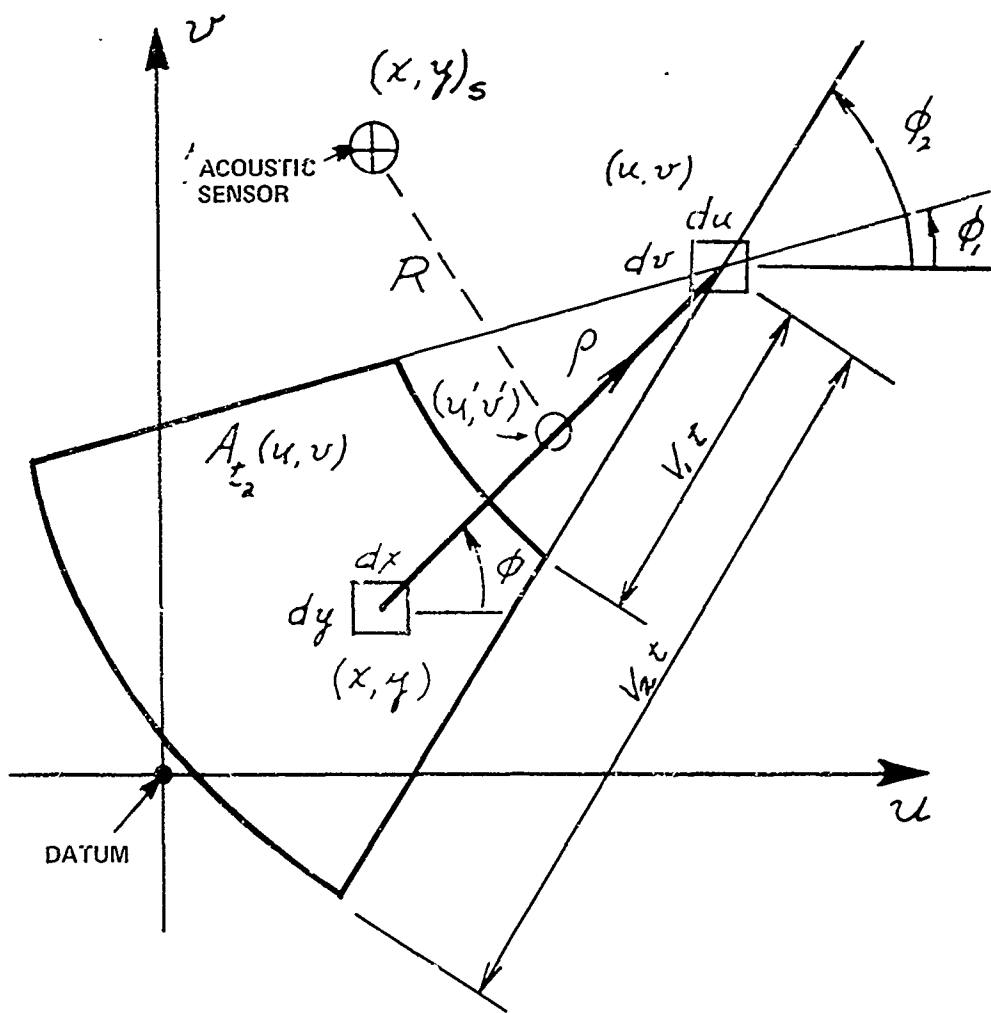


Figure 3-2 EFFECT OF DEPLOYING AN ACOUSTIC SENSOR ON PROBABILITY DENSITY MAP GEOMETRY

It should be noted that the division shown in the equation above is a constant which is independent of  $u, v$ . Therefore, it need not be calculated since its effect is to normalize the total area to unity.

If  $P_{t_1}(x, y) \Delta x \Delta y$  is the probability density map for time  $t_1$ , then

$$\begin{aligned}
 (**) \quad P_{t_2}(u, v) \Delta u \Delta v &= \sum_{A_{t_2}(u, v)} \frac{1}{t_2} g_1(\rho/t_2) g_2(\phi) [1 - G(R)] \frac{1}{\rho} f(x, y) \Delta x \Delta y \Delta u \Delta v \\
 &\div \sum_{\text{all}(x, y)} (1 - G(R)) P_{t_1}(x, y) \Delta x \Delta y,
 \end{aligned}$$

where  $A_{t_2}(u, v), \rho, \phi$  are defined as indicated previously, and  $R$  denotes the range from the target to the sensor. In the numerator, the range  $R$  is measured from the sensor at  $(x, y)_s$  to the point  $(u', v')$  described above. In the denominator, the range is measured from the sensor at  $(x, y)_s$  to the points  $(x, y)$  over which the summation is made.

The diagram shown previously in Figure 3-2 depicts the probability density map geometry at time  $t_2$  when the sensor is deployed at location  $(x, y)_s$  at time  $t_1$ .

If several acoustic sensors located at  $(x, y)_{s_1}, \dots, (x, y)_{s_n}$ , respectively, report failures to detect the target at time  $t_1$ , then  $(1 - G(R))$  is replaced by:

$$\prod_{k=1}^n (1 - G(R_k)) \text{ in the above expressions,}$$

where  $R_k$  is the range from the  $k$ 'th sensor to the point  $(u', v')$  or  $(x, y)$ , as described above.

#### a. Sensor Nondetection at Successive Time Increments

If an acoustic sensor fails to detect the target at several times past,  $t_1, \dots, t_m$  with the sensor placed at  $(x, y)_{s_1}^1, \dots, (x, y)_{s_m}^m$ , respectively, the expression for the uncertainty map probability  $P_{t_m}(u, v) \Delta u \Delta v$  is modified by replacing  $(1 - G(R))$  with  $\prod_{k=1}^m (1 - G(R^k))$  in the

numerator, and  $\sum (1-G(R)) P_{t_k} (x, y) \Delta x \Delta y$  with  $\prod_{k=1}^m (\sum (1-G(R^k)) \times P_{t_k} (x, y) \Delta x \Delta y)$  in the denominator of (\*\*). As stated before,  $R^k$  in the numerator is the distance from the sensor at time  $t_k$  to the point  $t_k/t$  of the way between  $(x, y)$  and  $(u, v)$ . In the denominator,  $R^k$  is the distance from the sensor to the point  $(x, y)$ .  $P_{t_k}$  denotes the probability density map generated for time  $t_k, k=1, \dots, m$ .

#### 4. Target Motion Changes at t

The probability densities associated with target motion,  $g_1(V)$  and  $g_2(\phi)$  are replaced by  $g_1^*(V)$ ,  $g_2^*(\phi)$  and  $f(x, y) \Delta x \Delta y$  is replaced by  $P_{t^*}(x, y) \Delta x \Delta y$  in (\*), with  $t^*$  denoting the new time datum.

#### 5. Target Location Probability Density Versus Time

Target location probability density  $g_t(u, v)$  at time  $t$  is derived as follows: Probability densities  $g_1(V)$ ,  $g_2(\phi)$  are given on target velocity and track heading. Also given is an initial target location density  $f(x, y)$ . The first step is to find the conditional probability

density of  $u, v$  given  $x, y$ . Letting  $\rho = Vt$ , the density of  $\rho$  is  $g_1(\frac{\rho}{t})$ . By measuring  $\rho$  and  $\phi$  with respect to the point  $x, y$ , one obtains:

$$g_t(\rho, \phi | x, y) = g_1\left(\frac{\rho}{t}\right) g_2(\phi)$$

By referring again to Figure 3-2, it is evident that the following relationships exist:

$$\begin{aligned} u &= x + \rho \cos \phi \\ v &= y + \rho \sin \phi \end{aligned}$$

Thus,

$$g_t(u, v, x, y) = \frac{1}{t} g_1(Vt) g_2(\phi) \frac{\partial(\rho, \phi)}{\partial(u, v)}$$

where

$$\rho = [(u-x)^2 + (v-y)^2]^{1/2}, \quad \phi = \tan^{-1} \left( \frac{v-y}{u-x} \right)$$

Here,

$$\frac{\partial(\rho, \phi)}{\partial(u, v)} = \frac{1}{\rho} \frac{\partial(u, v)}{\partial(\rho, \phi)} = \frac{1}{\rho} = \frac{1}{[(u-x)^2 + (v-y)^2]^{1/2}} \quad \text{is the Jacobian}$$

of  $\rho$ ,  $\phi$  with respect to  $u, v$  ( $x, y$  are considered to have fixed values in computing the conditional probability density).

Hence,

$$g_t(u, v | x, y) = \frac{1}{t} g_1 \left( \frac{1}{t} \left[ (u-x)^2 + (v-y)^2 \right]^{1/2} \right) g_2 \left( \tan^{-1} \left( \frac{v-y}{u-x} \right) \right) \frac{1}{\left[ (u-x)^2 + (v-y)^2 \right]^{1/2}}$$

Finally,

$$\begin{aligned} g_t(u, v) &= \iint g_t(u, v | x, y) f(x, y) dx dy \\ &= \iint_{A_t(u, v)} g_t(u, v | x, y) f(x, y) dx dy, \end{aligned}$$

where  $A_t(u, v)$  is the set of points  $(x, y)$  such that transit to  $(u, v)$  is possible under the constraints of  $g_1$  and  $g_2$ .

The equation for  $P_t(u, v) \Delta u \Delta v$  is an approximation to  $g_t(u, v) du dv$ .

## B. DESCRIPTION OF "EXACT" SOLUTION COMPUTER PROGRAM

### 1. Method of Determining Probability Density Map of Target Position With Time.

A computer program has been developed which closely models the exact mathematical relationships governing the Search Director concept. The principal approximation in this program is that the continuous probability densities are approximated by discrete functions. The program first divides the initial probability density area or SPA into  $N_x \times N_y$  grids and then calculates the probability of the target being in each  $\Delta x$  by  $\Delta y$  grid at time equal to zero when the target is initially detected by SOSUS and a SPA is formed. This probability is given by:

$$P_{i,j} = f(x_i, y_j) \Delta x \Delta y$$

where  $P_{i,j}$  is the probability of the target submarine starting in the  $i, j$  grid and  $f(x, y)$  is described by a joint circular normal probability density (SPA). The point  $x_i, y_j$  is at the center of a grid of size  $\Delta x$  by  $\Delta y$ .

From the estimates of the heading and velocity probability densities, four grids ( $V_B, B=1,2,3 \text{ or } 4$ ) are calculated for the probability of the target starting in grid  $i, j$  and going to grid  $m, n$  in time  $t$ . The four grids are calculated for the following constraints on  $i, j$  and  $m, n$ :

Grid 1	$m \geq i$ $n \geq j$
Grid 2	$m \geq i$ $n \leq j$
Grid 3	$m < i$ $n > j$
Grid 4	$m < i$ $n < j$

## 2. Method of Inserting Sonobuoy Field

The sonobuoy field is inserted into the computer model by first calculating a composite probability of miss grid for all the sonobuoys at each "look" interval. The position ( $k, l$ ) of the target going from grid  $i, j$  to  $m, n$  at the time of the ath look is given by:

$$k_a = i + \frac{T_a}{T}(m-i)$$

$$l_a = j + \frac{T_a}{T}(n-j)$$

Where  $T_a$  is the time of the ath look and  $T$  is the time for which the probability density is to be calculated. The above equations are valid for the assumption that a covert search operation is conducted and thus, target heading and speed remain constant. The composite probability of miss for a target starting in grid  $i, j$  and going to grid  $m, n$  is given by:

$$PM = \prod_{a=1}^{NLOOK} PM_a(k_a, l_a)$$

where  $NLOOK$  is equal to the number of discrete "looks" by the sonobuoy field and  $PM_a$  is the composite probability of miss grid for the ath look.

To find the probability of the target submarine being in the  $m, n$  grid at the update time  $T$ , the following operation is performed.

$$P \{m, n\} = \sum_i \sum_j V_B (m-i, n-j) \cdot \left( \prod_{a=1}^{N_{LOOK}} P M_a (k_a, l_a) \right) \cdot P_{i,j}$$

where  $V_B$  is the grid representing the velocity and heading distributions.

### C. DESCRIPTION OF MONTE CARLO COMPUTER PROGRAM

#### 1. Method of Determining Probability Density Map of Target Position With Time

Algorithms have been developed to "grow" the initial probability functions such that a general purpose computer can be used to provide probability density maps of target uncertainty areas on an accelerated time basis. One of these algorithms has been developed to grow the initial probability grid by a Monte Carlo (MC) method. The computer program solves the initial probability density distribution (SPA) in the same manner described previously for the exact solution. The initial distribution is assumed to be a joint normal distribution in which the  $x$  and  $y$  components are assumed to be independent but their variances need not be equal.

A number of Monte Carlo elements (MC submarines) are then placed in each  $\Delta x$  by  $\Delta y$  grid. The same number of MC submarines is inserted in each  $\Delta x$  by  $\Delta y$  grid. From the velocity and heading distribution,  $x$  and  $y$  components of velocity are assigned to the MC submarines. The same set of velocity components are used for the MC submarines in each  $\Delta x$  by  $\Delta y$  grid. A discussion of the method used in this model to obtain the velocity components is presented in Subsection C-6 of Section III of this report.

The computer program then converts the velocity components into the number of  $\Delta x$  by  $\Delta y$  grids in which the MC submarines move at the update time  $T$ . Knowing the MC subs starting grid and the number of grids that the MC submarines travel in the  $x$  and  $y$  direction, the coordinates of the MC submarines

end grid at the update time  $T$  may be found. A count is then performed on the number of MC submarines in each grid at the update time weighted by the probability of the MC submarine starting grid. This count is normalized by dividing by the number of MC submarines placed in each  $\Delta x$  by  $\Delta y$  start grid.

2. Comparison of Monte Carlo Computer Program Sample Results With Exact Solution For Initial Probability Density Distribution

Figure 3-3 presents results from a computer run from the Monte Carlo program together with those for the exact solution. The initial distribution (SPA) is a joint circular normal with a standard deviation of one ( $\sigma_{SPA} = 1$ ) for the  $x$  and  $y$  components. The velocity components ( $v_x, v_y$ ) were each generated from a  $N(0, 1)^*$  random number generator. The curve shown for the Monte Carlo method has been calculated for the time  $t=1$  and is a cross section of the joint distribution passing approximately through the mean of the distribution.

The curve shown for the exact solution is calculated in the following manner:

$$\text{Let } u = x + v_x t$$

$$v = y + v_y t$$

Hence,  $(u, v)$  gives the position of the target starting at  $x, y$  with velocity components  $(v_x, v_y)$  at the time  $t$ .

The random variables  $x$  and  $y$  are described by the distribution governing the SPA  $N(0, 1; 0, 1)^*$ , and  $v_x, v_y$  are also described by a joint normal.

The expected value of  $u(E\{u\})$  is given by

$$E\{u\} = E\{x + v_x t\}$$

$$= 0$$

\*The notation  $N(0, 1)$  denotes a normal distribution having 0 mean and variance = 1.

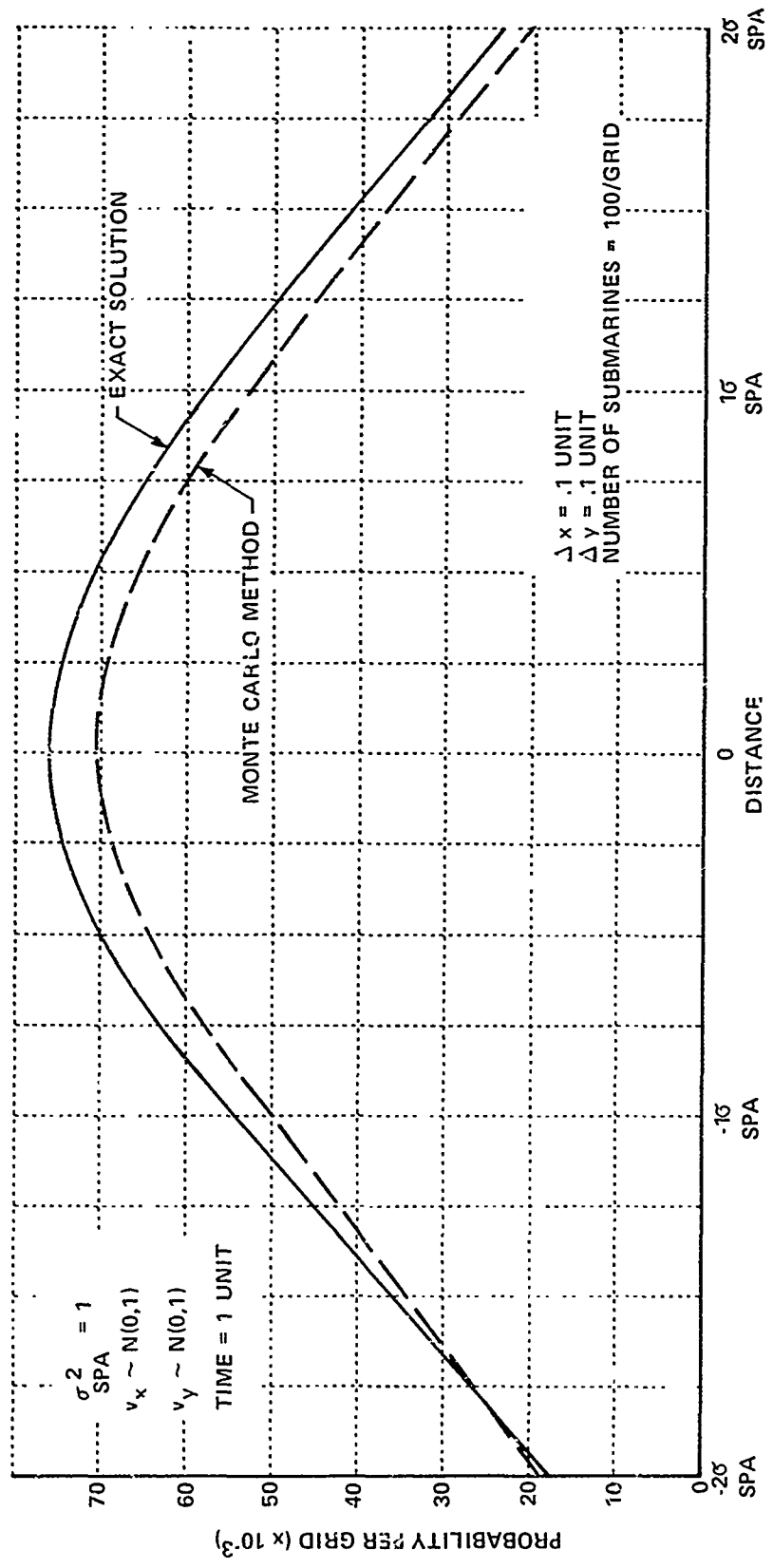


Figure 3-3 DISTRIBUTION OF A MOVING TARGET: X AND Y VELOCITIES ARE N(0, 1)



The variance of  $u$  ( $Var(u)$ ) is given by

$$\begin{aligned} Var\{u\} &= E\{x + v_x t\}^2 \\ &= E\{x^2 + 2xv_x t + v_x^2 t^2\} \\ &= E\{x^2\} + t^2 E\{v_x^2\} \\ &= \sigma_{SPA}^2 + t^2 \sigma_{v_x}^2 \end{aligned}$$

Since  $u$  is described by the sum of two normal random variables,  $u$  is also a normal random variable with a mean of zero and a variance equal to  $\sigma_{SPA}^2 + t^2 \sigma_{v_x}^2$ . The expected value of  $v$  is also zero and has a variance of  $\sigma_{SPA}^2 + t^2 \sigma_{v_y}^2$ .

A comparison of the two curves in Figure 3-3 indicates that the probability density distribution obtained utilizing the Monte Carlo Method closely approximates that obtained from the exact solution. The relatively small differences shown are negligible for CRT display of the probability densities as variations in light intensities. Thus, it is concluded that the Monte Carlo method which has considerably less run time requirements on the computer is the preferred technique to use.

### 3. Methods For Inserting Sonobuoy Field Into Monte Carlo Program

Three methods have been investigated to insert the sonobuoy field into the Monte Carlo program. It is assumed in each of these methods that the sonobuoy field searches the area in discrete "looks". This in effect assumes that the output stage of the signal processor is an integrator and that this output is sampled at the Nyquist rate. Also, it is assumed that all integrated outputs of the signal processors are sampled at the same rate and at the same time.

In all the results presented in this report, the probability that the sonobuoy detects the target at each of the discrete "looks" is assumed to be of the form:

$$PD = \exp\{-\alpha R^2\}$$

where  $R$  is the distance of the sonobuoy to the position of the target submarine at the time of the "look" and  $\alpha$  is an input to the model. This probability of detection curve is not a limiting factor in the model but is only used for convenience in analyses conducted during this study.

The concept of Search Director make use of the negative information that the target has not been detected which is given by  $1-PD$  and is denoted by  $PM$ .

a. Method I

In this method of inserting the sonobuoy field into the Monte Carlo program, the location of all the sonobuoys and the "looks" on each sonobuoy that have been monitored are put into machine storage. It is assumed that the "looks" by the individual sonobuoys are at equal increments of time so that one  $PM$  grid can be used for all sonobuoys and "looks". A two dimensional grid  $PM(i, j)$  is then calculated as a function of the  $x$  and  $y$  offsets of the target from the sonobuoy. A more detailed description of the probability of miss grid is presented in Subsection C-5 of Section III of this report. As an MC submarine moves from grid  $i, j$  to grid  $m, n$  the location of the MC submarine at each look by the sonobuoy field is calculated from the following relationship:

$$k_a = i + \frac{T_a}{T} (m-i)$$

$$l_a = j + \frac{T_a}{T} (n-j)$$

By knowing the position of the MC submarine at each "look", the distance of the MC submarine from each sonobuoy is calculated.

Utilizing the relationships above, the accumulated probability that an MC submarine remains undetected is calculated by the following relationship:

$$\overline{PM} = \prod_{i=1}^{NSONO} \prod_{j=1}^{NLOOK} pm_{ij}$$

where  $p_{m_{ij}}$  is the value taken from the  $PM$  grid to represent the probability that the  $i$ th sonobuoy does not detect the MC submarine on the  $j$ th look. Also,  $NSONO$  is the number of sonobuoys deployed and  $NLOOK$  is equal to the number of "looks" by the sonobuoy field. If the  $i$ th sonobuoy is not being monitored on the  $j$ th "look", then  $p_{m_{ij}} = 1$ . Having the value of  $\overline{PM}$ , the count of each MC submarine in grid  $m, n$  is weighted by  $P_{ij} \cdot \overline{PM}$ .

b. Method II

Assume that the initial probability density distribution of a SPA is given by:

$$f(x, y) = \frac{1}{2\pi\sigma_x\sigma_y} \exp \left\{ -\frac{1}{2} \left( \frac{x^2}{\sigma_x^2} + \frac{y^2}{\sigma_y^2} \right) \right\}$$

Let  $V(v, \theta)$  be the joint distribution describing the motion of the target. By making the following transformation:

$$v_x = v \cos(\theta)$$

$$v_y = v \sin(\theta)$$

the joint distribution,  $g(v_x, v_y)$ , of the velocity components is obtained.

Let the start grid of the submarine target be denoted by  $x_i, y_j$  and the end grid by  $x_m, x_n$  then the probability that the target moves a distance  $x_m - x_i$  in the  $x$  direction and  $y_n - y_j$  in the  $y$  direction in time  $t$  is given by:

$$g(v_x, v_y) \Delta v_x \Delta v_y = \frac{1}{t^2} g\left(\frac{x_m - x_i}{t}, \frac{y_n - y_j}{t}\right) \Delta x_m \Delta y_n$$

The probability of the submarine starting in the grid  $x_i, y_j$  is given by:

$$f(x_i, y_j) \Delta x_i \Delta y_j$$

Hence, the probability of the submarine being in the grid  $x_m, y_n$  at time  $t$  is obtained by summing over all possible starting grids:

$$h(x_m, y_n, t) \Delta x_m \Delta y_n = \frac{1}{t^2} \sum_i \sum_j f(x_i, y_j) g\left(\frac{x_m - x_i}{t}, \frac{y_n - y_j}{t}\right) \Delta x_i \Delta y_j \Delta x_m \Delta y_n$$

Assume that one "look" at the area is made by a field of sonobuoys and that the probability that the sonobuoy does not detect the target is given by:

$$PM(x_x - x_o, y_x - y_o)$$

where  $(x_x, y_x)$  denotes the location of the target and  $(x_o, y_o)$  the location of the sonobuoy.

The joint probability of the target starting in grid  $x_i, y_j$  and going to grid  $(x_m, y_n)$  and that the target is not detected is given by:

$$h(x_m, y_n, t) \Delta x_m \Delta y_n = \frac{K}{t^2} \sum_i \sum_j f \cdot g \cdot PM\left(x_i + \frac{t_1}{t}(x_m - x_i) - x_o, y_j + \frac{t_1}{t}(y_n - y_j) - y_o\right)$$

where  $t_1$  is the time of the "look",  $t$  is the time of the update and  $K$  is a normalizing constant.

At the time of the first "look",  $t_1 = t$ ,  $PM$  is not a function of the increments being summed over:

$$h(x_m, y_n, t=t_1) = PM \sum_i \sum_j f \cdot g$$

At the second look consider:

$$h(x_m, y_n, t=t_1 + \Delta t) = PM_2 \sum_i \sum_j n(x_i, y_i, t) \cdot g$$

The result of this method approximates the motion of the target as a random walk. That is, at each new time update the target is allowed to turn to a new heading governed by the heading probability density.

When no sonobuoys are deployed, the effect of utilizing the above method is that at the end of  $N$  steps of  $\Delta t$  length, the variance of the resultant probability distribution is proportional to:

$$\sum_{i=1}^N (\Delta t)^2$$

while the assumption that the target maintains a constant heading and velocity the desired variances is proportional to:

$$\left( \sum_{i=1}^N \Delta t \right)^2$$

One method of correcting this is to multiply the components of velocity by a constant at each step so that the resultant variance is equal to the desired variance. Thus, a series of constants,  $a_i$ , are chosen so that

$$\sum_{i=1}^N (a_i \Delta t)^2 = \left( \sum_{i=1}^N \Delta t \right)^2 \quad \text{for all values of } i$$

c. Sample Results Utilizing Method II

Sample results utilizing Method II are presented in Figures 3-4 and 3-5 for the case in which sonobuoys have not been deployed. Figure 3-4 shows results for a tactical situation in which the velocity of the target is known and its heading is uniformly distributed between 0 and  $2\pi$ . Curves I, II and III show a comparison of the probability density distribution of a moving target for a 1-step, 2-step and 4-step random walk (changes in target heading during a specified time interval) respectively. Curve II most closely approximates the exact distribution whereas, considerable deviation occurs for Curves I and III. Thus, it is concluded that a random walk of more than one step will alter the actual probability density map considerably.

Computer run results in which the target velocity components are  $N(0,1)$  are presented in Figure 3-5. Curves I and II show a comparison of the probability density of a moving target for a 4-step and 1-step random walk respectively with that computed for the exact solution. In both runs the velocity components of the MC submarines are multiplied by a constant at each step so that the variance is equal to the desired variance. On this basis, it is concluded that both Curves I and II closely approximate the curve for the exact solution.

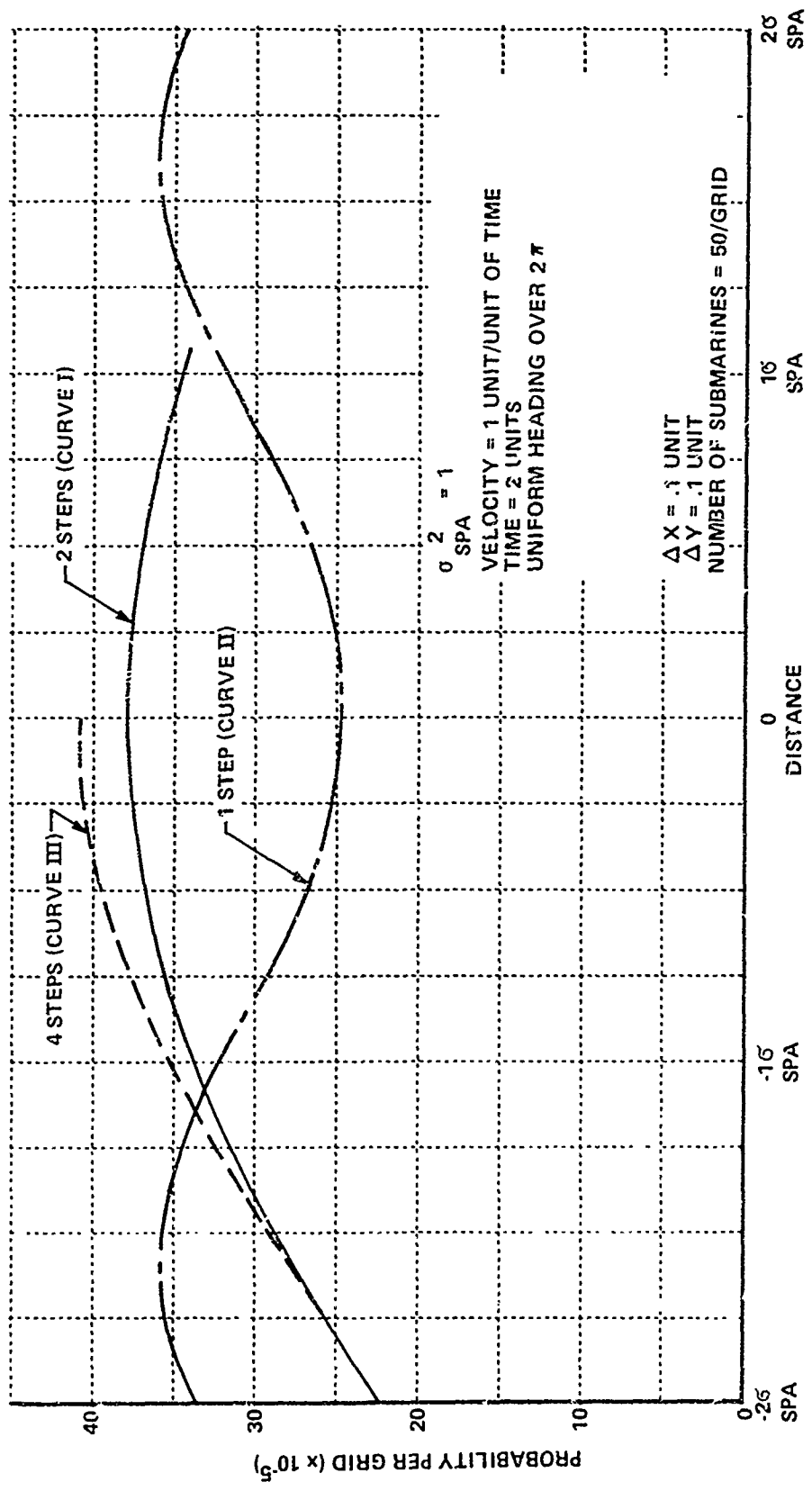


Figure 3-4 DISTRIBUTION OF A MOVING TARGET WITH KNOWN CONSTANT VELOCITY AND UNIFORM HEADING: RANDOM WALK

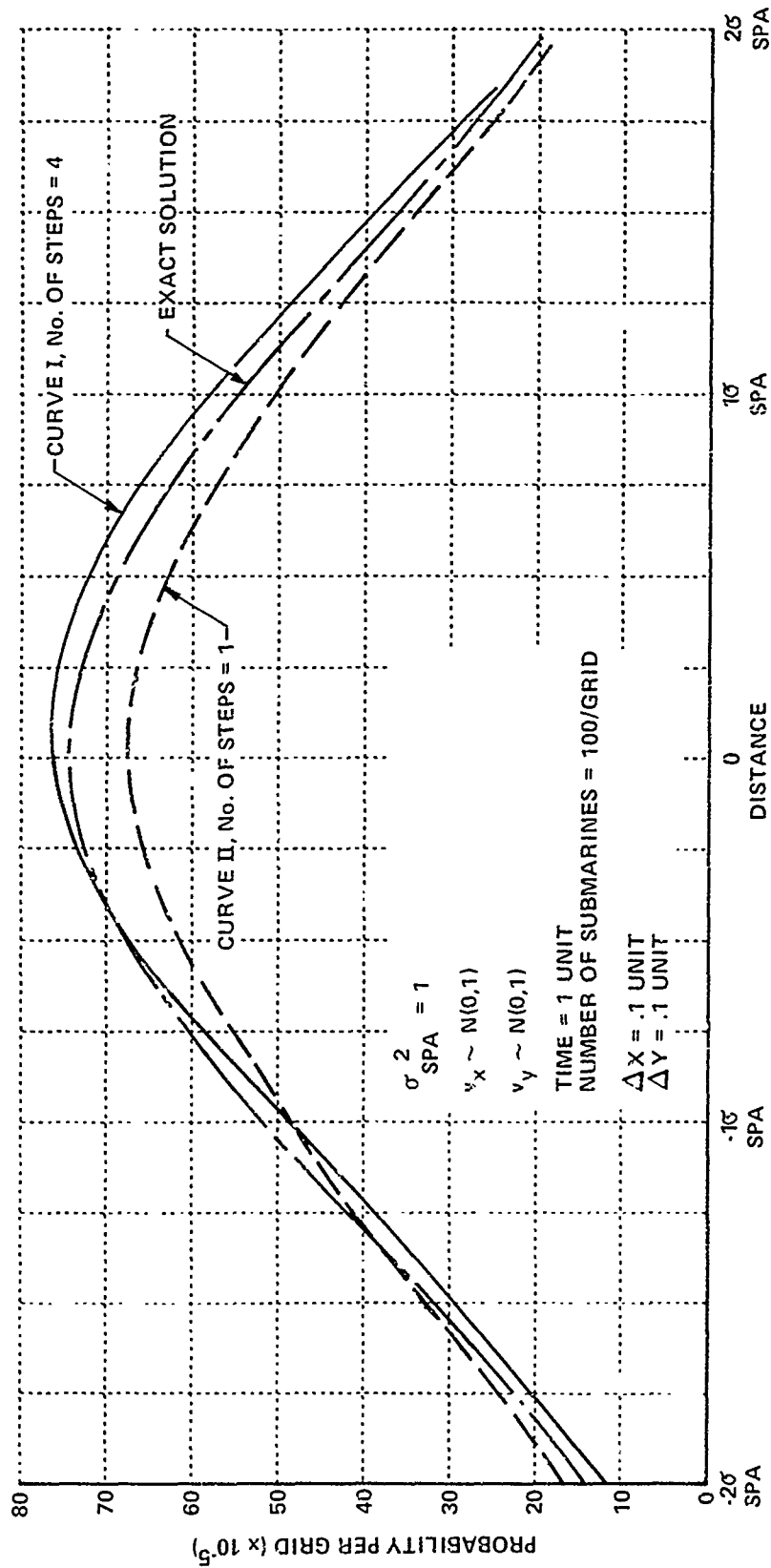


Figure 3-5 DISTRIBUTION OF A MOVING TARGET WHEN X & Y VELOCITY COMPONENTS ARE  $N(0, 1)$ : RANDOM WALK

d. Method III

This method approximates the update probability density as follows:

$$\sum \sum f \cdot g \cdot PM \cong p(x, y, t) \cdot \overline{PM}(x, y, t)$$

where  $p(x, y, t) = \sum \sum f \cdot g$ .

The method of obtaining  $p(x, y, t)$  is by the Monte Carlo method described previously. The  $\overline{PM}$  grid is then "grown" separately from the  $p(x, y, t)$  term. The only case modeled in this study for a heading distribution of the target which is assumed to be uniform between  $0-2\pi$ .

The  $\overline{PM}$  grid is set equal to the probability that the target is not detected on the first "look" by the sonobuoy field. Between successive "looks" the  $PM$  grid is then "grown" by the following operation:

$$\overline{PM}(x_i, y_j, t) = \frac{1}{4} \left\{ \overline{PM}(x_i, y_{j-1}, t - \Delta t) + \overline{PM}(x_{i-1}, y_j, t - \Delta t) \right. \\ \left. + \overline{PM}(x_{i+1}, y_j, t + \Delta t) + \overline{PM}(x_i, y_{j+1}, t - \Delta t) \right\}$$

For heading distributions other than for a uniform heading between  $0$  and  $2\pi$ , the above operation would be performed by weighting each term in the sum.

At the time of each "look", the  $\overline{PM}$  grid is multiplied by the probability that the sonobuoy field does not detect the target during that "look". The term  $\Delta t$  in the above equation is set equal to  $\Delta x/E\{v\}$  where  $\Delta x$  is the grid size (assuming  $\Delta x = \Delta y$ ) and  $E\{v\}$  is equal to the expected value of the target's velocity. Let  $T$  be the time increment between "looks", then the above operation is performed  $N$  times between "looks" where  $N$  is defined as:

$$N = T/\Delta t^2$$



e. Sample Computer Run Results For Methods I, II and III

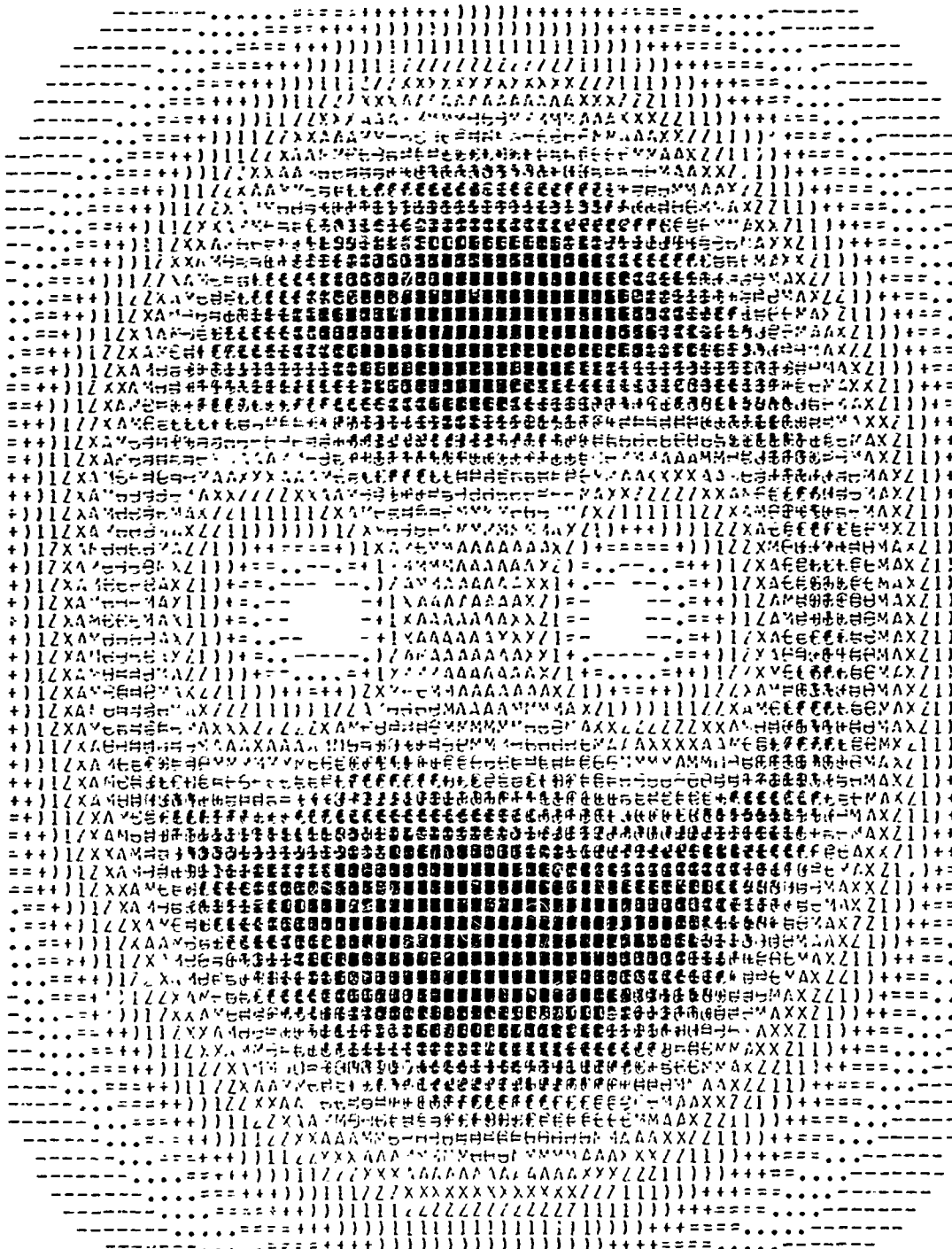
Figures 3-6 through 3-11 present results of some sample computer runs for the three methods of inserting the sonobuoys into the Monte Carlo program. The plots were obtained from an on-line printer used in conjunction with the IBM 370 Model 165 computer system. Since the printer prints 10 characters per inch in the horizontal direction and 8 characters per inch in the vertical direction, some distortion is present in these figures. The symbols on these figures indicate various probability density levels with the darker areas indicating higher probability density levels. These levels are stepped in approximately 5% increments.

Each typewriter character shown on the figures represents a grid of .1 unit by .1 unit. The standard deviation of the initial probability density of the SPA is a joint circular normal with a standard deviation of 1 unit in both the  $x$  and  $y$  directions. The SPA is centered approximately in the center of each figure. This point is also called datum.

The number of emplaced sonobuoys shown in each figure is two with each sonobuoy having 5 "looks". The sonobuoys are located 1 unit to the right and left of datum. In all cases, the target submarine heading is uniformly distributed between 0 and  $2\pi$ .

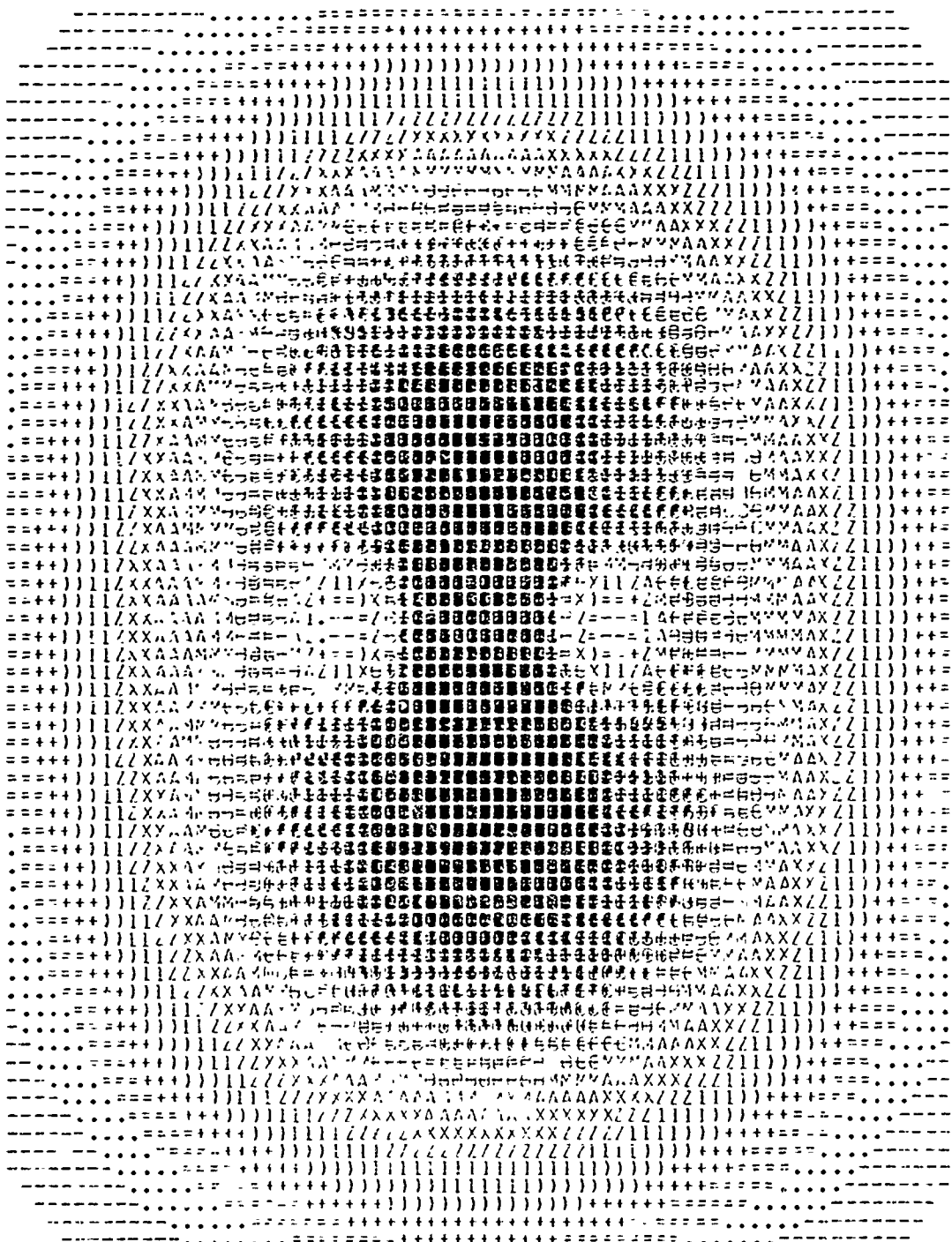
For Figures 3-6, 3-7 and 3-8, the target submarine has a known velocity of 1 unit/unit of time. The display (elapsed) time is 2 units. In Figure 3-6 the sonobuoys are inserted by Method I. Figure 3-7 by Method II and in Figure 3-8 by Method 3. Figures 3-9 and 3-10 are the same as Figures 3-6 through 3-8 except that the velocity component of the MC Submarines have a normal distribution ( $N(0, 1)$ ). The magnitude of the velocity has a Rayleigh distribution. In Figure 3-9 the sonobuoys are inserted by Method I, Figure 3-10 by Method II and in Figure 3-11 by Method III. A comparison of these and additional results indicate that Method I of inserting the sonobuoys into the Monte Carlo program provides the best results. For this reason, a major

SYMBOLS INDICATE VARIOUS PROBABILITY DENSITY LEVELS  
DARKER AREAS INDICATE HIGHER PROBABILITY DENSITY AREAS



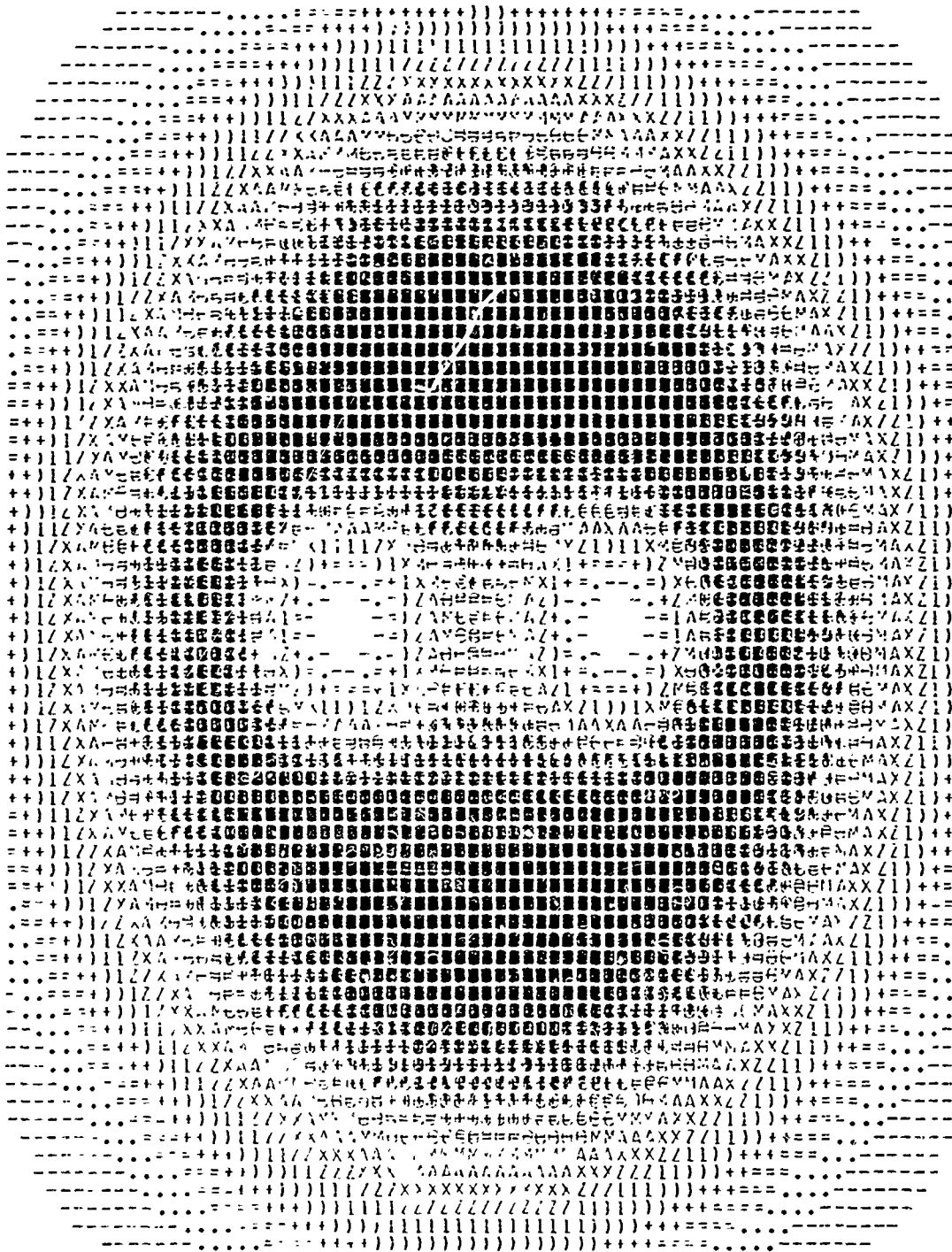
SUBMARINE HEADING: UNIFORM DISTRIBUTION 0-2 $\pi$   
SUBMARINE VELOCITY: 1 UNIT/UNIT OF TIME  
ELAPSED TIME: 2 UNITS  
NUMBER OF SONOBUOYS: 2 NUMBER OF "LOOKS": 5  
TIME OF "LOOKS": 1.0, 1.25, 1.5, 1.75, 2.0

Figure 3-6 PROBABILITY DENSITY OF SUBMARINE'S POSITION WITH KNOWN  
CONSTANT VELOCITY AND UNIFORM HEADING: METHOD I



SUBMARINE HEADING: UNIFORM DISTRIBUTION 0-2 $\pi$   
 SUBMARINE VELOCITY: 1 UNIT/UNIT OF TIME  
 ELAPSED TIME: 2.0 UNITS  
 NUMBER OF SONOBUOYS: 2 NUMBER OF "LOOKS": 5  
 TIME OF "LOOKS": 1.0, 1.25, 1.5, 1.75, 2.0

Figure 3-7 PROBABILITY DENSITY OF SUBMARINE'S POSITION WITH KNOWN CONSTANT VELOCITY AND UNIFORM HEADING: METHOD II



SUBMARINE HEADING: UNIFORM DISTRIBUTION 0-2 $\pi$   
 SUBMARINE VELOCITY: 1 UNIT/UNIT OF TIME  
 ELAPSED TIME: 2.0 UNITS  
 NUMBER OF SONOBUOYS: 2 NUMBER OF "LOOKS": 5  
 TIME OF "LOOKS": 1.0, 1.25, 1.50, 1.75, 2.0

Figure 3-8 PROBABILITY DENSITY OF SUBMARINE'S POSITION WITH KNOWN CONSTANT VELOCITY AND UNIFORM HEADING: METHOD III







portion of the Search Director study effort has been concentrated toward the full development of this computer program.

#### 4. Start and End Grids Development

The initial probability density distribution of target location within a SPA at  $t=0$  is described by joint normal probability distributions. The computer model initially computes  $f(x_i) \Delta x$  and  $f(y_j) \Delta y$  and stores each in a one-dimensional array. The model as presently configured saves on computer core size and a minimal amount on computer run time compared with computing the above functions over the total initial distribution (SPA) and then storing this array in machine memory.

The locus of points in the  $x$ - $y$  plane such that  $f(x, y)$  is a constant  $C_1$  is an ellipse given by:

$$x^2/\sigma_x^2 + y^2/\sigma_y^2 = C_1$$

Therefore, the boundary of the starting grid in the model is an ellipse which is determined by  $C_1$ . The value of  $C_1$  is an input to the model. The target submarine is thus assumed to be within an ellipse of specified area (SPA SIZE) with a given confidence, e.g., 90% at time = 0. The region outside the ellipse is not considered in the analysis.

The  $\Delta x$  by  $\Delta y$  start grid size need not be of equal size in the  $x$  and  $y$  direction. That is,  $\Delta x$  is not required to be the same size as  $\Delta y$ . This allows  $f(x)$  and  $f(y)$  to be subdivided into an equal number of grids even when their variances are unequal. The end grid calculated at the update time  $t$  is circular in shape. The grid center and radius are inputs to the model. A limitation of the model is that for the end grid  $\Delta x = \Delta y$ , the value of  $\Delta x$  should not be larger than the maximum of the values of  $\Delta x$  or  $\Delta y$  of the start grid.



## 5. Probability-of-Miss (PM) Grid Development

One limitation of the present computer model is that all deployed sonobuoys are assumed to have the same probability of detection curve. The probability of detection of the target by a sonobuoy is assumed to be of the form  $e^{-\alpha R^2}$  where  $R$  is the distance from the target to the sonobuoy and  $\alpha$  is an input to the model. All sonobuoys being monitored are assumed to be sampled at the same time. It is also assumed that the sampling rate remains constant throughout the search time.

The probability that a sonobuoy does not detect the target is given by:

$$1 - e^{-\alpha R^2}$$

In the computer model the  $PM$  grid is calculated utilizing the following relationship:

$$pm_{i,j} = 1 - \exp \left\{ -\alpha \left( \left( \frac{\Delta x}{2} + (i-1) \Delta x \right)^2 + \left( \frac{\Delta y}{2} + (j-1) \Delta y \right)^2 \right) \right\} \quad \text{for } i, j < K$$

where  $i, j$  represents the number of  $x$  grids and  $y$  grids from the sonobuoy to the target and  $K$  is an input to the model. Also, the  $\Delta x \Delta y$  grid size of the  $PM$  grid can be an integer subdivision of the end grid  $\Delta x \Delta y$  size. This allows for a finer sampling of the  $PM$  curves. Hence, the model has three different grid sizes that can be used and are listed below:

Start Grid	$\Delta x_{SG}$	$\Delta y_{SG}$
End Grid	$\Delta x_{EG}$	$\Delta y_{EG}$
$PM$ Grid	$\Delta x_{PM}$	$\Delta y_{PM}$

Also,  $\alpha$  may be adjusted to become a function of velocity for a limited number of target velocity and heading distributions and when the velocity is a random variable. This will adjust the probability density map for these limited cases to account for an increase in source level of the target as it's velocity increases. The model is presently being extended to include any sensor Probability of Detection versus range functions for both direct path and convergence zone detection.

For each "look" by the sonobuoy field, the model checks each sonobuoy to determine whether that sonobuoy was monitored for that "look". If the sonobuoy is not being monitored,  $pm_{ij}$  is set equal to one. The computer model calculates the  $x$  and  $y$  component of range of each MC submarine to each sonobuoy for all sonobuoys which are being monitored. If either the  $x$  or  $y$  components (scaled to the number of grids) is greater than  $K$ ,  $pm_{ij}$  is again set equal to one. If  $x$  and  $y$  are both less than  $K$ , the model looks up the value of  $pm_{ij}$  in the  $PM$  grid. The accumulated probability of miss of the MC submarines is then the product of all the probability of misses for each sonobuoy on each "look".

#### 6. Methods of Assigning Velocity Components to MC Submarines

The objective in analyzing different methods of assigning velocity components to MC submarines is to find a method which allows the minimum number of MC submarines to be placed in each  $\Delta x_{SG}$  by  $\Delta y_{SG}$  grid in order to satisfactorily compute the probability density map. Three methods are available to obtain the set of numbers representing the headings of the MC submarines for this distribution:

- I. Generate a set of random numbers from this distribution.
- II. Equally space the headings of the MC submarines between 0 and  $2\pi$  and weight the count of the MC submarines by the probability that the target actually has that heading within some  $\Delta\theta$  range.
- III. Space the heading of MC submarines at equal probability increments between 0 and  $2\pi$ .

##### a. Uniform Heading Case

The first attempt at assigning velocity components to the submarines has been to use a random number generator for the "random" portion of the velocity and/or heading distribution. An example, consider

the case where the magnitude of the velocity,  $v$ , is known and the heading of the distribution is assumed to be uniformly distributed between 0 and  $2\pi$ . Let  $N$  be the number of MC submarines placed in each  $\Delta x$  by  $\Delta y$  grid. A uniform random number generator supplies a list of  $N$  "random" numbers between 0 and 1. Each number of the set is then multiplied by  $2\pi$  to obtain a set of random numbers which are uniformly distributed between 0 and  $2\pi$ . The velocity components for the  $i$ th MC submarines are then formed from the following relationship:

$$v_{x_i} = v \cos(\theta_i)$$

$$v_{y_i} = v \sin(\theta_i)$$

where  $\theta_i$  is the  $i$ th number in the random number set.

Another approach is to equally space the headings of the submarines in each grid around 0 to  $2\pi$ , that is, to assign "expected values"\* of headings to the MC submarines. Thus, if four MC submarines are to be placed in each  $\Delta x$  by  $\Delta y$  grid, the following headings would be assigned to the MC submarines in that grid:

$$0, 90^\circ, 180^\circ, 270^\circ$$

Sample results using these two methods are presented in Figure 3 12. Comparison of the two methods of assigning velocity components to MC submarines is shown in determining the probability density distribution of a moving target submarine having a known constant velocity and uniform heading. In Curve I the headings of the MC submarines are obtained utilizing

\*"Expected value" is used in the following sense: If a probability density function is divided into  $N$  subdivisions in which the area in each segment is equal (equal probabilities) and  $N$  random samples are obtained from the distribution, it is expected that one sample would fall in each of the  $N$  subdivisions.

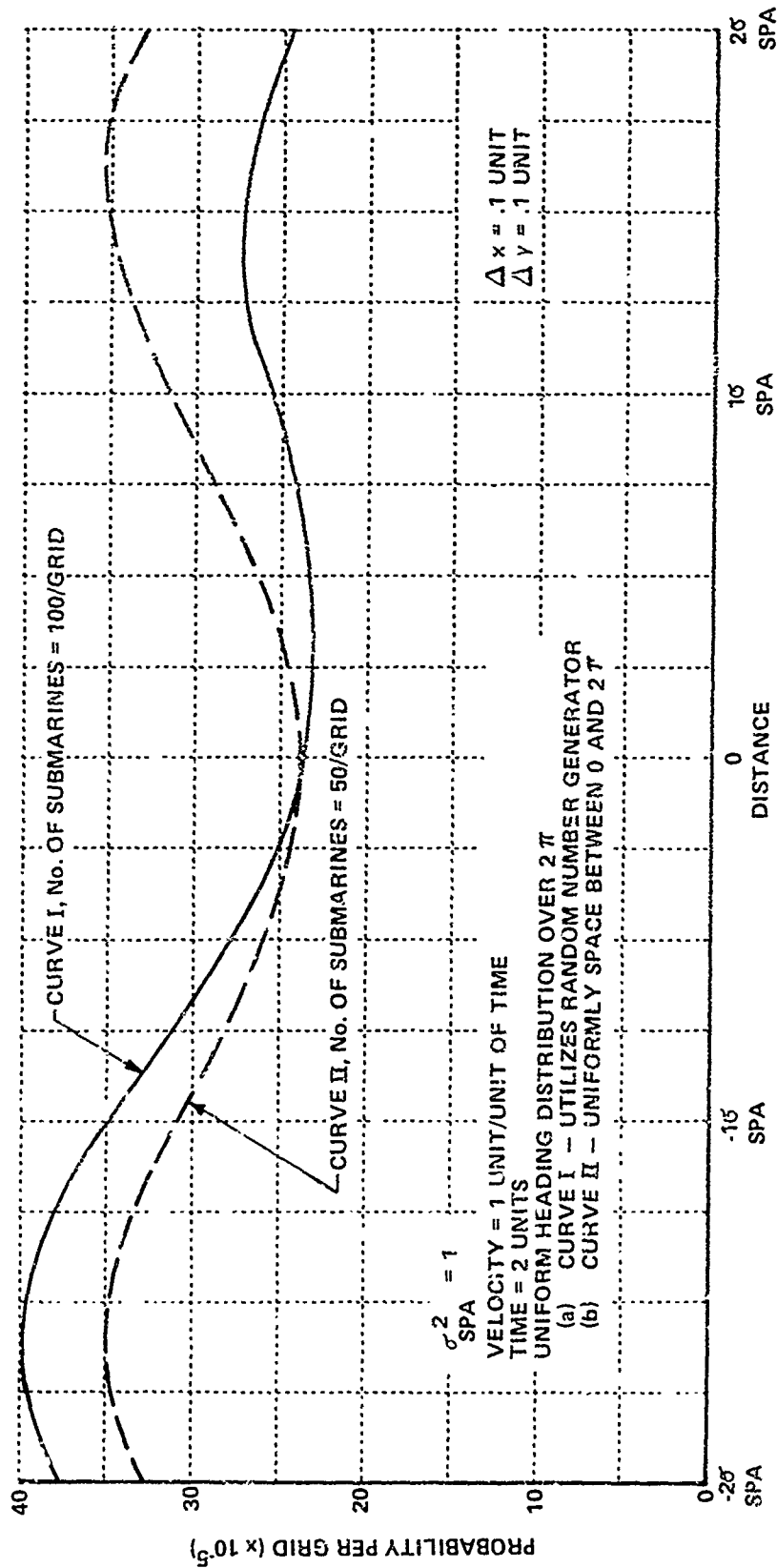


Figure 3-12 DISTRIBUTION OF A MOVING TARGET WITH CONSTANT VELOCITY AND UNIFORM HEADING: FOR TWO METHODS OF ASSIGNING VELOCITY COMPONENTS OF MC SUBMARINES

the random number generator. In Curve II the headings are equally spaced between 0 and  $2\pi$ . Unlike Curve I, Curve II corresponds closely to the exact results presented in Reference 1.\* These results indicate that equally spacing the headings of the MC submarines allows the minimum number of submarines to be used in each grid.

b. Biased Heading Case

Consider the example where the magnitude of the velocity is known and the heading is a random variable described by the following probability distribution:

$$p(\theta, \Lambda_m) = \frac{1}{2\pi I_0(\Lambda_m)} \exp\{\Lambda_m \cos(\theta)\} \quad -\pi \leq \theta \leq \pi$$

The function  $I_0(\Lambda_m)$  is a modified Bessel function of the first kind which is included so that the density will integrate to unity. The parameter  $\Lambda_m$  can be regarded simply as a parameter that controls the spread of the density. From the above equation it is determined that for  $\Lambda_m = 0$ .

$$p(\theta) = \frac{1}{2\pi}$$

As  $\Lambda_m$  increases, the density becomes more peaked and as  $\Lambda_m \rightarrow \infty$  it approaches the case where the heading is known. Therefore, the above distribution allows a wide range of headings distribution to be modeled. Due to the kind of results obtained for the uniform heading case, no attempt has been made to model a random number generator for the above distribution.

Results for the biased heading case utilizing Methods II and III are presented in Figure 3-13. These indicate that Method II (Illustration 13a) provides a better representation of the probability density map in the fourth quadrant than Method III (Illustration 13b). However, the reverse situation occurs for

\*Reference 1: Status Summary - Research at CAL on Analysis of Airborne Anti-Submarine Warfare (ASW) Operations CAL Report - no number, May 1962, SECRET.



EQUALLY SPACED

13-a

NUMBER OF MC SUBMARINES/GRID = 24

VELOCITY = 12 knots

$$p(\theta, 2) = \frac{1}{2\pi I_0(2)} \exp \left\{ 2 \cos \theta \right\}$$

NUMBER OF SONOBUOYS: 15  
 NUMBER OF LOOKS: 24  
 DISPLAY TIME: 9 HOURS



EQUAL PROBABILITY INCREMENTS

13-b

SPA SIZE  $\sigma_x = 25$  n.mi.

$\sigma_y = 25$  n.mi.

$\Delta x = \Delta y = 3$  n.mi.

Figure 3-13 PROBABILITY DENSITY OF SUBMARINE'S POSITION WITH CONSTANT VELOCITY AND RANDOM HEADING: FOR TWO METHODS OF ASSIGNING VELOCITY COMPONENTS OF MC SUBMARINE'S

the second quadrant. It is believed that both methods can be extended to provide improved results. However, this has not been attempted up to the present time.

c. Random Velocity Component Case

Consider the example where the velocity is a random variable described by the following joint normal:

$$f(v_x, v_y) = \frac{1}{2\pi\sigma_{v_x}\sigma_{v_y}} \exp \left\{ -\frac{1}{2} \left( \frac{(v_x - v_{x_0})^2}{\sigma_{v_x}^2} + \frac{(v_y - v_{y_0})^2}{\sigma_{v_y}^2} \right) \right\}$$

The velocity components for this distribution may be obtained from a random number generator in the following way: The first step is to obtain two sets of  $N$  random numbers from the following  $N(0, 1)$  distribution:

$$f(z) = \frac{1}{\sqrt{2\pi}} \exp \left\{ -\frac{1}{2} z^2 \right\}$$

The next step is to multiply each number in one of the sets by  $\sigma_{v_x}$  and add  $v_{x_0}$ . The third step is to multiply each member of the other set by  $\sigma_{v_y}$  and add  $v_{y_0}$ . The final step is to pair the numbers of the two sets to obtain a new set which corresponds to a set of random numbers from  $f(v_x, v_y)$ . Each member of this set is then paired with one of the MC submarine as its velocity component.

Another approach in assigning velocity components to the submarines is to obtain a set of "expected values" of velocity components from the distribution  $f(v_x, v_y)$  as follows:

$$\begin{aligned} \text{Let } \bar{v}_x &= v_x - v_{x_0} \\ \bar{v}_y &= v_y - v_{y_0} \end{aligned}$$

then

$$f(\bar{v}_x, \bar{v}_y) = \frac{1}{2\pi\sigma_{v_x}\sigma_{v_y}} \exp \left\{ -\frac{1}{2} \left( \frac{\bar{v}_x^2}{\sigma_{v_x}^2} + \frac{\bar{v}_y^2}{\sigma_{v_y}^2} \right) \right\}$$

Let

$$\bar{v}_y = \bar{v}_y \frac{\sigma_{v_y}}{\sigma_{v_x}}$$

then

$$f(\bar{v}_x, \bar{v}_y) = \frac{1}{2\pi\sigma_{v_x}^2} \exp\left\{-\frac{1}{2\sigma_{v_x}^2} (\bar{v}_x^2 + \bar{v}_y^2)\right\}$$

Now let

$$\bar{v} = \sqrt{\bar{v}_x^2 + \bar{v}_y^2}$$

The random variable  $\bar{v}$  has a Rayleigh density given by:

$$g(\bar{v}) = \frac{\bar{v}}{\sigma_{v_x}^2} \exp\left\{-\frac{\bar{v}^2}{2\sigma_{v_x}^2}\right\} \quad \text{for } \bar{v} > 0$$

Solve for  $M$  velocities along the curve  $g(\bar{v})$  spaced at equal probability increments.

Next, take the first of the  $M$  values of velocity,  $v_1$ , above and divide  $\theta$  into equal increments over  $2\pi$  in the same manner as in the case for uniform heading. The reason for this is that the random variable

$$\theta = \tan^{-1}\left(\frac{\bar{v}_y}{\bar{v}_x}\right)$$

is uniformly distributed between 0 and  $2\pi$ .

$$\bar{v}_x(\theta_i) = \bar{v} \cos(\theta_i)$$

$$\bar{v}_y(\theta_i) = \bar{v} \sin(\theta_i)$$

It is now necessary to transform the set of expected values from the distribution  $f(\bar{v}_x, \bar{v}_y)$  to a set from  $f(v_x, v_y)$ .

Therefore,

$$v_y(\theta_i) = \frac{\sigma_{v_x}}{\sigma_{v_y}} \bar{v}_y(\theta_i) + v_{y_0}$$

$$v_x(\theta_i) = \bar{v}_x(\theta_i) + v_{x_0}$$



Let  $\alpha$  be the angle between  $v_x$  of the  $v_x v_y$  plane and  $x$  of the  $xy$  SPA. Then rotate the values of  $v_x(\theta_i)$  and  $v_y(\theta_i)$  into the  $xy$  plane of the SPA by the following equations:

$$v_x^*(\theta_i) = v_x(\theta_i) \cos(\alpha) + v_y(\theta_i) \cos\left(\alpha + \frac{\pi}{2}\right)$$

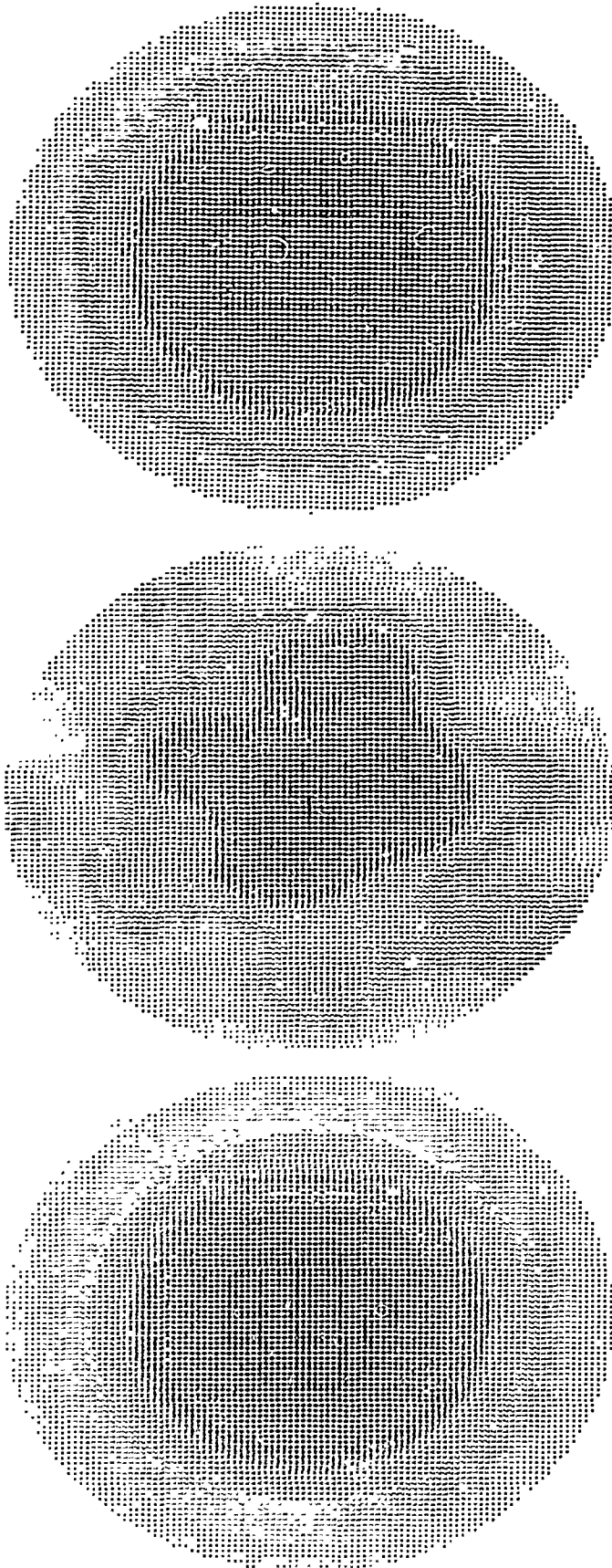
$$v_y^*(\theta_i) = v_x(\theta_i) \sin(\alpha) + v_y(\theta_i) \sin\left(\alpha + \frac{\pi}{2}\right)$$

The above operation is repeated for each of the  $M$  original velocities to obtain the complete set of velocity components to model  $f(v_x, v_y)$ .

Sample results are presented in Figure 3-14 of the probability density of a submarine's position for a Rayleigh distribution in velocity and uniform heading utilizing the random number generator and expected value methods. This is also presented for the exact solution for comparison purposes. In the three illustrations (14a, 14b and 14c)  $v_x$  and  $v_y$  are both described by a normal distribution with a mean of zero and a standard deviation of 12 knots. The resultant vector velocity is described by a Rayleigh density and hence the expected value of the vector velocity is approximately 15 knots. The initial SPA has a standard deviation of 25 n. miles for both the  $x$  and  $y$  components. The  $\Delta x$  by  $\Delta y$  grid size is 4 x 4 n. miles. The display time is 8 hours.

Illustration 14a is the exact solution density map for the sample problem. In illustration 14b, the velocity components are generated from a normal random number generator. The velocity components for illustration 14c have been obtained using expected values. The number of MC submarines in each grid are the same for both illustrations 14b and 14c. These examples indicate that using the expected value method gives the best results since they more closely approximate those shown for the exact solution.

Additional results are presented in Figure 3-15 using the expected value method. The parameter values used are the same as those for Figure 3-14 except for the number of MC submarines placed in each grid.



EXACT  
14a

RANDOM NUMBER  
GENERATOR  
14b

EXPECTED VALUE  
14c

VELOCITY:

RAYLEIGH DISTRIBUTION

SPA SIZE:

$\sigma_x = 25$  n.mi.

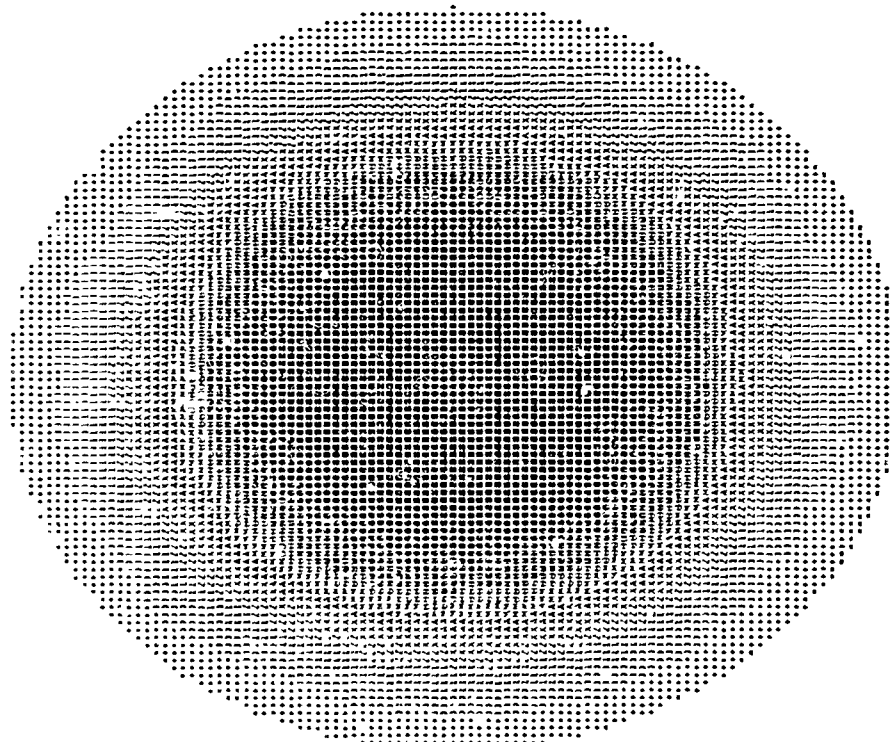
HEADING:

UNIFORM DISTRIBUTION  $0-2\pi$

$\Delta x = \Delta y = 4$  n.mi.

DISPLAY TIME: 8 HOURS

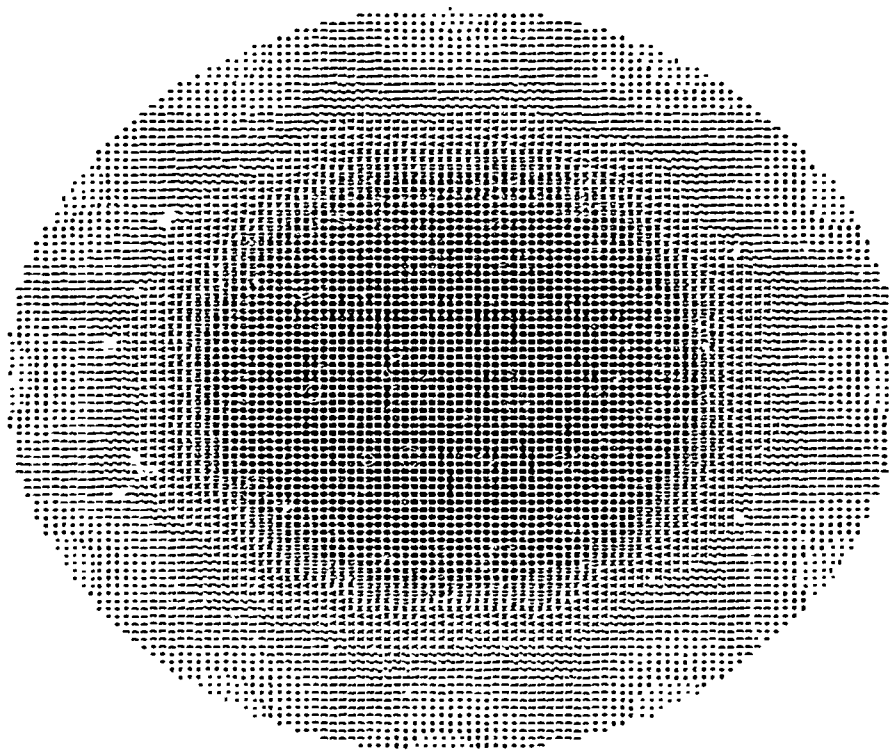
Figure 3-14 PROBABILITY DENSITY OF SUBMARINE'S POSITION WITH RAYLEIGH DISTRIBUTION IN VELOCITY AND UNIFORM HEADING: FOR TWO METHODS OF ASSIGNING VELOCITY COMPONENTS TO MC SUBMARINES



SMALL SAMPLE SIZE M

VELOCITY: RAYLEIGH DISTRIBUTION

HEADING: UNIFORM DISTRIBUTION  $0-2\pi$



LARGE SAMPLE SIZE M

SPA SIZE:

$\sigma_x = 25$  n.mi.

$\sigma_y = 25$  n.mi.

$\Delta x = \Delta y = 4$  n.mi.

DISPLAY TIME: 8 HOURS

Figure 3-15 PROBABILITY DENSITY OF SUBMARINE'S POSITION WITH  
 RAYLEIGH DISTRIBUTION IN VELOCITY AND UNIFORM  
 HEADING: FOR TWO VARIATIONS IN NUMBER OF MC  
 SUBMARINES/GRID

Illustration 15a in Figure 3-15 is the result of a computer run in which the function  $g(\bar{v})$  is sampled at a relatively small sample size,  $M$ , and a relatively large number of MC submarines is assigned to each sampled velocity. In 15b,  $g(\bar{v})$  is sampled at a large sample size,  $M$ , but the number of submarines assigned to each sampled velocity is small.

Referring to 15a, a readily discerned effect resulting from under sampling  $g(\bar{v})$  is that a "hole" in the probability density pattern appears at the datum. On the other hand, assigning relatively few submarines to each sampled velocity (15b) causes the constant contour levels to have the effect of a circle modulated by a sine function. Thus, additional tradeoff analyses are necessary to minimize or eliminate these adverse effects.

#### 7. Sub-Optimal Sonobuoy Drop Point Determination

A limited effort has been conducted on a modification to the Monte Carlo program for use as a possible improved aid in determining sub-optimal sonobuoy drop points. Instead of solving for the joint probability that the target is in some grid at time  $T$  and that the target will not be detected in moving to this grid, the modified program calculates the joint probability that the target passes through some grid during the search time from  $T_1$  to  $T_2$  and that the target is not detected during this time by the deployed sonobuoys.

The modified program would be used in the following manner: First, the operator determines the time on station (from  $T_1$  to  $T_2$ ). The model then computes the probability that the target will pass through each  $\Delta x$  by  $\Delta y$  grid during this time period. Having this display the operator then decides on a drop point for one or more sonobuoys. The model then calculates the joint probability that the target passes through the  $\Delta x$  by  $\Delta y$  grid and is not detected by the deployed sonobuoys. For this calculation the operator must make a reasonable estimate of the monitoring schedule of the deployed sonobuoys.

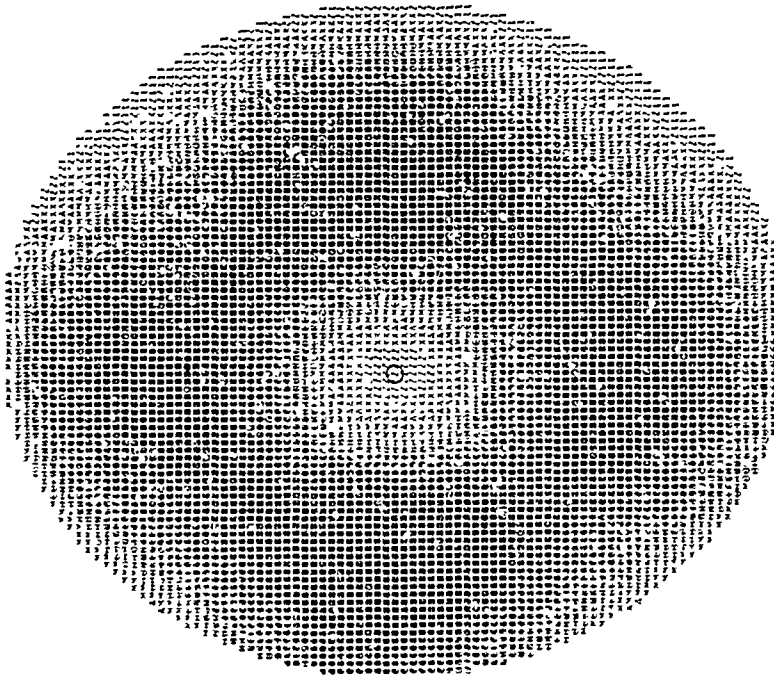
Presently, a problem area exists in this model which is caused by the use of a rectangular coordinate system. The reason is that submarines with a heading of  $0^\circ$  may be counted as passing through more grids than those with a heading of  $45^\circ$  for example. A correction factor has been inserted into the model to account for this difference. However, a complete analytical justification of this factor has not yet been made.

Sample results from this model are presented in Figure 3-16. Illustrations 16a and 16b respectively show the probability density maps without and with application of the correction factor. In both cases the target's velocity of 13 knots with a uniform heading between 0 and  $2\pi$  is assumed to be known. The grid size is  $2.5 \times 2.5$  n. mi. The SPA is described by a joint circular normal distribution with a standard deviation of 25 n. mi. In summary, although complete analytical justification for the correction factor has not been made computer run results (16b) indicate that it appears to work satisfactorily.

#### 8. Analog-Hybrid Computer Program

A limited effort has also been conducted toward determining the feasibility of using an analog/hybrid computer system to obtain the probability density maps of target uncertainty areas. This limited program has been completed on the CAL COMCOR CI 5000 Analog computer. Typical results of the CRT display obtained from this program are illustrated in Figure 3-17. The tactical situation shown is for the case where the velocity of the submarine is a constant value and its heading is uniformly distributed between 0 and  $2\pi$ . Referring to Illustration 17a, one "look" is taken with two sonobuoys offset on both sides of the center of the uncertainty area. In 17b, two looks with one sonobuoy are shown for the case in which the sonobuoy is dropped at the center of the uncertainty area.

A general purpose computer could be used in conjunction with the Analog computer (Hybrid system). This system would use the GP computer



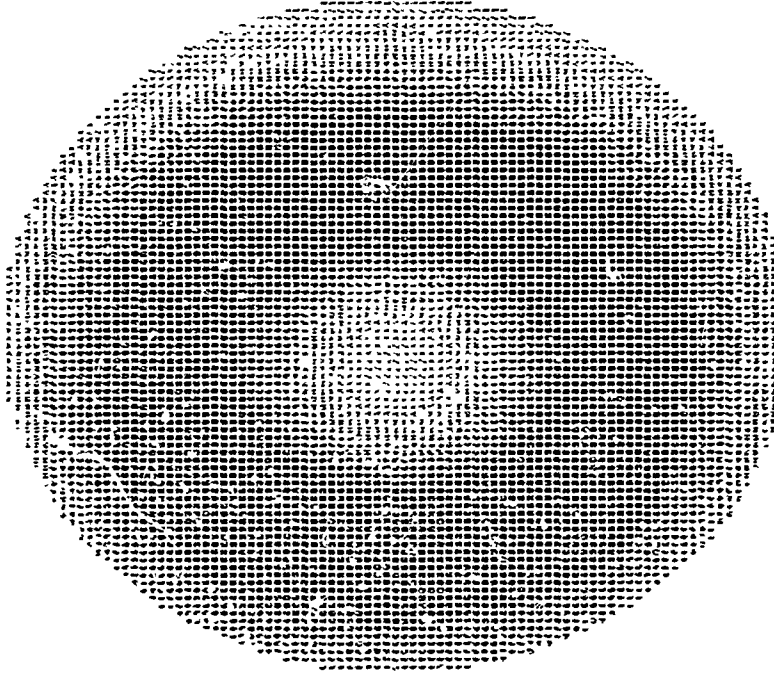
WITHOUT CORRECTION FACTOR

16a

VELOCITY: 13 knots

HEADING: UNIFORM DISTRIBUTION  $0-2\pi$

O DATUM



WITH CORRECTION FACTOR

16b

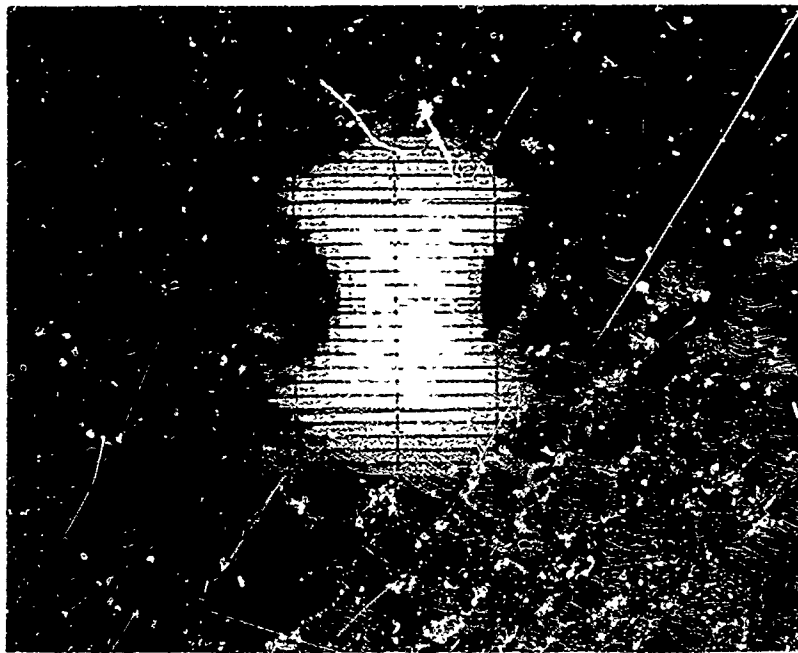
SPA SIZE:  $\sigma_x = 25$  n.mi.

$\sigma_y = 25$  n.mi.

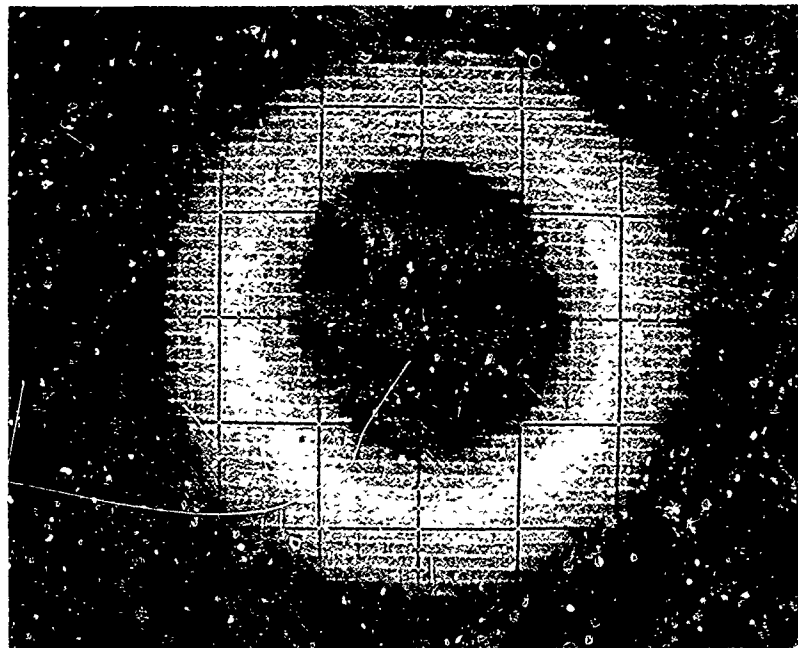
$\Delta x = \Delta y = 2.5$  n.mi.

ACCUMULATED TIME: 3.9 HOURS

Figure 3-16 ACCUMULATED PROBABILITY DENSITY OF SUBMARINE'S POSITION WITH KNOWN CONSTANT VELOCITY AND UNIFORM HEADING: EFFECT OF CORRECTION FACTOR



5a



5b

SUBMARINE HEADING:	UNIFORM DISTRIBUTION $0-2\pi$	
SUBMARINE VELOCITY:	CONSTANT	
NUMBER OF SONOBOUY:	A = 2	LIGHTER AREAS INDICATE HIGHER PROBABILITY DENSITY AREAS
	B = 1	
NUMBER OF "LOOKS":	A = 1	
	B = 2	

Figure 3-17 CRT DISPLAY OF PROBABILITY DENSITY AND SUBMARINE'S POSITION WITH KNOWN CONSTANT VELOCITY AND UNIFORM HEADING: UTILIZING ANALOG COMPUTER

primarily for storage while the analog computer would be used to "compute" the probability density maps.

#### 9. Possible Search Director Display Techniques

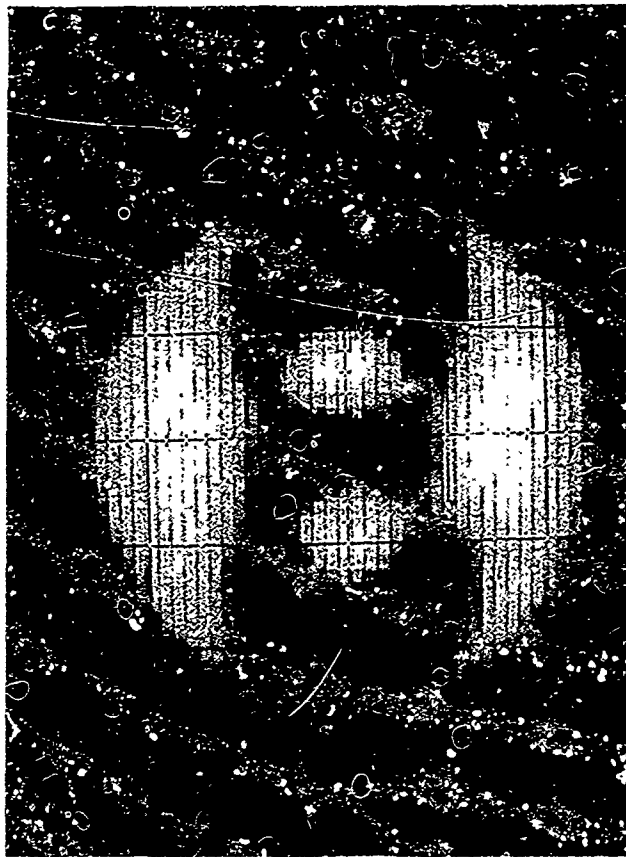
A limited study has been conducted of several techniques for displaying probability density maps of target uncertainty areas in which sonobuoys have been deployed. Figure 3-18 illustrates several display techniques which have been photographed from a CRT connected to the output processor of the CAL analog computer. These presentations vary the amount of fill-in between the calculated value for each  $\Delta x$  by  $\Delta y$  grid. In illustration 18a the fill-in is almost complete. In 18b a partial fill-in is utilized for display purposes. In 18c the probability level is indicated both by the intensity of the point and by its size.

A capability also exists in future study, for the analog computer to pass the output grid through a non-linear amplifier. This capability provides a method for investigating the effects, for example, of intensifying the highest probability density levels.

#### 10. Comparison of Display Techniques Utilizing the CAL Flying Spot Scanner

A limited effort has been conducted on the CAL Flying Spot Scanner for the purpose of comparing various display techniques. A description of this CAL equipment is summarized in Appendix A. In brief, the values of the calculated grid of the Monte Carlo program are converted to integer values ranging from 0 to 60. The lowest number in the grid is set equal to zero, the highest to 60 and the intermittent values are linearly spaced between 0 and 60. A 1024 x 1024 grid is then formed from the calculated grid by linearly smoothing between the calculated points. A color code is assigned to each of the 61 levels in the grid. The possible shades of gray for a black and white photograph are shown in Figure 3-19.





6a



6b



6c

Figure 3-18 CRT DISPLAY TECHNIQUES OF THE PROBABILITY DENSITY MAP

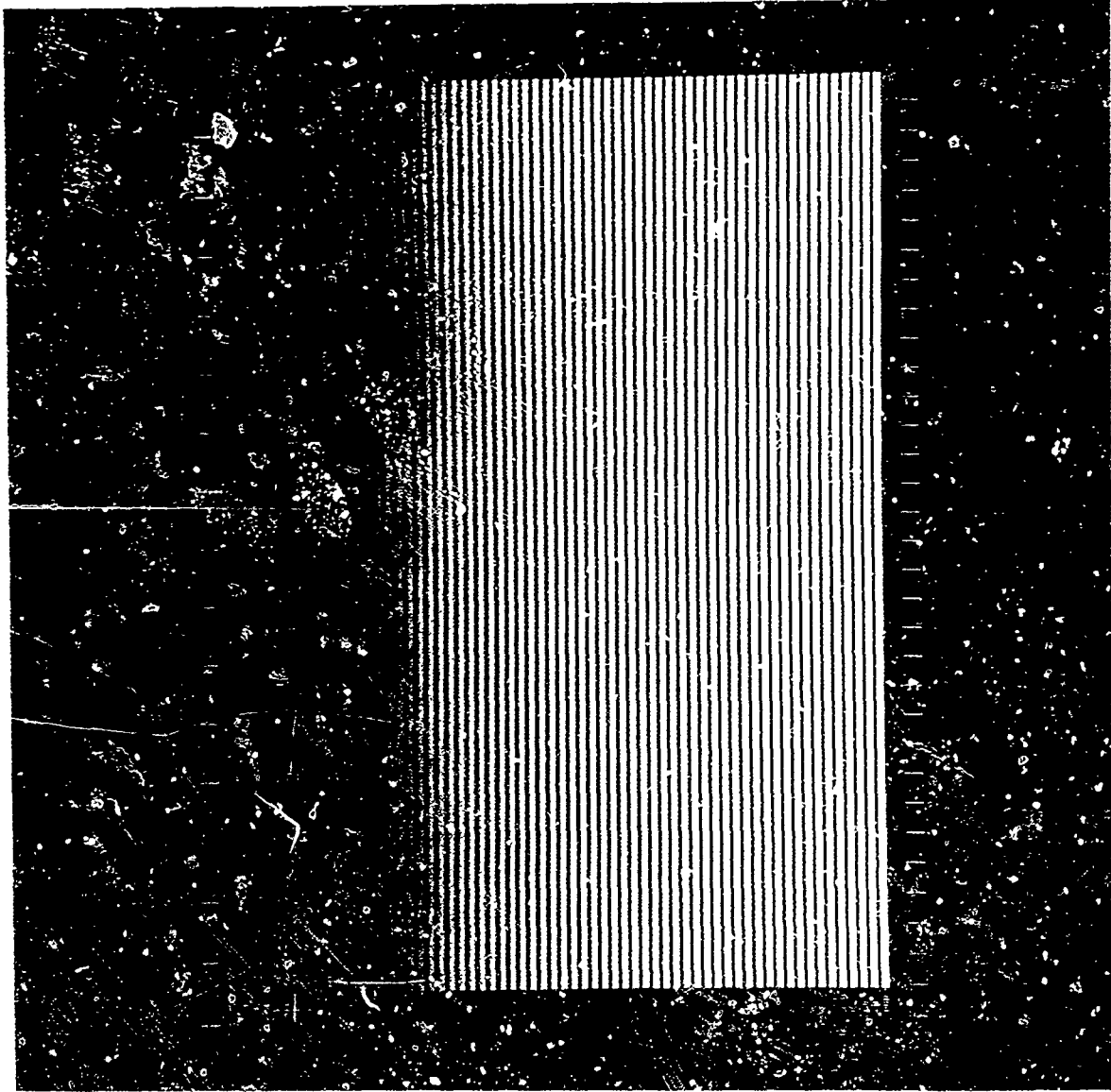


Figure 3-19 GREY SCALE FOR BLACK AND WHITE PHOTOGRAPHS

Figures 3-20 and 3-21 are examples in which all the different levels of gray have been used. The brighter areas indicate higher probability levels. Figure 3-20 is presented for the case where the submarine target velocity is known to be 12 knots and its heading is uniformly distributed between 0 and  $2\pi$ . The SPA is described by a circular normal distribution with a standard deviation of 25 n. mi. The displayed circle has a diameter of 252 n. mi. The display time for this example is 9 hours. A total of 15 sonobuoys are deployed. Each sonobuoy is monitored on every other "look" starting at a time late equal to 3 hours in increments of 15 minutes for a total of 24 "looks". This photograph is for the same probability density map as shown in Figure 4-7c of Section IV of this report in which an on-line computer printer has been used to create the map. Figure 4-7 also shows the locations of the deployed sonobuoys.

An example is shown in Figure 3-21 in which the velocity of the target is described by a Rayleigh distribution with a mean velocity of 15 knots. The diameter of the display is 420 n. mi. and the center of the figure is the datum point. Figure 4-12b is a presentation of the same display using the on-line printer (Refer to Section IV).

Figures 3-22 and 3-23 present the same probability density map that is shown in Figure 3-20 except for the coding of the shades of gray. In Figure 3-22, 31 intensity levels have been used which are equally spaced over the gray-scale range of 0-60. Figure 3-23 shows six intensity levels linearly spaced over the dynamic range 0-60.

Figure 3-24 presents the same probability density map that is shown in Figure 3-20 except that in this example, the blacker areas indicate higher probability levels. This is accomplished by making a positive of Figure 3-20.

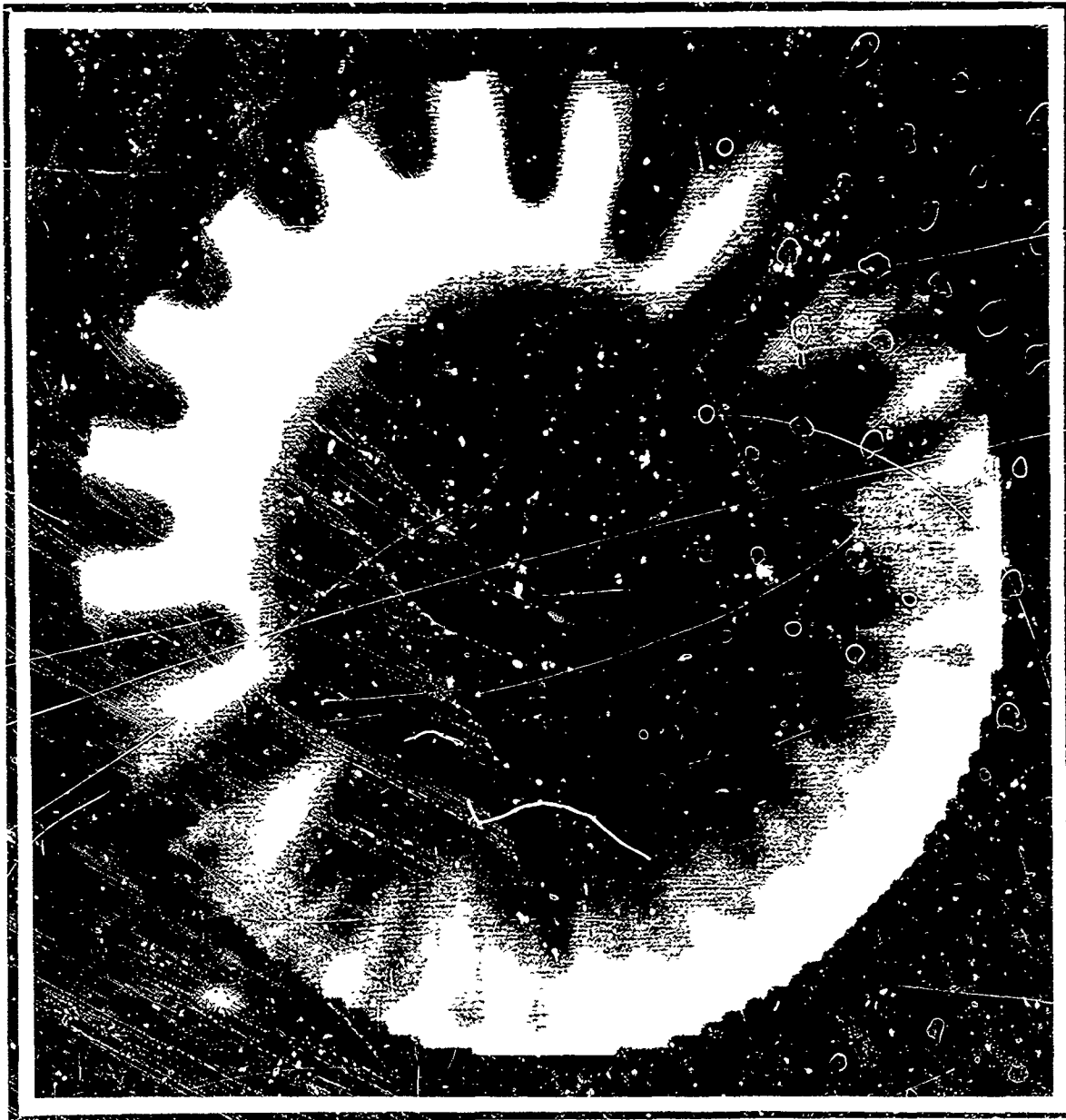


Figure 3-20 FLYING SPOT SCANNER DISPLAY OF PROBABILITY DENSITY MAP:  
EXAMPLE 1

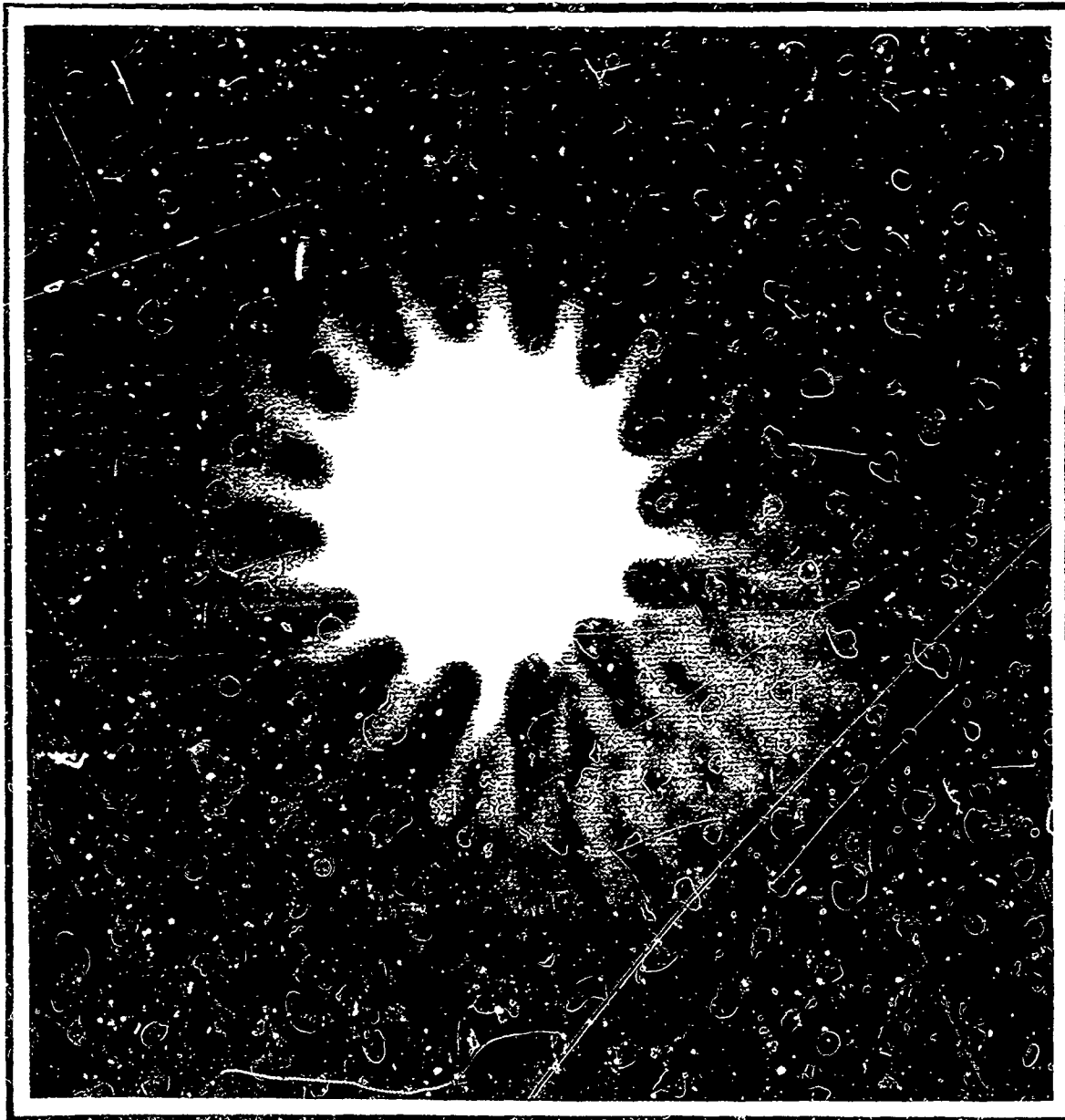


Figure 3-21 FLYING SPOT SCANNER DISPLAY OF PROBABILITY DENSITY MAP:  
EXAMPLE 2

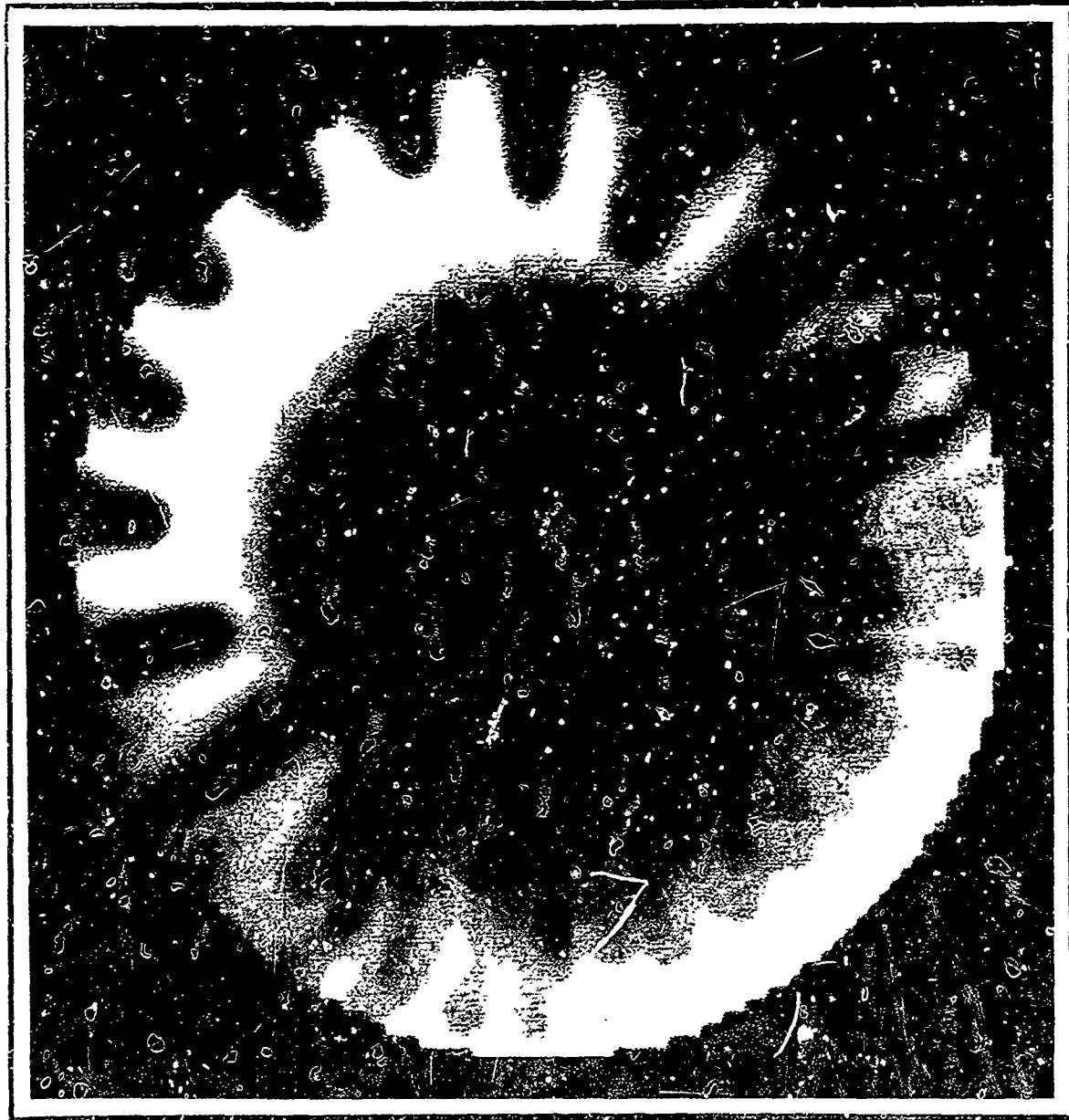


Figure 3-22 FLYING SPOT SCANNER DISPLAY OF PROBABILITY DENSITY MAP:  
EXAMPLE 3

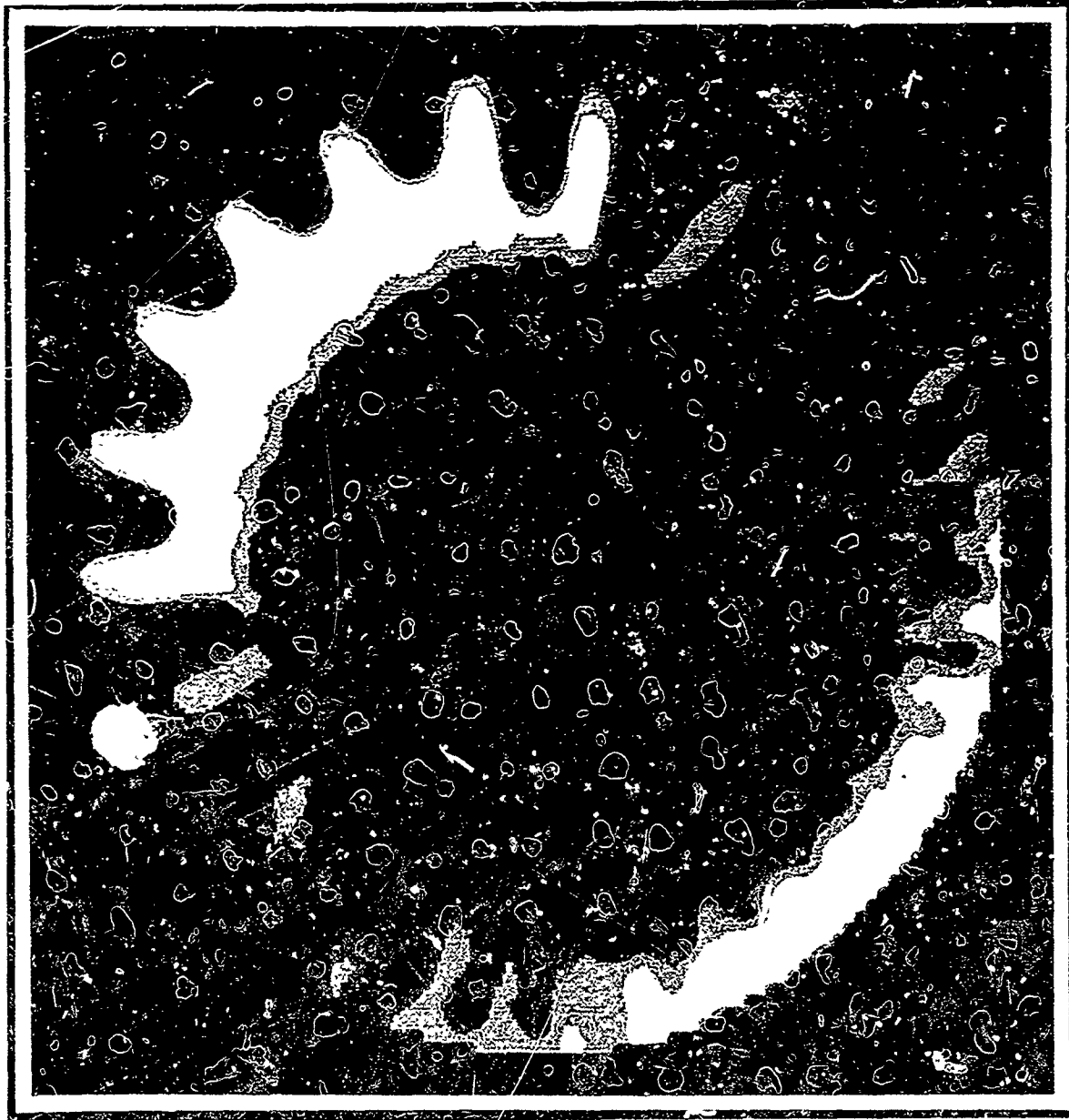


Figure 3-23 FLYING SPOT SCANNER DISPLAY OF PROBABILITY DENSITY MAP:  
EXAMPLE 4

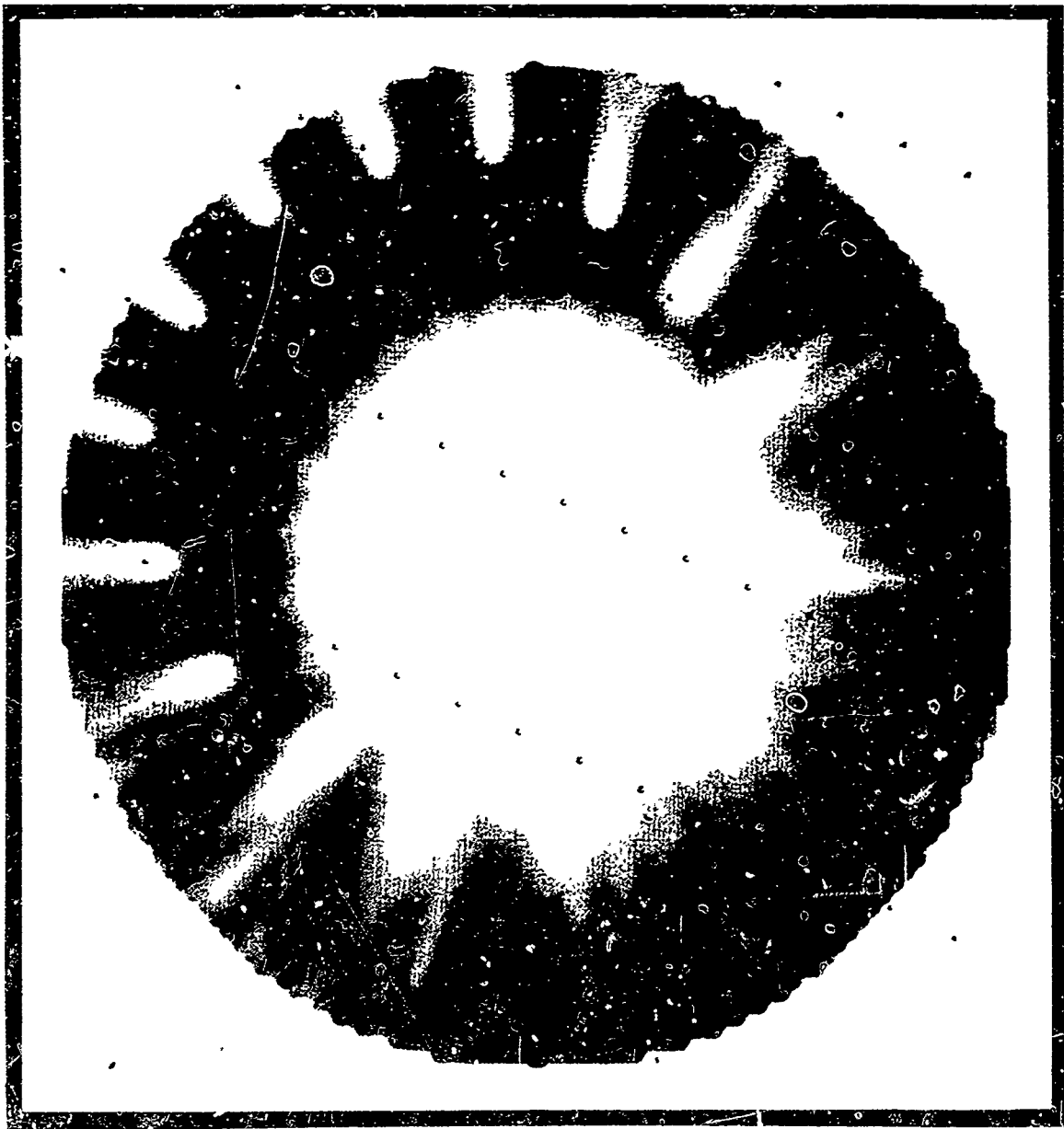


Figure 3-24 FLYING SPOT SCANNER DISPLAY OF PROBABILITY DENSITY MAP:  
EXAMPLE 5



Figure 3-25 shows an example of a color display with Figure 3-26 being its equivalent black-and-white photograph using 61 shades of gray. It should be noted that no effort has been attempted to determine the "best" color code and, therefore, Figure 3-25 is presented only as an example of the capability of the CAL Flying Spot Scanner.

Another method of presenting a probability density map to an ASW operator is to display it as a series of contour lines representing iso-probability density levels. Thus, in order to evaluate the merits of this method of display, a contour plotting routine has been added to the Monte Carlo model. Sample contour plots based on computer runs made utilizing this routine are shown in Figures 3-27, 3-28 and 3-29.

A contour plot of probability density levels for the initial SPA ( $N(0,1)$ ) is shown in Figure 3-27 at zero elapsed time. In Figures 3-28 and 3-29, the target is assumed to have a known constant velocity and the heading is uniformly distributed between 0 and  $2\pi$ . Contour plots for display elapsed times of 1 unit and 2 units are presented respectively in Figures 3-28 and 3-29. The probability density levels associated with zero and one unit of elapsed time are listed in Table 3-1. Those for two units of elapsed time are listed in Table 3-2.

In summary, the limited results achieved to date provide some indication that an intensity display in shades of gray can supply ASW aircraft personnel with the necessary information required for conducting Search Director operations. Still to be finally determined, however, are the number of intensity levels needed and the size of the display scope.



Figure 3-25 FLYING SPOT SCANNER DISPLAY OF PROBABILITY DENSITY MAP:  
EXAMPLE 6

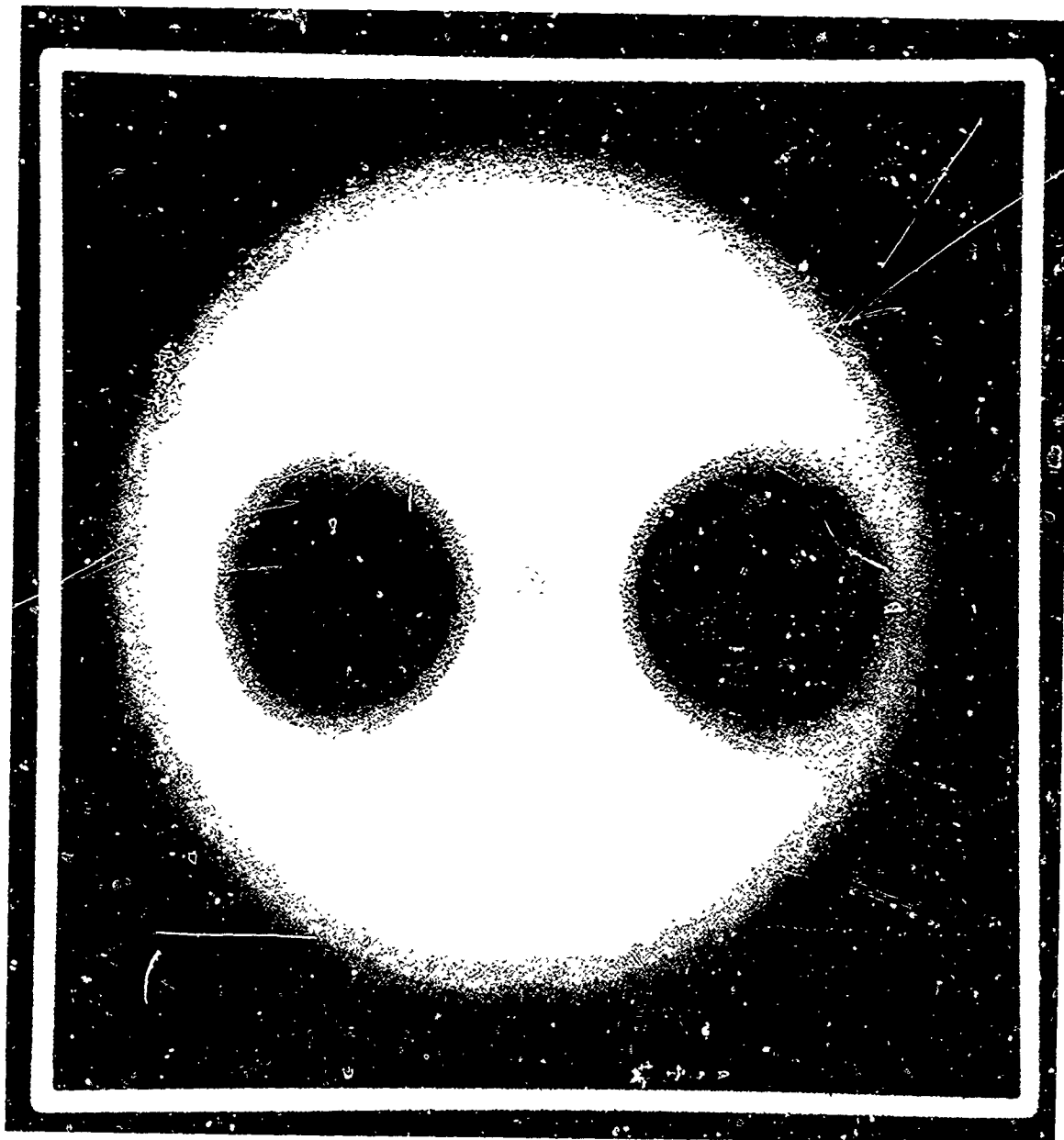
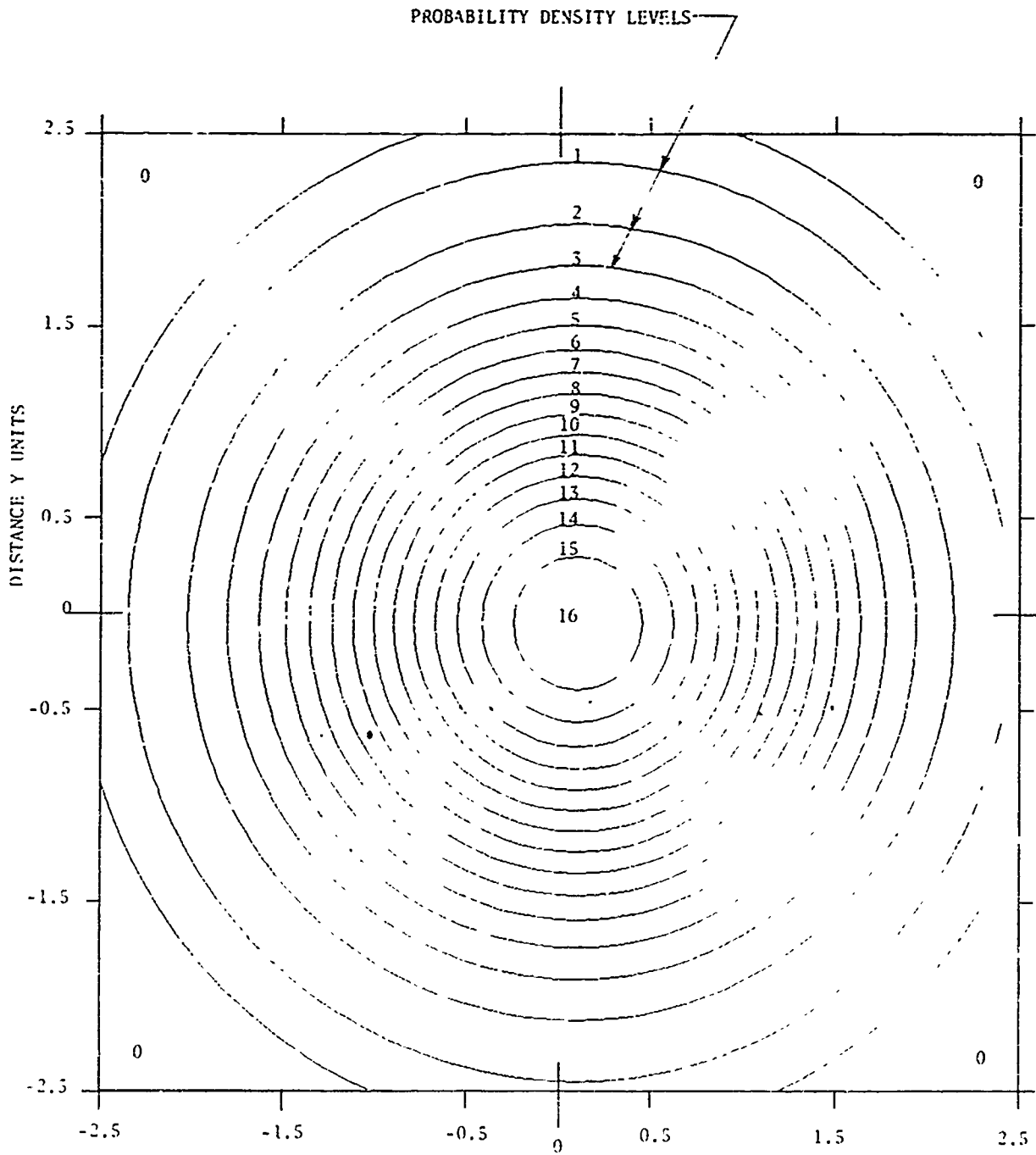


Figure 3-26 FLYING SPOT SCANNER DISPLAY OF PROBABILITY DENSITY MAP:  
EXAMPLE 7



DISTANCE X-UNITS

VELOCITY: 1 UNIT/UNIT OF TIME  
 HEADING: UNIFORM DISTRIBUTION 0-2 $\pi$   
 ELAPSED TIME: 0 UNITS  
 $\sigma_{SPA}$ : 1 UNIT

Figure 3-27 PROBABILITY DENSITY CONTOUR MAP OF SUBMARINE'S POSITION WITH KNOWN CONSTANT VELOCITY AND UNIFORM HEADING: ELAPSED TIME = 0 UNITS

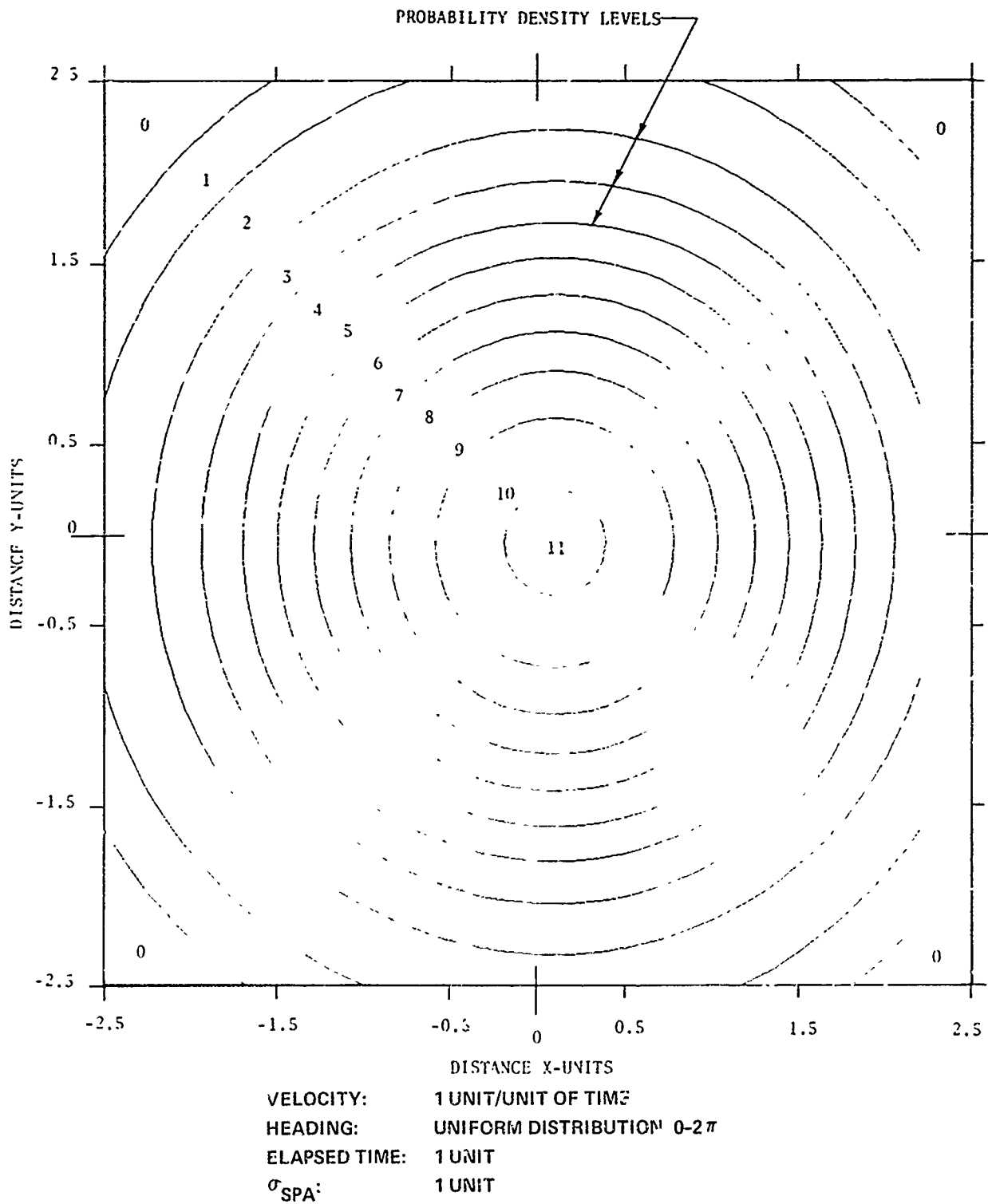


Figure 3-28 PROBABILITY DENSITY CONTOUR MAP OF SUBMARINE'S POSITION WITH KNOWN CONSTANT VELOCITY AND UNIFORM HEADING: ELAPSED TIME = 1 UNIT

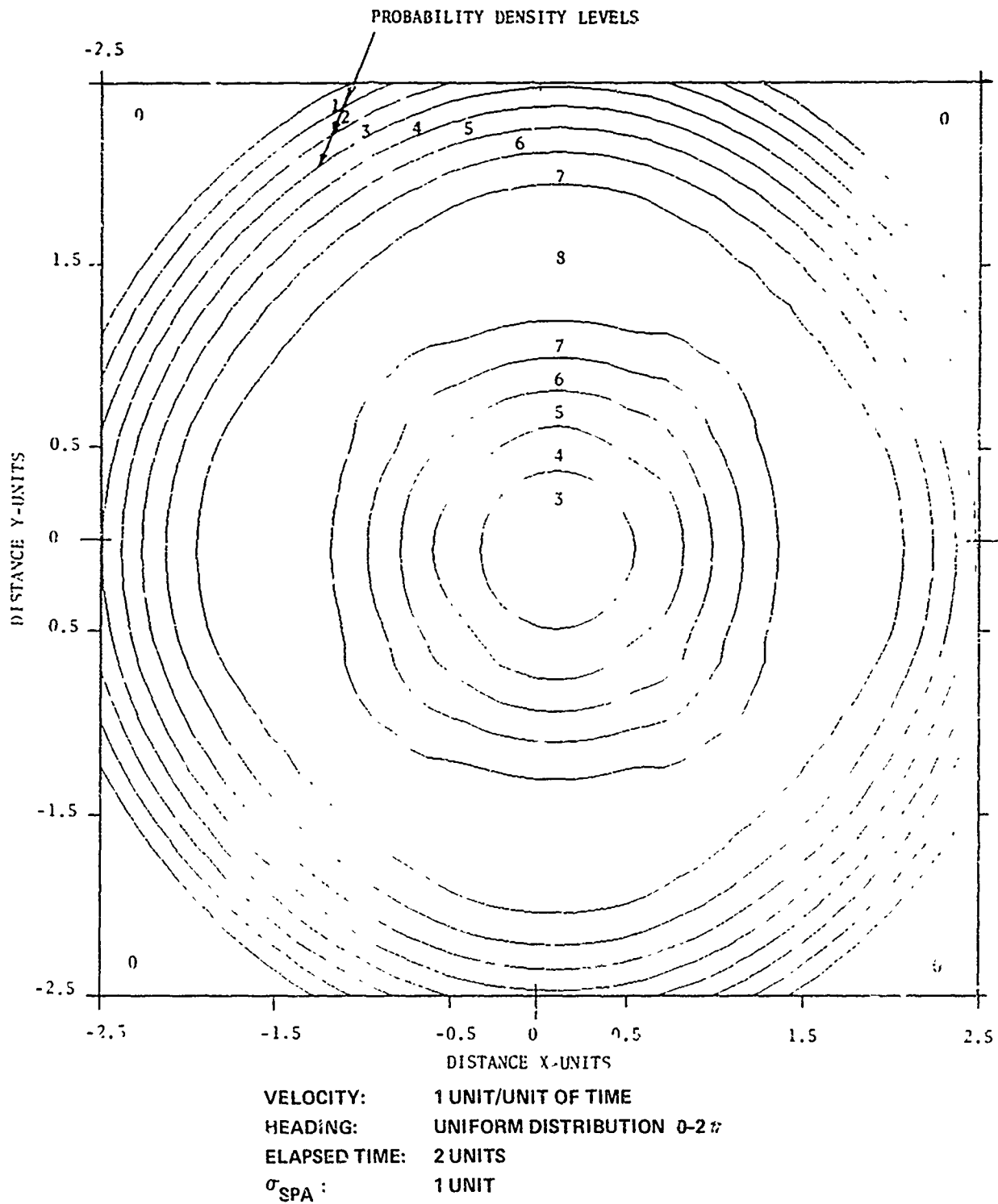


Figure 3-29 PROBABILITY DENSITY CONTOUR MAP OF SUBMARINE'S POSITION WITH KNOWN CONSTANT VELOCITY AND UNIFORM HEADING: ELAPSED TIME = 2 UNITS

TABLE 3-1 PROBABILITY DENSITY LEVELS FOR ZERO AND ONE UNIT OF ELAPSED TIME

<u>PROBABILITY DENSITY LEVEL</u>	<u>H(u,v)</u>	<u>u</u>	<u>v</u>
0	0 ≤ Prob. < .0005		
1	.0005		.0001
2	.0001		.0002
3	.0002		.0003
4	.0004		.0004
5	.0004		.0005
6	.0005		.0006
7	.0006		.0007
8	.0007		.0008
9	.0008		.0009
10	.0009		.0010
11	.0010		.0011
12	.0011		.0012
13	.0012		.0013
14	.0013		.0014
15	.0014		.0015
16	.0015		

TABLE 3-2 PROBABILITY DENSITY LEVELS FOR TWO UNITS OF ELAPSED TIME

<u>PROBABILITY DENSITY LEVEL</u>	<u>h(u,v)</u>	<u>u</u>	<u>v</u>
0	0 ≤ Prob. < .0002		
1	.0002		.00022
2	.00022		.00024
3	.00024		.00026
4	.00026		.00028
5	.00028		.00030
6	.00030		.00032
7	.00032		.00034
8	.00034		

#### IV. GENERAL STUDY RESULTS

##### 1. Comparison of Sample Results for Exact Solution and Monte Carlo Program

An illustrative comparison of results obtained from an "exact" solution versus those from the Monte Carlo program is shown in Figures 4-1 and 4-2. In these examples it is assumed that the target's velocity components are described by  $N(0,1)$ . The SPA is assumed to be described by a joint circular normal with unity variance and zero mean. The display time is one unit. One sonobuoy is deployed in the uncertainty area and one "look" is obtained at 0.75 units elapsed time.

The similarity between the probability density maps shown in Figures 4-1 and 4-2 appears to be excellent. It should be noted that the computing time on the IBM 370-165 computer utilizing the exact solution is, although not optimum, 92 seconds compared to less than 2.5 seconds for the Monte Carlo program.

##### 2. Effect of Varying Start Grid Size

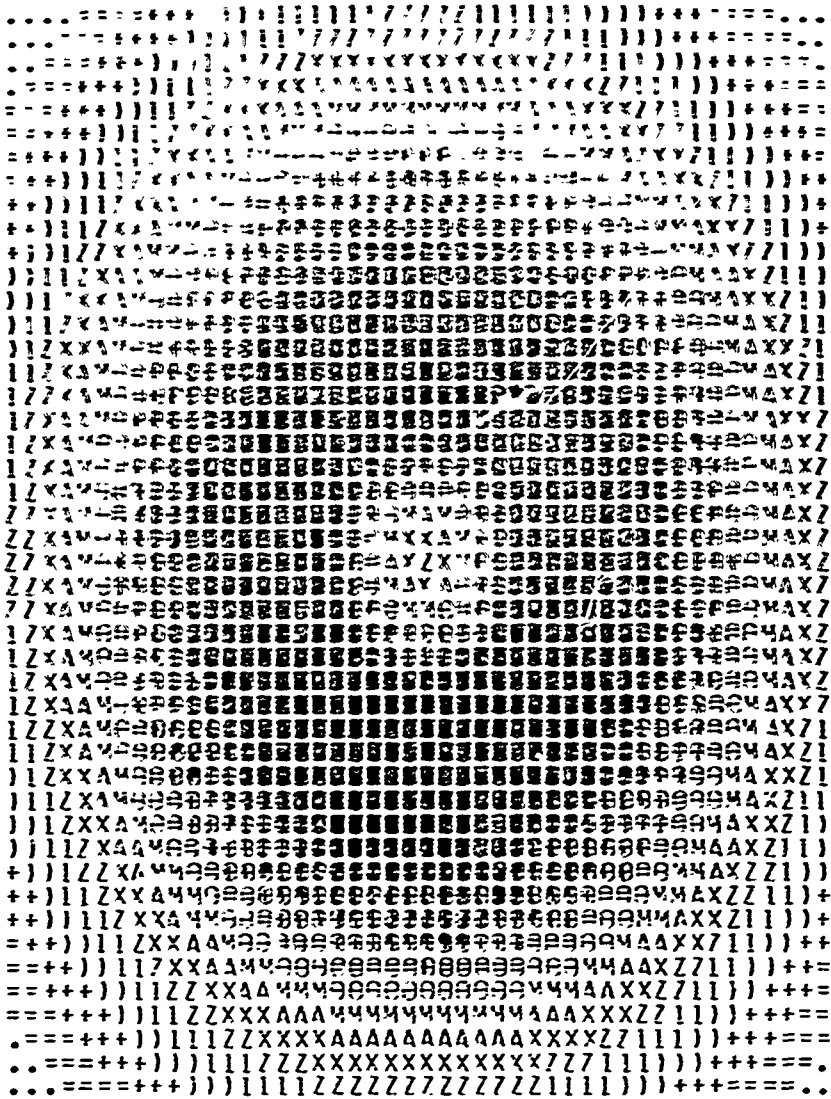
The results shown in Figures 4-3 and 4-4 indicate the effect of varying the size of the start grid. That is, the effect of varying  $C_1$  to determine the boundary of the start grid from the following equation:

$$\frac{x^2}{\sigma_x^2} + \frac{y^2}{\sigma_y^2} = C_1^2$$

The importance of limiting the size of the start grid is that doubling the size of the grid (with  $\Delta x$  and  $\Delta y$  remaining constant) increases the computer run time of the Monte Carlo program by more than a factor of four.



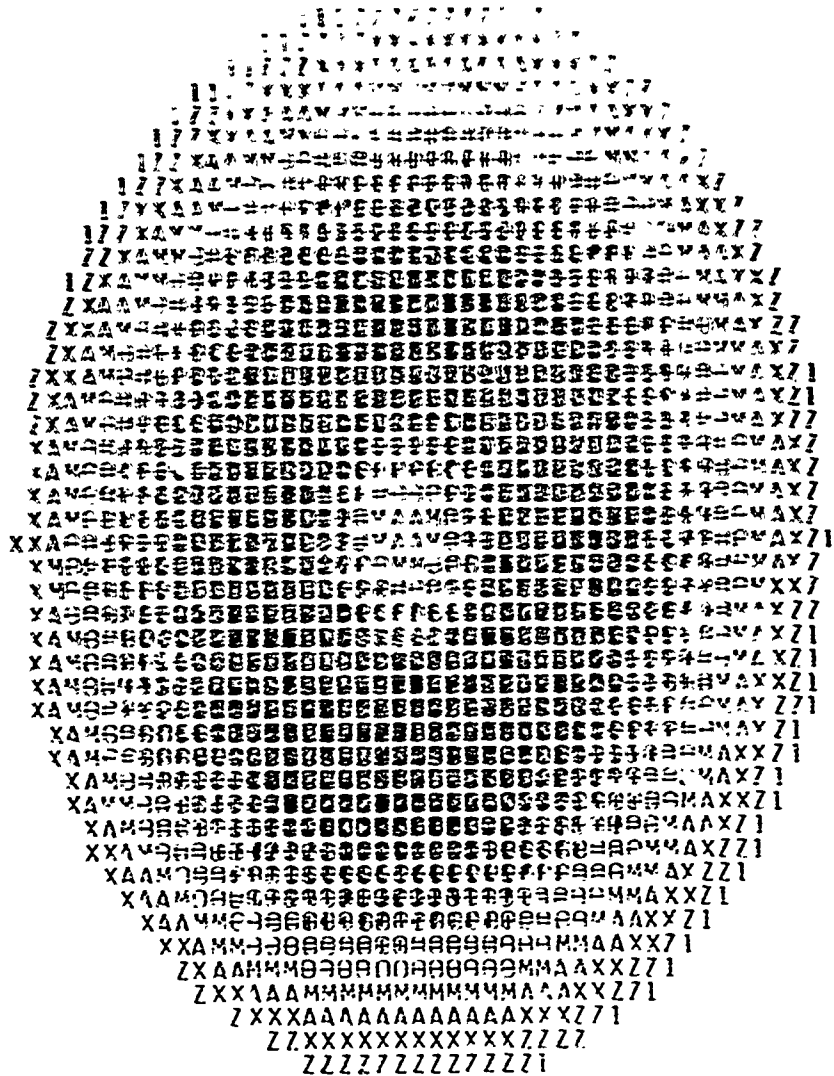
SYMBOLS INDICATE VARIOUS PROBABILITY DENSITY LEVELS  
DARKER AREAS INDICATE HIGHER PROBABILITY DENSITY AREAS



SUBMARINE HEADING: UNIFORM DISTRIBUTION 0-2  $\pi$   
 SUBMARINE VELOCITY: x & y COMPONENTS NORMAL WITH  
 ZERO MEAN AND UNITY VARIANCE  
 ELAPSED TIME: 1 UNIT  
 NUMBER OF  
 SONOBUOYS: 1, NUMBER OF "LOOKS": 1  
 TIME OF "LOOK": 0.75

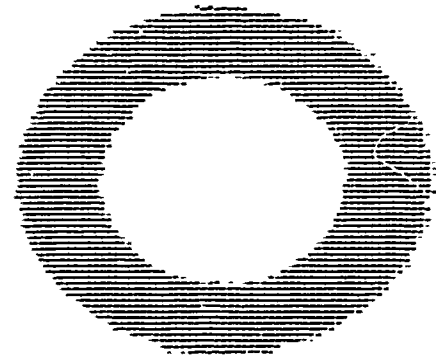
Figure 4-1 PROBABILITY DENSITY OF SUBMARINE'S POSITION WITH RAYLEIGH DISTRIBUTION IN VELOCITY AND UNIFORM HEADING: EXACT COMPUTATIONAL METHOD

SYMBOLS INDICATE AREAS PROBABLE BY DENSITY LEVELS  
 DARKER AREAS INDICATE HIGHER PROBABILITY DENSITY AREAS



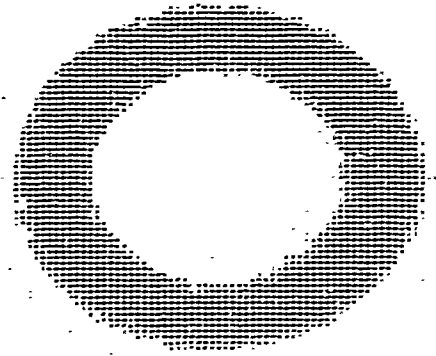
SUBMARINE HEADING: UNIFORM DISTRIBUTION 0-2 $\pi$   
 SUBMARINE VELOCITY: x & y COMPONENTS NORMAL WITH  
 ZERO MEAN AND UNITY VARIANCE  
 ELAPSED TIME: 1 UNIT  
 NUMBER OF  
 SONOBUOYS: 1, NUMBER OF "LOOKS": 1  
 TIME OF "LOOK": 0.75

Figure 4-2 PROBABILITY DENSITY OF SUBMARINE'S POSITION WITH RAYLEIGH  
 DISTRIBUTION IN VELOCITY AND UNIFORM HEADING: MONTE  
 CARLO METHOD



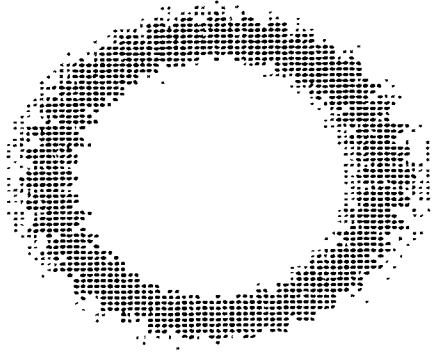
$C_1 = 2.40$

30



$C_1 = 2.0$

3b



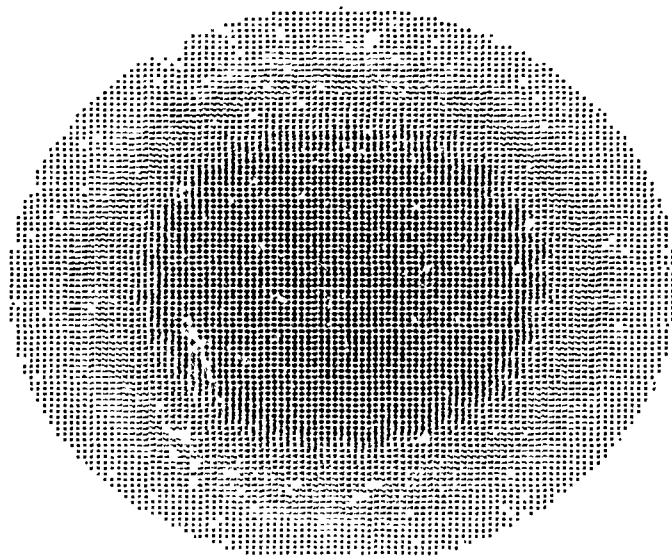
$C_1 = 0$

3a

VELOCITY: 12.5 KNOTS  
 HEADING: UNIFORM DISTRIBUTION 0-2  $\pi$

SPA SIZE:  $\sigma_x = 25$  n.mi.  
 $\sigma_y = 25$  n.mi.  
 $\Delta x = \Delta y = 4$  n.mi.  
 DISPLAY TIME: 8 HOURS

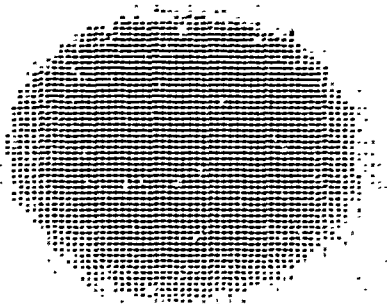
Figure 4-3 PROBABILITY DENSITY OF SUBMARINE'S POSITION WITH KNOWN  
 CONSTANT VELOCITY AND UNIFORM HEADING: FOR VARIATIONS  
 IN START GRID SIZE



$C_1 = 1.6 \sigma$

VELOCITY: RAYLEIGH DISTRIBUTION

HEADING: UNIFORM DISTRIBUTION 0-2 $\pi$



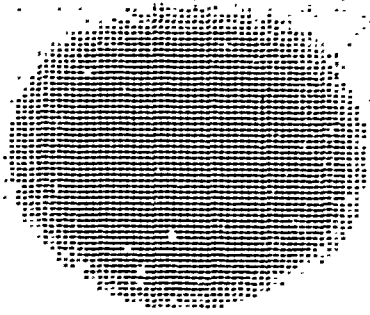
$C_1 = 2 \sigma$

SPA SIZE:

$\sigma_x = 25$  n.mil.

$\sigma_y = 25$  n.mil.

$\Delta x = \Delta y = 4$  n.mil.



$C_1 = 3 \sigma$

DISPLAY TIME: 8 HOURS

Figure 4-4 PROBABILITY DENSITY OF SUBMARINE POSITION WITH RAYLEIGH DISTRIBUTION IN VELOCITY AND UNIFORM HEADING: FOR VARIATION IN START GRID SIZE

For both Figures 4-3 and 4-4, the SPA is assumed to be a joint circular normal with a standard deviation of 25 n. mi. In Figure 4-3 the target is assumed to have a known constant velocity of 12.5 knots and a uniformly distributed heading between 0 and  $2\pi$ . In Figure 4-4 the target's velocity is described by a Rayleigh distribution having a mean of 15 knots and a uniform heading between 0 and  $2\pi$ .

The following list associates the radius,  $C_1$ , of the start grids with each of the illustrations shown on the two Figures 4-3 and 4-4.

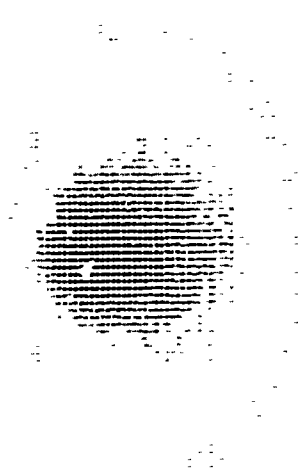
<u>Illustration</u>	<u><math>C_1</math></u>
4-3a	$1\sigma$
4-3b	$2\sigma$
4-3c	$2.4\sigma$
4-4a	$1.6\sigma$
4-4b	$2\sigma$
4-4c	$3\sigma$

From these limited results, the  $2\sigma$  boundary appears to be satisfactory for use in analyses. Thus, for the additional results presented in this report, the  $2\sigma$  boundary is used for the start grid. This encompasses approximately 90% of the probability density which describes the SPA.

### 3. Effect of Varying the Variance in Target Heading

Figure 4-5 presents results obtained due to varying the amount of spread (variance) of the probability density function describing the target's heading. In this example the target's velocity is given by the following probability density:

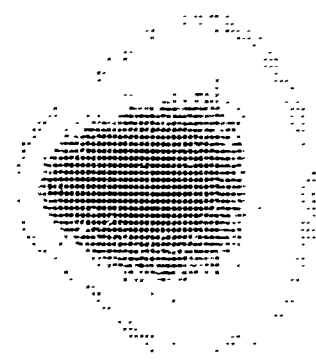
$$f(v) = K \exp \left\{ -\frac{1}{2} \frac{(v-12.5)^2}{64} \right\} \quad -16 < v < 16$$



$\Lambda_m = 1$   
5a



$\Lambda_m = 2$   
5b



$\Lambda_m = 4$   
5c



$\Lambda_m = 3$   
5d

VELOCITY:  $k \exp(-1/2 \frac{(v-12.5)^2}{64}) - 16 < v < 16$

HEADING:  $\frac{1}{2\pi I_0(\Lambda_m)} \exp(\Lambda_m \cos \Theta)$

SPA SIZE:  $\sigma_x = 25$  n.mi.  
 $\sigma_y = 25$  n.mi.  
 $\Delta x = \Delta y = 4$  n.mi.

DISPLAY TIME: 8 HOURS

□ DATUM

Fig. 4-5 PROBABILITY DENSITY OF SUBMARINE'S POSITION WITH RANDOM VELOCITY AND HEADING: FOR VARIANCE VARIATION IN HEADING DISTRIBUTION

In this case the velocity is assumed to be a constant (12.5 knots) plus a random part described by a normal distribution over the interval from  $-2\sigma$  to  $2\sigma$  (where  $\sigma^2 = 64$ ). The constant,  $K$ , is inserted so that the function will integrate to one. It should be noted that only the magnitude of the velocity is determined from  $\hat{r}(\gamma)$ .

The heading distribution is given by:

$$p(\theta, \Lambda_m) = \frac{1}{2\pi I_0(\Lambda_m)} \exp\{\Lambda_m \cos \theta\}$$

The results shown in Figure 4-5 are obtained for a number of values of  $\Lambda_m$ . The values of  $\Lambda_m$  associated with each of the illustrations shown are listed below:

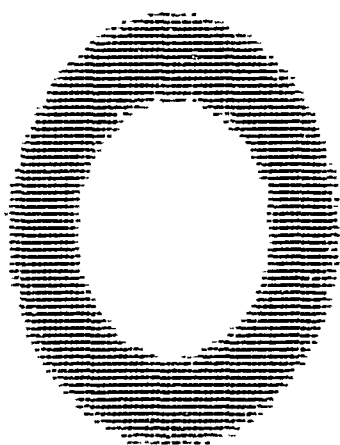
<u>Illustration</u>	<u><math>\Lambda_m</math></u>
4-5a	1
5b	2
5c	4
5d	8

Curves of  $p(\theta, \Lambda_m)$  can be found in Reference 2\* page 338 for a number of values of  $\Lambda_m$ .

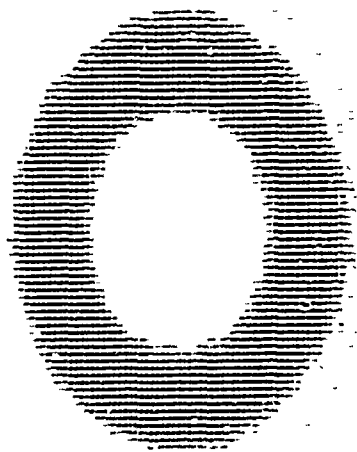
#### 4. Effect of Varying the Variance in Target Velocity

A presentation of selected examples to show the effect of varying the variance of target velocity when the target's heading is uniformly distributed between 0 and  $2\pi$  is presented in Figure 4-6.

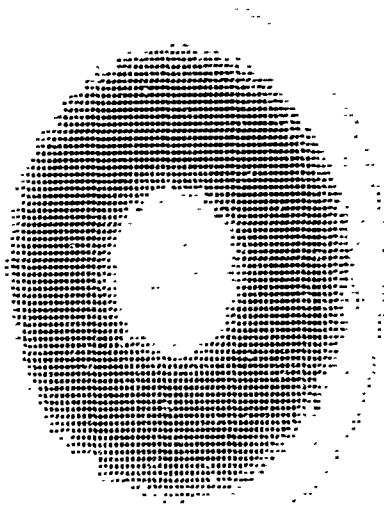
\*Reference 2. Detection, Estimation and Modulation Theory, Part I, Harry L. Van Trees, Published 1968 by John Wiley and Sons



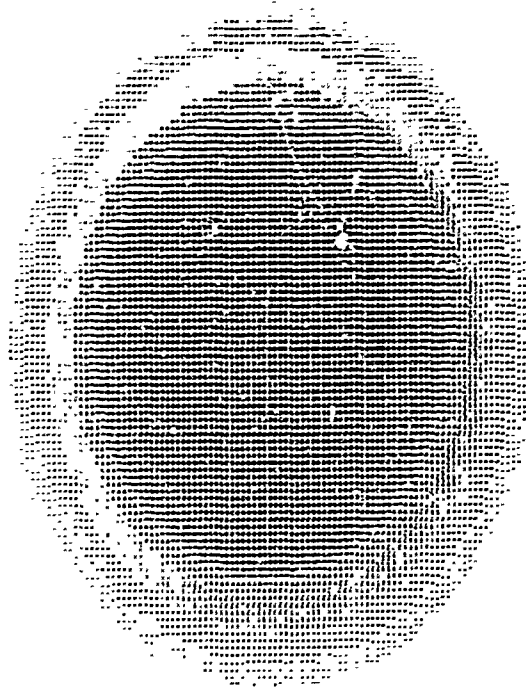
$\sigma_v = 1$   
6a



$\sigma_v = 4$   
6b



$\sigma_v = 16$   
6c



$\sigma_v = 36$   
6d

VELOCITY:  $k \exp \left( -\frac{1}{2} \frac{(v - 12.5)^2}{\sigma_v^2} \right) \cdot 2\sigma_v < v < 2\sigma_v$   
HEADING: UNIFORM DISTRIBUTION  $0 - 2\pi$

SPA SIZE:  $\sigma_x = 25$  n.mi.  
 $\sigma_y = 25$  n.mi.  
 $\Delta x = \Delta y = 4$  n.mi.

DISPLAY TIME: 8 HOURS

Figure 4-6 PROBABILITY DENSITY OF SUBMARINE'S POSITION WITH RANDOM VELOCITY AND UNIFORM HEADING: FOR VARIANCE VARIATION IN VELOCITY DISTRIBUTION



The probability density which describes the velocity is:

$$p(v) = K \exp \left\{ -\frac{1}{2} \frac{(v - 12.5)^2}{\sigma_v^2} \right\} \quad -2\sigma_v < v < 20\sigma_v$$

The target's heading is assumed to be uniformly distributed between 0 and  $2\pi$ .

The values of  $\sigma_v^2$  associated with each of the illustrations shown in Figure 4-6 are listed below:

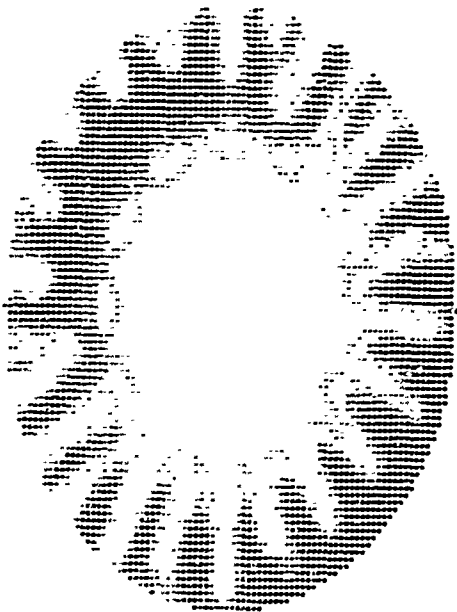
<u>Illustration</u>	<u><math>\sigma_v^2</math></u>
4-6a	1
6b	4
6c	16
6d	36

It is interesting to note that as  $\sigma_v^2$  increases the high probability areas spread more toward the datum than away from it. That is, the radius of a circle contouring the outer edge of the darker area has very little change over the range of  $\sigma_v^2$  while the radius of a circle containing the inner edge of the darker area decreases as  $\sigma_v^2$  increases.

#### 5. Effect of Varying the Number of MC Submarines/Start Grid

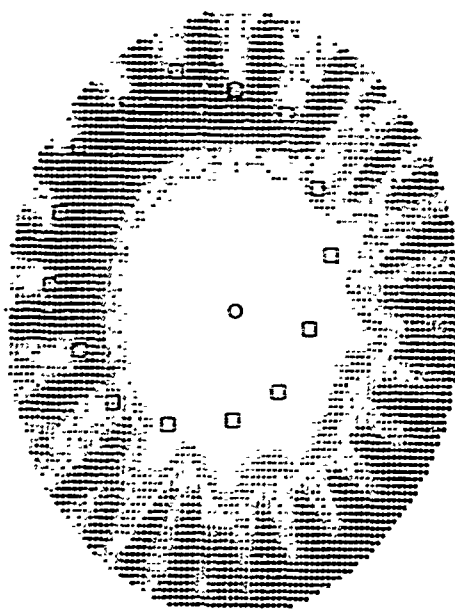
Sample computer results obtained by varying the number of MC submarines in each  $\Delta x$  by  $\Delta y$  area of the start grid are shown in Figure 4-7. This example is for the case of known target velocity with a uniform heading over the interval  $0-2\pi$ . There are 15 sonobuoys deployed in this example. Each sonobuoy is monitored on every other "look" period. The sonobuoys "looks" are spaced at 15 minute intervals over the period from 3 to 9 hours giving a total of 24 "looks".

The importance of limiting the number of MC submarines/grid is that the computing time on the IBM 370-165 computer increases linearly as the number of MC submarines in each  $\Delta x$  by  $\Delta y$  grid increases. The number



NUMBER OF MC  
SUBMARINES/GRID = 12

7a



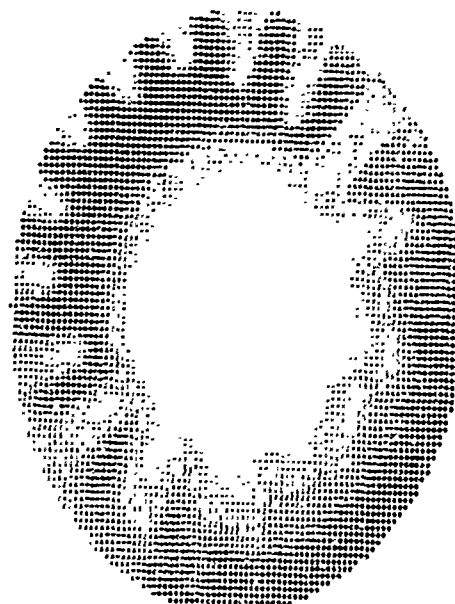
NUMBER OF MC  
SUBMARINES/GRID = 18

7b



NUMBER OF MC  
SUBMARINES/GRID = 24

7c



NUMBER OF MC  
SUBMARINES/GRID = 40

7d

VELOCITY: 12 knots

HEADING: UNIFORM DISTRIBUTION  $0-2\pi$

NUMBER OF SONOBUOYS: 15

NUMBER OF LOOKS: 24

DISPLAY TIME: 9 HOURS

O DATUM

□ DEPLOYED SONOBUOYS

SPA SIZE:  $\sigma_x = 25$  n.mi.

$\sigma_y = 25$  n.mi.

$\Delta y = \Delta x = 3$  n.mi.

Figure 4-7 PROBABILITY DENSITY OF SUBMARINE'S POSITION WITH KNOWN CONSTANT VELOCITY AND UNIFORM HEADING: FOR VARIATION IN NUMBER OF MC SUBMARINES/GRID

of MC submarines/grid associated with each of the illustrations shown in Figure 4-7 is summarized below:

<u>Illustration</u>	<u>MC Submarines/Grid</u>
4-7a	12
7b	18
7c	24
7d	40

In comparing Illustration 4-7a (12 MC submarines/grid) with 4-7d (40 MC submarines/Grid) it is noted that the probability densities resulting from the number of MC submarines/grid are dependent on the location of the sonobuoys. It is for the purpose of showing this effect that the sonobuoys are placed in an offset pattern with respect to datum.

The computing time on the IBM 370-165 computer (central processing unit time) for Illustration 4-7d (40 MC submarines/grid) is 4.1 seconds while the computing time for 4-7c (24 MC submarines/grid) is 2.7 seconds. These times are for the case in which the size of the start grid is determined by a  $2\sigma$  boundary. If the range of the target to the sonobuoy is greater than 12 n. mi., the probability that the sonobuoy detects the target is assumed to be zero. An increase in the values of either of the above parameters will cause an increase in the computing time.

#### 6. Effect of Varying Search Aircraft Time Late in Arriving at Datum

The effect of varying ASW search aircraft time late in arriving at datum of a SPA area and conducting search operations for a constant 6 hour period is presented in Figure 4-8. In this example, the velocity of the target is described by the following joint normal probability distribution:

$$f(v_x, v_y) = \frac{1}{2\pi 96} \exp\left\{-\frac{1}{2} \left(\frac{v_x^2}{144} + \frac{v_y^2}{64}\right)\right\}$$



DISPLAY TIME: 11 HOURS  
 TIME LATE: 5 HOURS

8a



DISPLAY TIME: 9 HOURS  
 TIME LATE: 3 HOURS

8b



DISPLAY TIME: 11 HOURS  
 TIME LATE: 5 HOURS

8c



DISPLAY TIME: 13 HOURS  
 TIME LATE: 7 HOURS

8d

○ DATUM

$$\text{VELOCITY} \sim \frac{1}{\pi \cdot 96} \exp \left\{ -1/2 \left( \frac{v_x^2}{144} + \frac{v_y^2}{16} \right) \right\}$$

SPA SIZE:  $\sigma_x = 25$  n.mi.  
 $\sigma_y = 25$  n.mi.

$\Delta x = \Delta y = 5$  n.mi.

NUMBER OF SONOBUOYS: 15  
 NUMBER OF LOOKS: 24

Figure 4-8 PROBABILITY DENSITY OF SUBMARINE'S POSITION WITH X AND Y VELOCITY COMPONENTS NORMALLY DISTRIBUTED: EFFECT OF TIME LATE

Also, there is an angle of  $45^\circ$  measured in the clockwise direction between the  $x-y$  axis of the SPA plane and the  $v_x-v_y$  axis of the velocity plane. The SPA is described by a joint circular normal distribution with a standard deviation of 25 n. mi.

Illustration 4-8a shows the "growth" of the SPA, without any sonobuoys deployed for an elapsed time interval of 11 hours. Time late for the other illustrations shown in Figure 4-8 are listed below:

<u>Illustration</u>	<u>Time Late, Hours</u>
4-8b	3
4-8c	5
4-8d	7

The results indicate the varying probability densities that occur as time late is increased from 3 and 5 hours to a maximum of 7 hours.

#### 7. Effect of Varying ASW Aircraft Search Time

Computer results which show the effect of varying ASW aircraft search time for a selected time late to datum are presented in Figure 4-9. The SPA is described by a joint circular normal with a standard deviation of 25 n. mi. The velocity components of the target are given by the following distribution:

$$f(v_x, v_y) = \frac{1}{2\pi \cdot 96} \exp \left\{ -\frac{1}{2} \left( \frac{v_x^2}{144} + \frac{v_y^2}{64} \right) \right\}$$

Also, there is an angle of  $45^\circ$  measured from the SPA axis in a clockwise direction between the  $x-y$  axis of the SPA and the  $v_x-v_y$  axis of the target velocity plane.

For each case shown in Figure 4-9 the search operation begins at seven hours time late. The display times and number of sonobuoy "looks" associated with the illustrations as shown in Figure 4-9 are listed below:



NUMBER OF LOOKS: 24  
 DISPLAY TIME: 13 HOURS  
 9c

SPA SIZE: = 25 n.mi.  
 = 25 n.mi.  
 $\Delta x = \Delta y = 5$  n.mi.



NUMBER OF LOOKS: 16  
 DISPLAY TIME: 11 HOURS  
 9b

NUMBER OF SONOBOOYS: 15  
 TIME LATE: 7 HOURS



NUMBER OF LOOKS: 8  
 DISPLAY TIME: 9 HOURS  
 9a

$$\text{VELOCITY} \sim \frac{1}{\pi \cdot 96} \exp \left\{ -1/2 \left( \frac{v_x^2}{144} + \frac{v_y^2}{16} \right) \right\}$$

O DATUM

Figure 4-9 PROBABILITY DENSITY OF SUBMARINE'S POSITION WITH X AND Y VELOCITY COMPONENTS NORMALLY DISTRIBUTED; FOR SELECTED SEARCH TIMES

<u>Illustration</u>	<u>Display Time, Hours</u>	<u>Number of Sonobuoy Looks</u>
4-9a	9	8
4-9b	11	16
4-9c	13	24

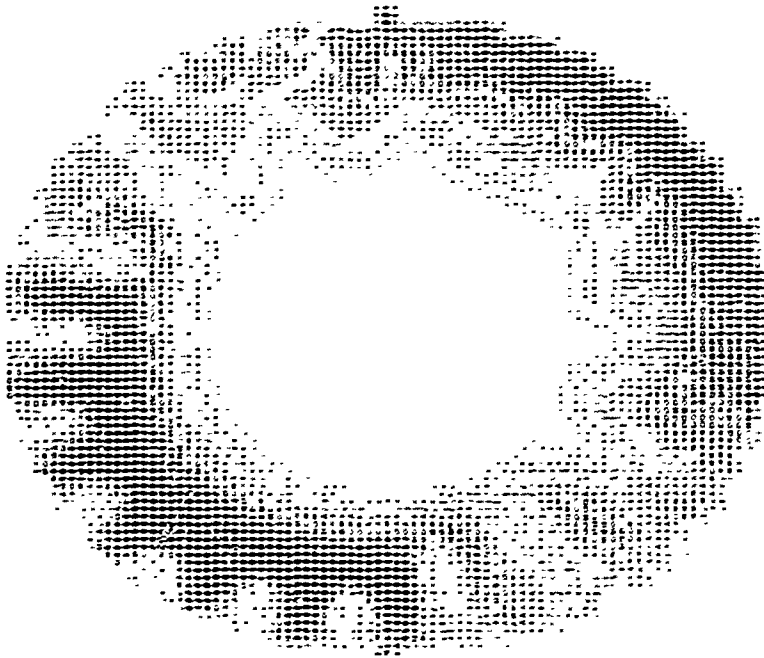
The results indicate that the sonobuoys in effect search out an increasing portion of the SPA as the search time and number of "looks" by the sonobuoy field increase from 9 to 13 hours and from 8 to 24 "looks" respectively.

#### 8. Effect of Linear Smoothing Between Grid Points

Figures 4-10 and 4-11 indicate the effect of linear smoothing between calculated grid points. Figure 4-10 presents results for a medium speed (12 knots) target and Figure 4-11 for a high speed (24 knots) target. The target's heading in both cases is uniformly distributed between 0 and  $2\pi$ . The SPA is described by a joint circular normal with a standard deviation of 25 n. mi. A field of 15 sonobuoys is deployed within the SPA. Each sonobuoy is monitored on every other "look". The "looks" are taken during the elapsed time interval from 3 to 9 hours at increments of 15 minutes.

In Illustration 4-10b the grid is calculated for a  $\Delta x = \Delta y = 6$  n. mi. Additional points are then calculated between these grid points by linearly averaging between adjacent grid points. This provides an effective grid size of 3 n. mi. on the display. Illustration 4-10a is calculated for a  $\Delta x = \Delta y = 3$  n. mi. for comparison purposes.

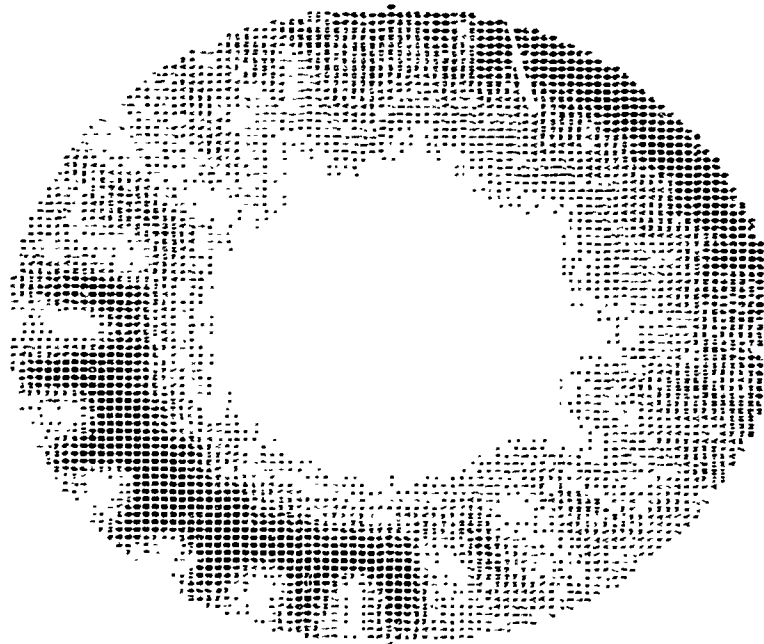
Referring to Illustration 4-11b in Figure 11, the display is first calculated for a grid size (  $\Delta x$  by  $\Delta y$  ) of 12 n. mi. and then reduced to one of 6 n. mi. by the above smoothing technique. Illustration 4-11a is calculated for  $\Delta x = \Delta y = 6$  n. mi. in order to compare the two cases. The resulting probability densities for these cases are fairly similar. Thus, the importance of the linear smoothing technique is in reducing computing time by a factor of approximately 4 for a specified  $\Delta y$  by  $\Delta x$  grid selected for the display.



WITH SMOOTHING

10 b

NUMBER OF SONOBUOYS: 15  
 NUMBER OF LOOKS: 24  
 DISPLAY TIME: 9 HOURS



WITHOUT SMOOTHING

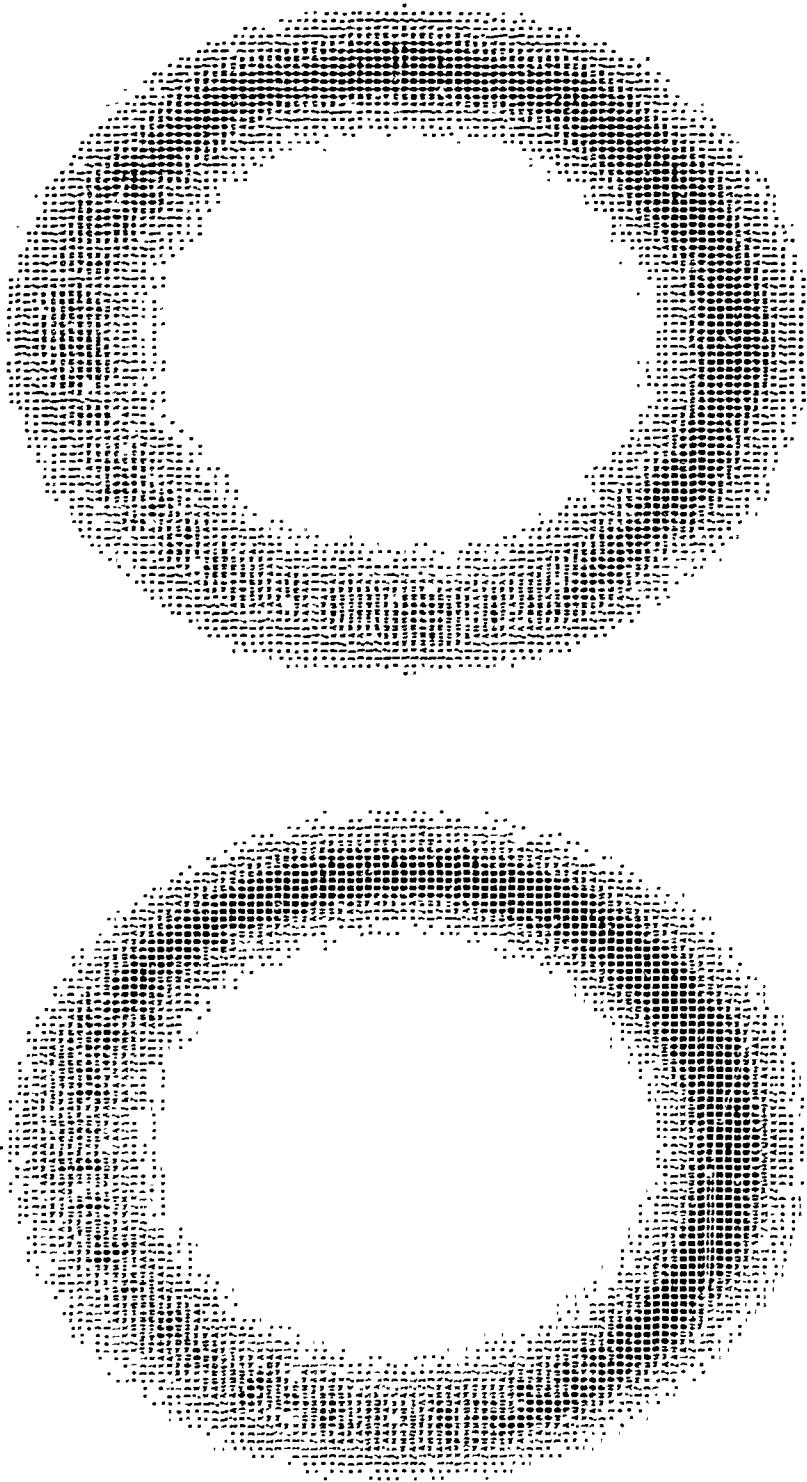
10 a

VELOCITY: 12 KNOTS  
 HEADING: UNIFORM DISTRIBUTION 0-2  $\pi$   
 SPA SIZE:  $\sigma_x = 25$  n.mi.  
 $\sigma_y = 25$  n.mi.

$\Delta x = \Delta y = 3$  n.mi.

Figure 4-10 PROBABILITY DENSITY OF SUBMARINE'S POSITION WITH KNOWN MEDIUM VELOCITY AND UNIFORM HEADING: EFFECT OF LINEAR SMOOTHING BETWEEN CALCULATED GRID POINTS





WITHOUT SMOOTHING

11-a

VELOCITY: 24 knots

HEADING: UNIFORM DISTRIBUTION  $0-2\pi$

NUMBER OF SONOBUOYS: 15

NUMBER OF LOOKS: 24

DISPLAY TIME: 9 HOURS

WITH SMOOTHING

11-b

SPA SIZE:

$\sigma_x = 25$  n.mi.

$\sigma_y = 25$  n.mi.

$\Delta x = \Delta y = 6$  n. mi.

Figure 4-11 PROBABILITY DENSITY OF SUBMARINE'S POSITION WITH KNOWN HIGH VELOCITY AND UNIFORM HEADING: EFFECT OF LINEAR SMOOTHING BETWEEN CALCULATED GRID POINTS

9. Effect of a Large Variation in Number of MC Submarines/Grid for a Uniform Target Heading and Rayleigh Distribution in Velocity

Figure 4-12 presents computer results obtained when target velocity is described by a Rayleigh distribution with a mean of 15 knots and target heading is described by a uniform distribution over the interval  $0-2\pi$ . Illustration 4-12a in Figure 4-12 presents results obtained for a display time of 9 hours for the case in which no sonobuoys are deployed. Illustrations 4-12b and 4-12c present results for the case in which 15 sonobuoys are deployed. Sonobuoy "looks" are taken at 15 minute intervals over the elapsed time interval from 3 to 9 hours for a total of 24 "looks". Each sonobuoy is monitored on every other "look". The number of MC submarines/grid is relatively small for the case shown in Illustration 4-12b whereas it is large for the case shown in Illustration 4-12c.

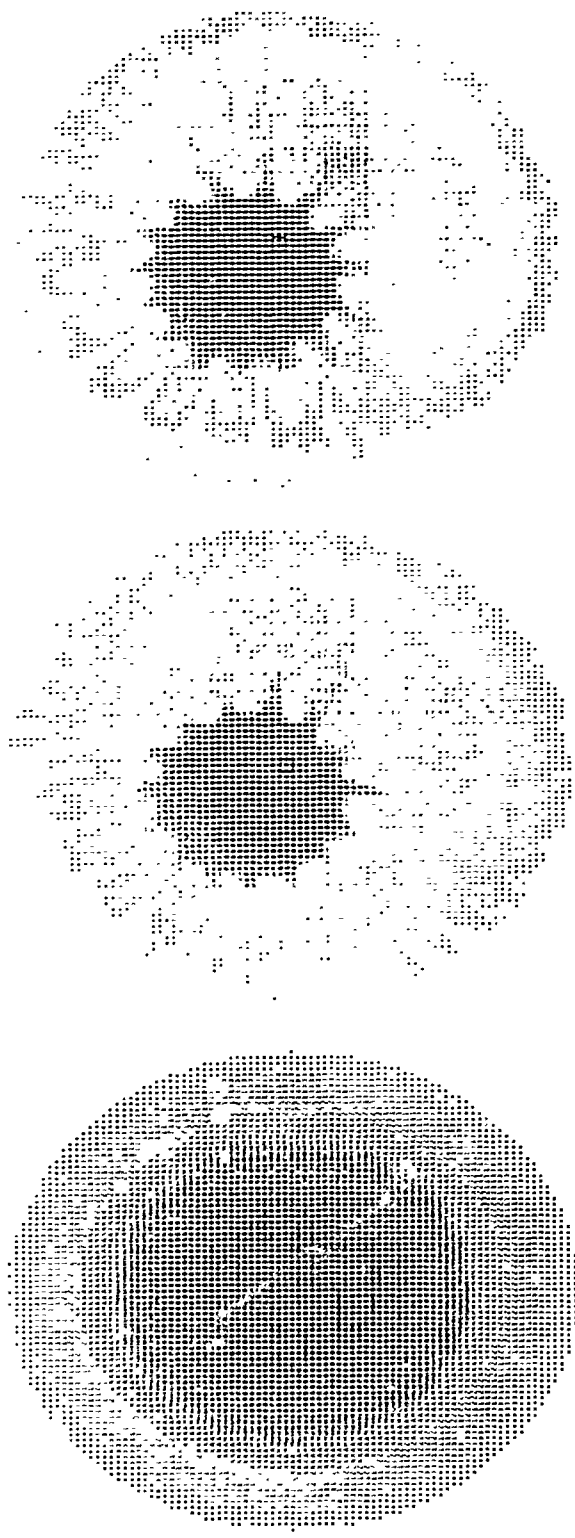
The computing time on the IBM 370-165 computer for the case shown in Illustration 4-12b is 6.53 seconds whereas, it is 11.64 seconds for 4-12c. The boundary of the start grid has a radius of  $2\sigma$ . If the target is more than 10 n. mi. from a sonobuoy, the probability of detection is assumed to be zero. Increasing the sonobuoy detection range from 10 n. mi. to 25 n. mi. increases the computing time of 4-12c from 11.64 seconds to 14.75 seconds.

10. Effect of Changes in Target Velocity on Probability of Detection

Figure 4-13 presents computer results for the case in which the probability of detection of the target by the sonobuoy field is a function of the target's velocity. As stated previously in Section III of this Report, the probability of detection is assumed to be:

$$PD = e^{-\alpha R^2}$$

where  $\alpha$  is an input to the model and  $R$  is the range from each sonobuoy to the target. Referring to Illustration 4-13b in Figure 4-13 the probability



WITHOUT SONOBUOYS  
12a

COMPUTING TIME: 6.53 sec  
12b

COMPUTING TIME: 11.64 sec  
12c

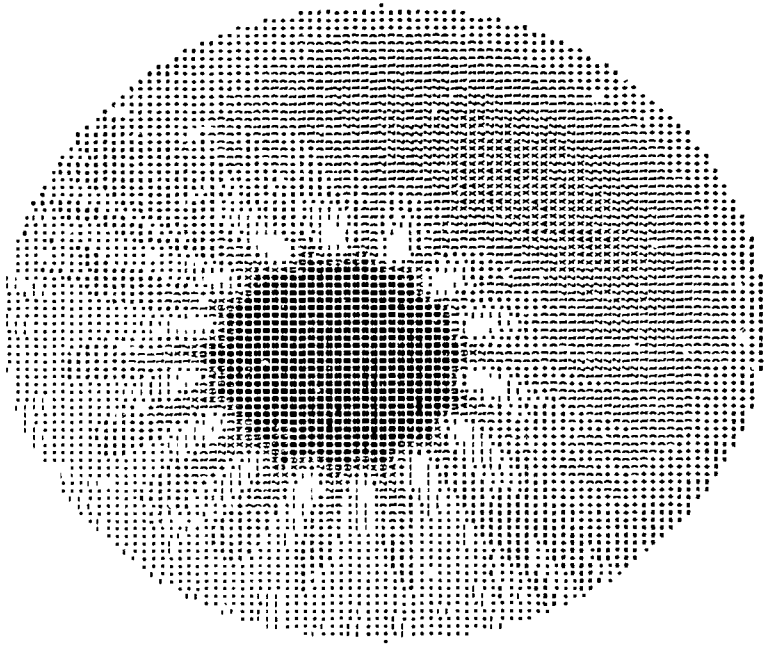
SPA SIZE:  $\sigma_x = 25$  n.mi.  
 $\sigma_y = 25$  n.mi.

$\Delta x = \Delta y = 5$  n.mi.

$$\text{VELOCITY: } \sim \frac{1}{\pi \cdot 144} \exp \left\{ -\frac{1}{2} \left( \frac{v_x^2}{144} + \frac{v_y^2}{144} \right) \right\}$$

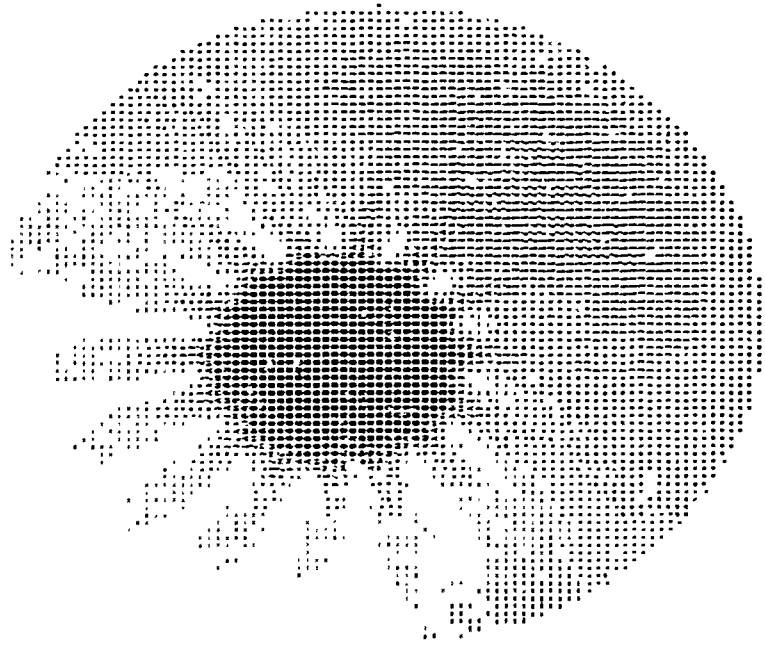
NUMBER OF SONOBUOYS: 15  
DISPLAY TIME: 9 HOURS

Figure 4-12 PROBABILITY DENSITY OF SUBMARINE'S POSITION WITH RAYLEIGH DISTRIBUTION IN VELOCITY AND UNIFORM HEADING: FOR VARIATION IN NUMBER OF MC SUBMARINE'S/GRID



CONSTANT PM GRID  
13a

$$\text{VELOCITY} \sim \frac{1}{\pi \cdot 144} \exp \left\{ -\frac{1}{2} \left( \frac{v_x^2}{144} + \frac{v_y^2}{144} \right) \right\}$$



VARIABLE PM GRID  
13b

SPA SIZE:  $\sigma_x = 25 \text{ n.mi.}$   
 $\sigma_y = 25 \text{ n.mi.}$   
 $\Delta x = \Delta y = 5 \text{ n.mi.}$

NUMBER OF SONOBUOYS: 15  
 DISPLAY TIME: 9 HOURS

Figure 4-13 PROBABILITY DENSITY OF SUBMARINE'S POSITION WITH RAYLEIGH DISTRIBUTION IN VELOCITY AND UNIFORM HEADING: EFFECT OF PM GRID AS A FUNCTION OF TARGET'S VELOCITY

of detection is assumed to be of the form:

$$PD = e^{-\alpha R^2 V_c / v} \quad \text{where } V_c < v$$

$$= e^{-\alpha R^2} \quad \text{where } V_c > v$$

where  $v$  is a velocity random variable and  $V_c$  is an input to the model. In effect, this indicates that the target's radiated noise is constant for velocities from 0 to  $V_c$  and that the radiated noise subsequently increases linearly as  $v > V_c$ . In this example,  $V_c$  is equal to 9 knots.

For the case shown in Illustration 4-13a of Figure 4-13,  $PD$  is equal to:

$$PD = e^{-\alpha R^2 V_c / 15}$$

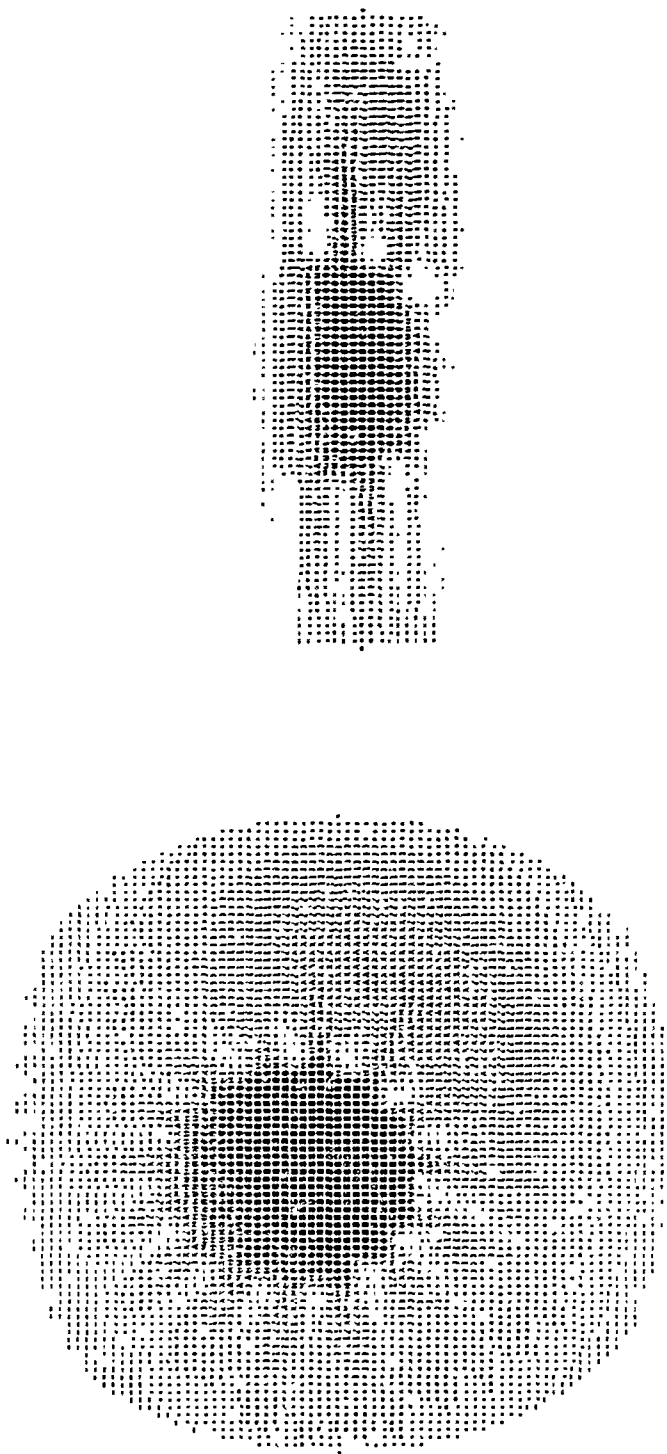
where  $v = 15$  knots is the expected value of the target's velocity which is described as a Rayleigh distribution. The heading of the target is assumed to be uniformly distributed between 0 and  $2\pi$ . The SPA is described by a joint circular normal with a standard deviation of 25 n. mi. A field of 15 sonobuoys is deployed and 24 "looks" are taken.

A comparison of these results show the increased capability of the sonobuoys to detect the target submarine as its' speed increases beyond a value  $v = 9$  knots. This is indicated by the changes in probability density in the second quadrant for the variable  $PM$  grid (Illustration 4-13b) compared to that for the constant  $PM$  grid (Illustration 4-13a).

#### 11. Effect of Variance of Variations in Target's Velocity

Figure 4-14 indicates the effect of variance variations in the velocity of the target. The target's velocity is described by the following probability distribution.

$$f(v_x, v_y) = \frac{1}{2\pi \cdot 12\sigma_{v_y}} \exp\left\{-\frac{1}{2} \left( \frac{v_x^2}{144} + \frac{v_y^2}{\sigma_{v_y}^2} \right)\right\}$$



$$\sigma_{v_y}^2 = 64$$

14a

$$\text{VELOCITY: } \sim \frac{1}{\pi \cdot 12 \sigma_{v_y}} \exp \left\{ -\frac{1}{2} \left( \frac{v_x^2}{144} + \frac{v_y^2}{\sigma_{v_y}^2} \right) \right\}$$

$$\sigma_{v_y}^2 = 1$$

14b

$$\text{SPA SIZE: } \sigma_x = 25 \text{ n.mi.}$$

$$\sigma_y = 25 \text{ n.mi.}$$

$$\Delta x = \Delta y = 5 \text{ n.mi.}$$

NUMBER OF SONOBUOYS: 15  
 NUMBER OF LOOKS: 24  
 DISPLAY TIME: 9 HOURS

O DATUM POINT

Figure 4-14 PROBABILITY DENSITY OF SUBMARINE'S POSITION WITH X AND Y VELOCITY COMPONENTS NORMALLY DISTRIBUTED: FOR VARIANCE VARIATIONS IN VELOCITY

In Illustration 14a the variance of the  $\sigma_{v_y}^2$  components of velocity is 64. It is equal to 1 for the case shown in Illustration 14b. The SPA is described by a joint circular normal distribution with a standard deviation of 25 n. mi. for both examples presented in Figure 4-14. Also, 15 sonobuoys are deployed with a total of 24 "looks".

Figure 4-14 indicates that as  $\sigma_{v_y}^2$  decreases (with  $\sigma_{v_x}^2$  remaining constant) the uncertainty of the target's heading decreases. Hence, when the velocity of the target is described by a joint normal and even when the means of the velocity components are zero, information is available on the target's heading when the variances of the velocity components are unequal.

## 12. Effect of Biasing Target Heading

Figure 4-15 presents results obtained for the case in which target velocity is described by the following probability density:

$$f(v_x, v_y) = \frac{1}{2\pi \cdot 144} \exp \left\{ -\frac{1}{2} \left( \frac{(v_x - 12)^2}{144} + \frac{v_y^2}{144} \right) \right\}$$

The initial SPA is described by a joint circular normal with a standard deviation of 25 n. mi. A field of 15 sonobuoys are deployed within the SPA. A total of 24 "looks" are taken during the elapsed time interval between 3 to 9 hours. Each sonobuoy is monitored on every other "look".

The effect of inserting a mean value of 12 knots to the component of target velocity is to bias the heading of the target. The joint probability density of the target's velocity and heading is given by:

$$g(v, \theta) = \frac{v}{2\pi\sigma^2} e^{-\frac{(v^2 + u_x^2)}{2\sigma^2}} e^{\frac{v u_x \cos \theta}{\sigma^2}}$$

(This equation is presented in Reference 3,\* page 196) where  $\sigma^2 = 144$  and  $u_x = 12$ . Integrating out  $\theta$  results in the following velocity distribution:

$$g(v) = \frac{v}{\sigma^2} \exp \left\{ -\frac{(v^2 + u_x^2)}{2\sigma^2} \right\} I_0 \left( \frac{v u_x}{\sigma^2} \right)$$

\*Reference 3: Probability Random Variables on Stochastic Processes by Athanasios Papoulis Published 1965 by McGraw-Hill.



$$E \{ v \} = 12 \text{ knots}$$

$$\text{VELOCITY} \sim \frac{1}{2\pi \cdot 144} \exp \left\{ -1/2 \left( \frac{v_x - 12}{144} \right)^2 + \frac{v_y^2}{144} \right\}$$

SPA SIZE:  $\sigma_x = 25 \text{ n.mi.}$   
 $\sigma_y = 25 \text{ n.mi.}$

$$\Delta x = \Delta y = 5 \text{ n.mi.}$$

NUMBER OF SONBUOYS: 15  
 NUMBER OF LOOKS: 24  
 DISPLAY TIME: 9 HOURS

Figure 4-15 PROBABILITY DENSITY OF SUBMARINE'S POSITION WITH X AND Y VELOCITY COMPONENTS NORMALLY DISTRIBUTED: EFFECT OF BIASED HEADING



Curves of  $g(\nu)$  and the heading distribution  $g(\theta)$  are presented in Reference 2 on page 362 and 363 for a number of values of  $\gamma = \frac{u_x^2}{2\sigma^2}$ .

The results shown in Figure 4-15 indicate that the effect of biasing submarine heading is to shift the high density area of probable target positions to a sector located outside of the ring of deployed sonobuoys.

### 13. Accumulated Probability Density of Target Position with Search Time

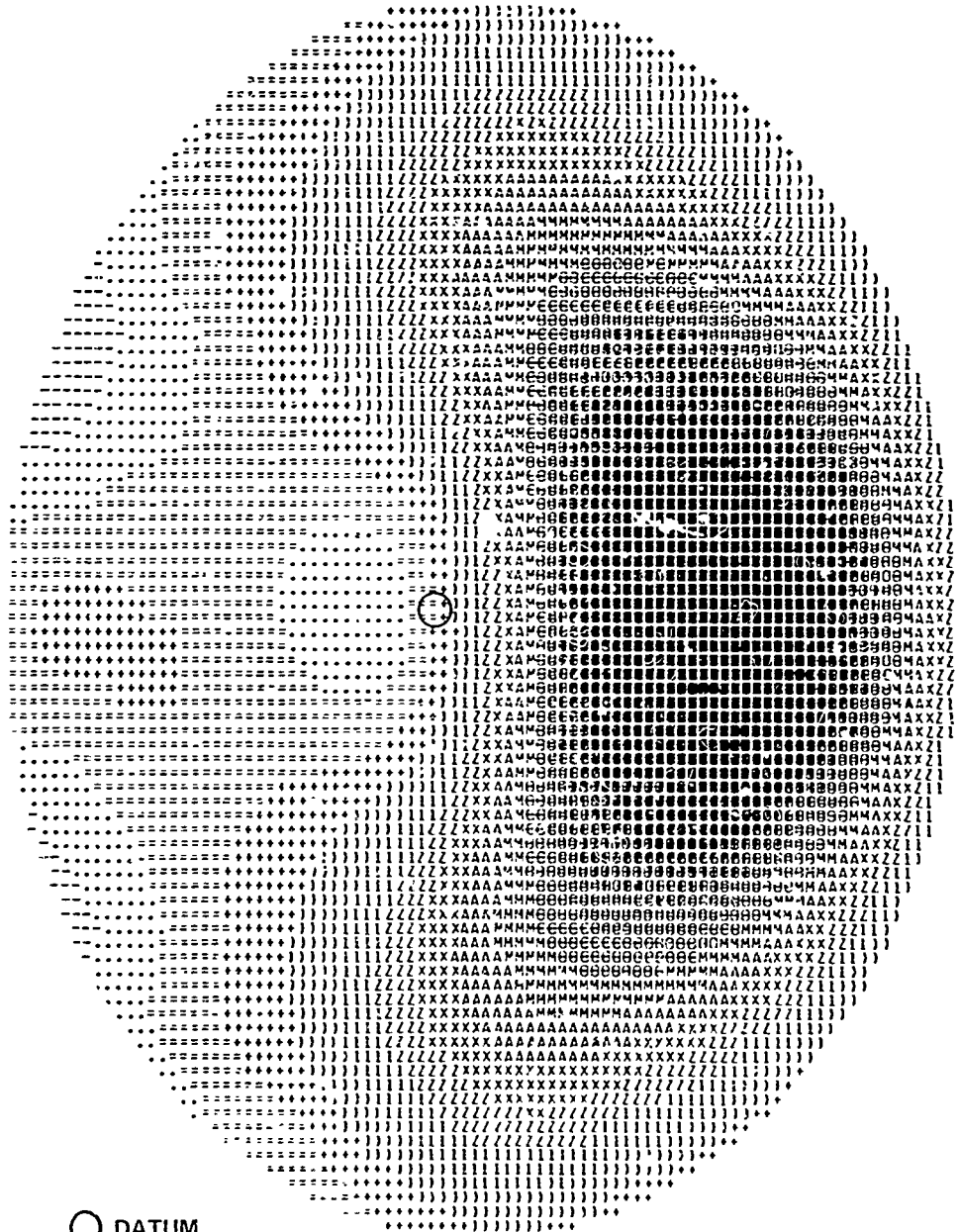
A limited effort has been conducted toward development of a program which computes the probability that the target will pass through a  $\Delta x$  by  $\Delta y$  grid during the search time from  $T_1$  to  $T_2$ . Some sample results of this effort are presented in Figures 4-17 and 4-18. For Figures 4-17 and 4-18 the velocity of the target is assumed to be 13 knots. The heading of the target is described by the following distribution:

$$P(\theta) = \frac{1}{2\pi I_0(1)} \exp\{\cos \theta\}$$

The accumulated time is the interval between 3 to 9 hours. Figure 4-17 presents results for the case in which no sonobuoys are deployed. Figure 4-18 presents results for the case in which one sonobuoy is deployed.

The example presented in Figure 4-18 is the same as that shown in Figure 4-17 with the exception that target heading is assumed to be uniformly distributed over the interval from  $0 - \frac{\pi}{2}$ . This angle is measured in the clockwise direction.

SYMBOLS INDICATE VARIOUS PROBABILITY DENSITY LEVELS  
DARKER AREAS INDICATE HIGHER PROBABILITY DENSITY AREAS



○ DATUM

SUBMARINE HEADING: 
$$p(\theta) = \frac{1}{2\pi I_0(1)} \exp\{\cos \theta\}$$

SUBMARINE VELOCITY: 13 KNOTS  
 TIME LATE: 3 HOURS  
 ACCUMULATED TIME: 3.9 HOURS  
 GRID SIZE: 2.5 x 2.5 N.MI.

Figure 4-16 ACCUMULATED PROBABILITY DENSITY OF SUBMARINE'S POSITION WITH KNOWN CONSTANT VELOCITY AND RANDOM HEADING: NO SONOBUOYS DEPLOYED

SYMBOLS INDICATE VARIOUS PROBABILITY DENSITY LEVELS  
 DARKER AREAS INDICATE HIGHER PROBABILITY DENSITY AREAS



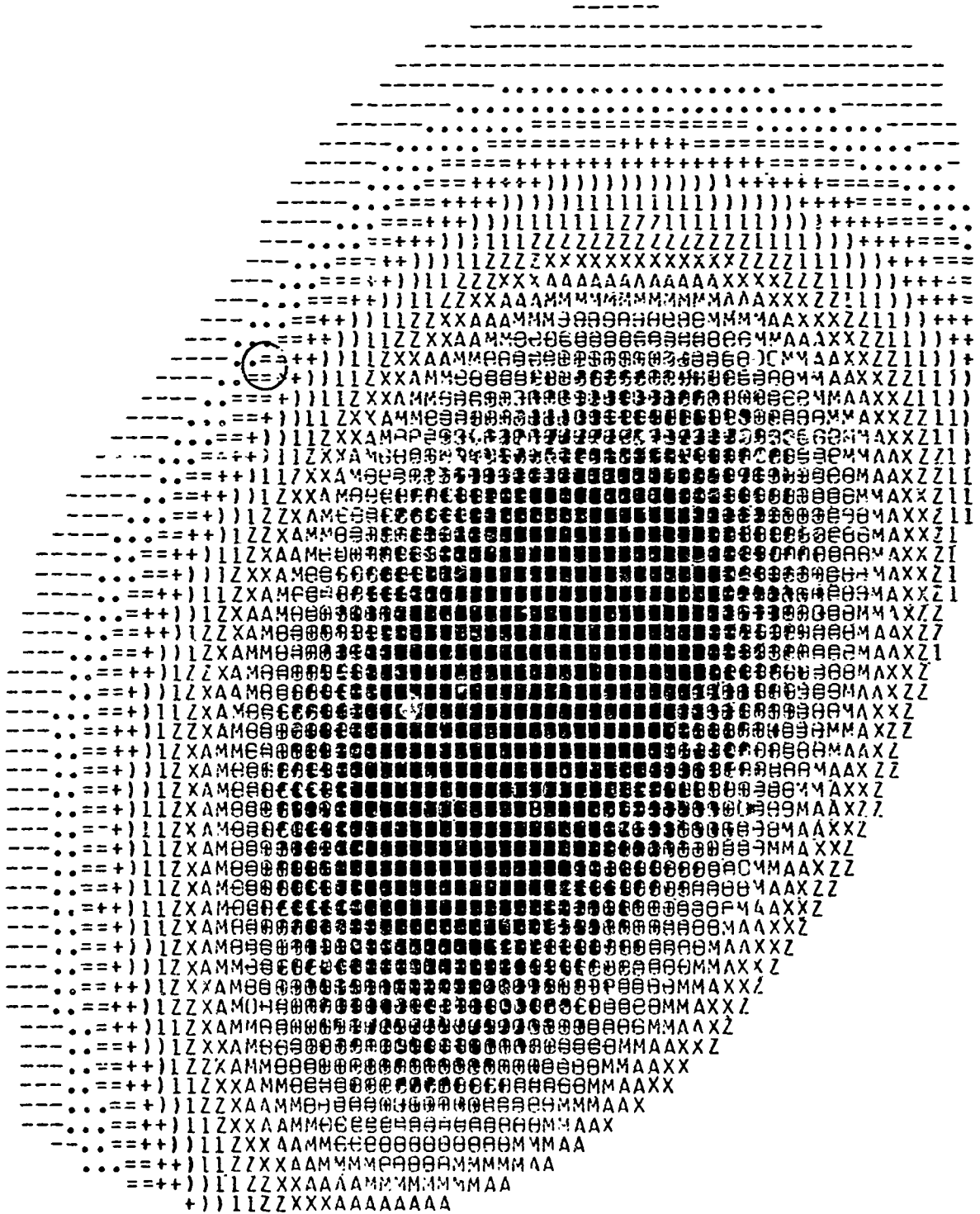
○ DATUM  
 □ SONOBUOY DROP POINT

SUBMARINE HEADING: 
$$p(\theta) = \frac{1}{2\pi I_0(1)} \exp\{\cos \theta\}$$

SUBMARINE VELOCITY: 13 KNOTS  
 TIME LATE: 3 HOURS  
 ACCUMULATED TIME: 3.9 HOURS  
 GRID SIZE: 2.5 x 2.5 N.MI.  
 NUMBER OF SONOBUOYS: 1, NUMBER OF "LOOKS": 24

Figure 4-17 ACCUMULATED PROBABILITY DENSITY OF SUBMARINE'S POSITION WITH KNOWN CONSTANT VELOCITY AND RANDOM HEADING: ONE SONOBUOY DEPLOYED

SYMBOLS INDICATE VARIOUS PROBABILITY DENSITY LEVELS  
 DARKER AREAS INDICATE HIGHER PROBABILITY DENSITY AREAS



○ DATUM

SUBMARINE HEADING: UNIFORM DISTRIBUTION 0-  $\pi/2$   
 SUBMARINE VELOCITY: 13 KNOTS  
 TIME LATE: 3 HOURS  
 ACCUMULATED TIME: 3-9 HOURS  
 GRID SIZE: 2.5 x 2.5 N.MI.

Figure 4-18 ACCUMULATED PROBABILITY DENSITY OF SUBMARINE'S POSITION WITH KNOWN CONSTANT VELOCITY AND UNIFORM HEADING BETWEEN 0 AND  $\pi/2$ : NO SONOBUOYS DEPLOYED

V. APPENDIX A: CAL FLYING SPOT SCANNER

The CAL Flying Spot Scanner was developed as a flexible research facility for investigation of pattern recognition/image analysis problems. It has been interfaced with various computers at the Computer Center as these have been updated from generation to generation and is currently capable of on line operation with either an IBM 370-165 or a PDP-9 computer. General software utility programs have been developed for reading and writing (computer input/output) operations. Recently, a new utility program has been developed to adapt the standard IBM 370 plotting routines, provided for use with electro-optical and electro mechanical plotters at the Center, to permit direct control of the Flying Spot Scanner as a plotter.

Plotting instructions to the Flying Spot Scanner can now be directly executed by FORTRAN and PL/I programs. Included is the capability to generate the standard character and symbol set. This feature together with the variety of photographic recording devices incorporated in the scanner has greatly expanded the utility of the system.

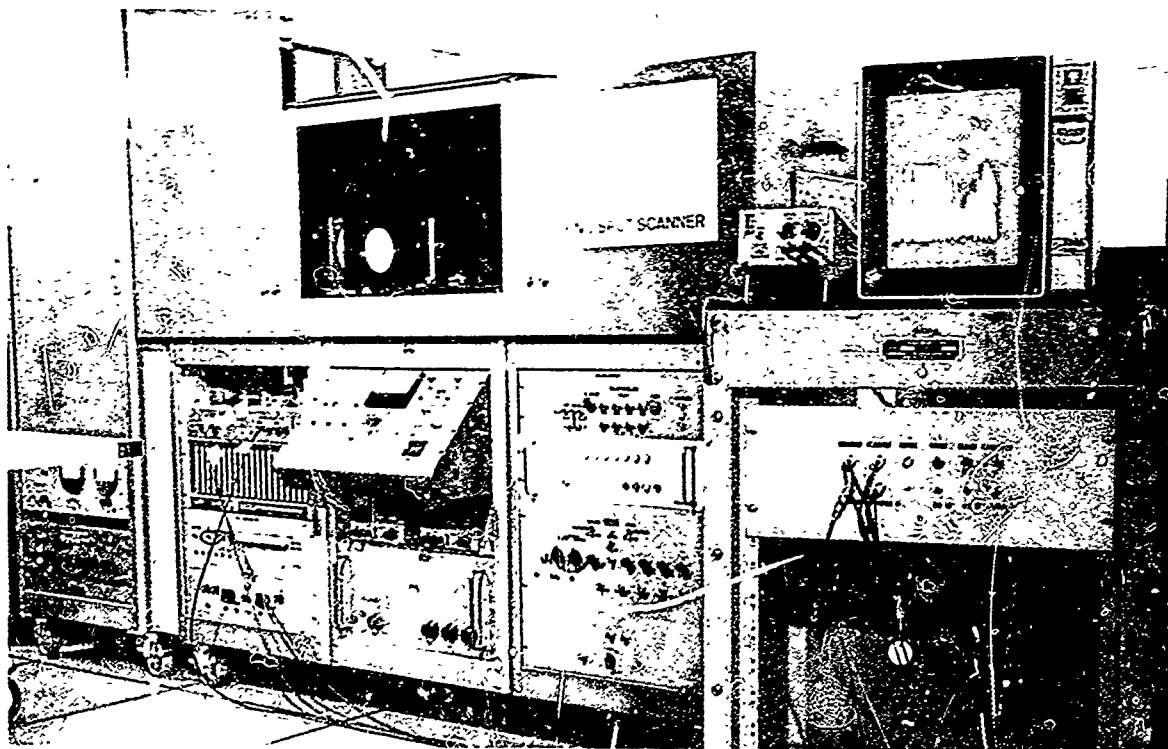
The Flying Spot Scanner features a cathode ray tube controlled by a precision magnetic deflection system. Nominal spot size is .0018" with 1024 discrete addresses per line horizontally and 1024 lines vertically. No programming restriction is placed on successive spot address location, a feature that facilitates operation in the plotting mode as well as in more complex interactive pattern reading modes. Two complete cathode ray tubes and deflection systems are provided which can be connected alternatively to common logic control and power supplies. One is configured to read opaque copy and is used only in the read mode. The second CRT is designed to read transparencies and to write on photographic material. A plate holder is provided to mount transparencies with a useful scan area of 3" x 3". A film transport which features pin registration to an accuracy of .001" under computer control is provided for reading 70mm and 35mm film. For recording purposes a variety of cameras and cut film holders as well as Polaroid backs are provided. A 35mm and a 16mm movie camera with single frame advance control by computer may be used alternatively. Provision is made for introducing color filters in the optical path thus allowing

v-30

A-1

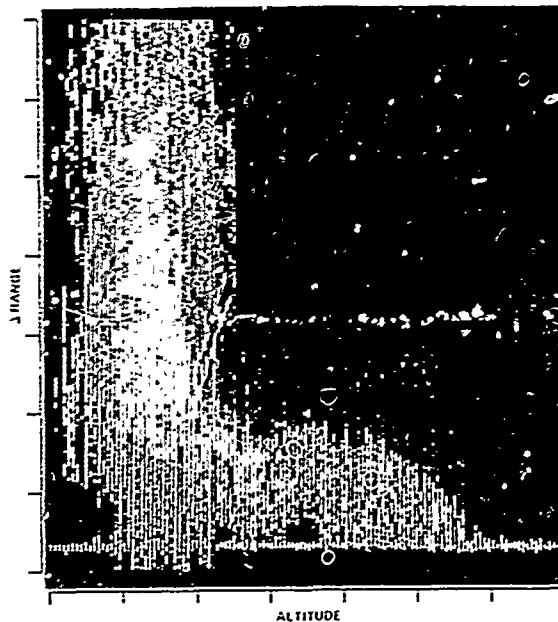
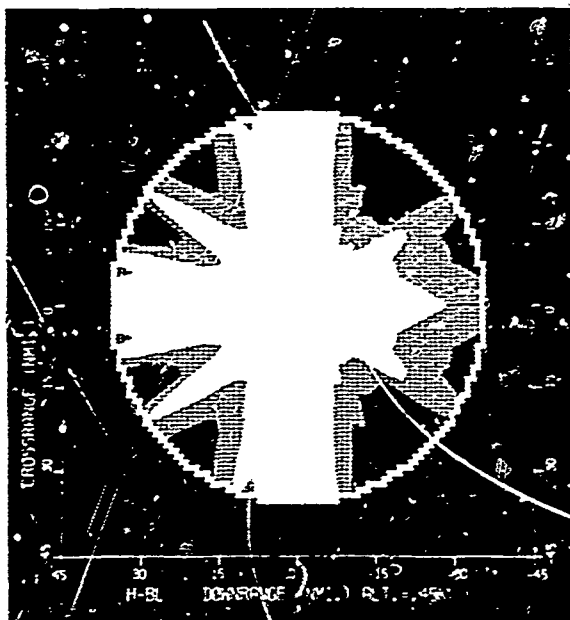
color separation in the read mode and color writing with appropriate color negative material. A large screen monitor CRT display is provided to observe the action of the scanner in the reading mode or to display in parallel the information being written on the photographic negative.

A VIEW OF THE FLYING SPOT SCANNER SHOWING THE CRT AND OPTICAL BENCH IN OPENING, TOP LEFT, AND THE LARGE SCREEN MONITOR ON RIGHT.

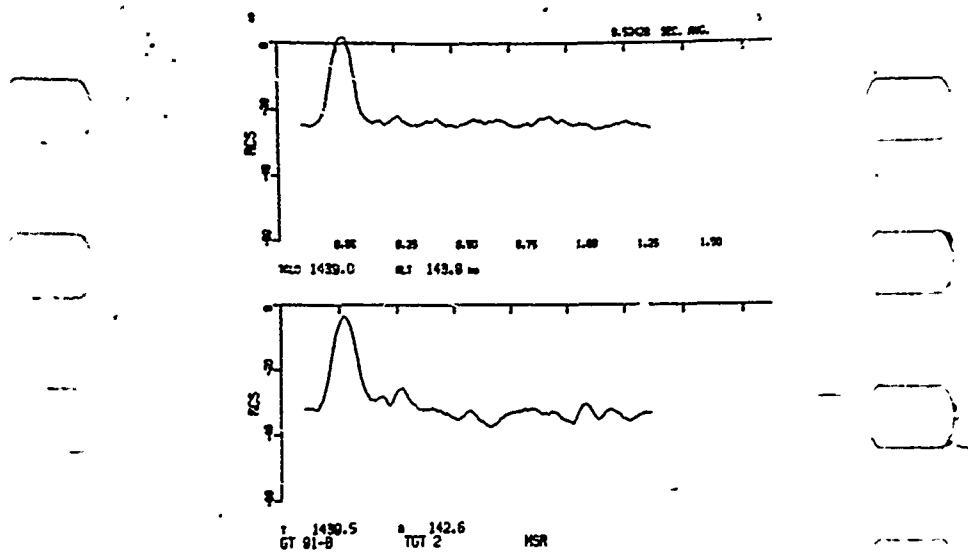


IV-31

ILLUSTRATIONS OF THREE DIMENSIONAL DATA PLOTS BY  
370/FLYING SPOT SCANNER SYSTEM



3 DIMENSIONAL GRAY SCALE PLOTS



LINE PLOT (35 mm)

*IV-32*